Pressure Measurements around a Circular Cylinder with and without Strake near Carved-out Boundary

by

VISHNU GUPTA

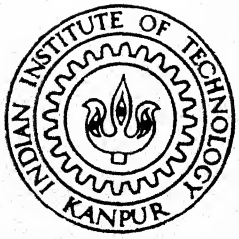

DEPARTMENT OF AEROSPACE ENGINEERING

INDIAN INSTITUTE OF TECHNOLOGY, KANPUR

June, 1996

Pressure Measurements around a Circular Cylinder with and without Strake near Carved-out Boundary

A Thesis Submitted
in Partial Fulfillment of the Requirements
for the Degree of
Master of Technology

by

Vishnu Gupta

to the

DEPARTMENT OF AEROSPACE ENGINEERING
INDIAN INSTITUTE OF TECHNOLOGY, KANPUR

June,1996

CERTIFICATE

It is certified that the work contained in the thesis entitled "*Pressure Measurements around a Circular Cylinder with and without Strake near Carved-out Boundary*", by Mr. *Vishnu Gupta*, has been carried out under my supervision and that this work has not been submitted elsewhere for a degree.

A. K. Gupta

(Dr. A. K. Gupta)

Professor,

Department of Aerospace Engineering,

Indian Institute of Technology,

Kanpur.

June,1996

Dedicated

to

My Parents

ABSTRACT

An experimental study of flow around a smooth and straked cylinder, near a plane and different carved-out surfaces, is carried out for different height of cylinder above the surface. The surfaces are carved-out for curvature radius of 0.7D, 0.9D, 1.2D from the centre of the cylinder, when the cylinder is resting on the plane surface. These curvature representing the various stages of the growth of scour. The cylinder spanned the test-section of the wind tunnel and their axis were parallel to each other. The flow is taking place normal to the cylinder axis. The cylinder was placed 20 diameters downstream of the leading edge of the plate. The cylinder can be fixed for three heights of 0.0D, 0.5D and 1.0D above the plane of the wind tunnel test-section. The strake has the width of 0.057D and height of the strake is 0.12D.The strake is fixed to the cylinder helically.

The experiments have been done at three values of 3m/s, 4m/s, 5m/s for the measurement of pressure around the cylinder and on the bed with the smooth cylinder and with velocity of 3m/s and 5m/s for the pressure distribution around the straked cylinder. The measurements have been done on the carved-out bed at 5m/s and for heights of 0.0D and 0.5D with the straked cylinder.

The experiments have indicated that pressure drops rapidly for smaller values of gap and the effect of the boundary is minimum for higher gap-ratios. It has been found that the minimum C_p lies just after the gap. The negative pressure peak is more pronounced for small gap between the cylinder and bed. The effect of curvature

is similar to the gap of that much between the cylinder and bed. At larger gap-ratios and large curvatures the pressure distribution around the cylinder becomes nearly symmetric about the front stagnation point and the negative pressure peak almost disappears. The effect of strake on the cylinder is that the pressure after the strake is more and for small curvature and low gap-ratio the pressure decreases under the cylinder but for increased gap-ratio the pressure increases. There is almost no effect of change in Reynold's number.

ACKNOWLEDGEMENTS

I express my deep gratitude and indebtedness to Dr. A. K. Gupta for his invaluable guidance and persevering supervision through out the course of this work. I feel proud of the privilege of receiving guidance from him who has readily helped me whenever I approached him to clear my doubts, and without whom this work would not have been possible.

I convey my sincerest greatfulness and heartful thanks to Dr. Kamal Poddar for his valuable suggestions and kind cooperation in my experimental work.

I whole heartedly convey my thanks to Mr. K. Mohan and Mr. Rameshwar whose valuable help and cooperation made my work easy in the Aerodynamics lab.

I feel myself bound to add the names of Abhishek, Amod, Tyagi, Gagan, Rahul, Rathore, Bhartendu, Sukumar, Rajeev, MPA, Binod, Avi, Sangeet, Maneesh and other E-Bot members who provided me not only a pleasant company during my stay at IIT Kanpur, but also a life long friendship.

NOMENCLATURE

D	diameter of circular cylinder
C_p	coefficient of pressure
G	clearance between the bed and cylinder
p	pressure at the point on interest
p_o	upstream undisturbed pressure
U	maximum freestream velocity
ω	frequency of vortex shedding
St	Strouhal number
Re	Reynold's number
ρ	density of fluid
α_{hs}	angle showing strake position with respect to flow direction

Contents

List of Tables

List of Figures

Chapter 1

INTRODUCTION

1.1 Introduction

The flow around a circular cylinder in a free stream has been studied in detail and has been understood with many variations. However the flow around a circular cylinder near a plane is also important to study for various engineering application. Now a days pipelines have been laid under the sea for transportation of petroleum from offshore drilling station to the coast and for under water communication cables and also for outfalls for disposal of industrial waste. These pipelines laid near the sea bed are exposed to tidal flows and waves. The action of these develops scour below the pipeline.

The development of the scour below the pipeline may be crucial in the structural failure. The scour underneath a submarine pipeline which is a hollow circular cylinder and is located on the sea bed, may expose a part of the pipe causing it to be suspended in the water. If the free span of the pipe is long enough, the pipe may experience a flow induced resonant oscillations, leading to pipe's structural failure. Therefore one of the main aims in the design of submarine pipeline is to avoid these oscillations by dealing with the cause of the problem; that is to reduce

the depth of the scour, or perhaps to prevent the scour underneath the pipe.

Bearman and Zdravkovich (1978) [1], while summing up what has been done till date on this problem threw light on an important aspect of the wall interference problem that had not been examined. How does the flow changes along the wall during the various phases of the interference with the cylinder? This question, they emphasised, was relevant for pipelines laid along the sea or a river bed, where the scouring could change considerably the gap between the pipe and the bed and also alter the shape of the bed itself.

The emphasis of this work is how the flow depth affect the flow pattern around a cylinder placed near a plane bed to a real scour like condition. The study also examines the effect of the gap openings between cylinder and bed on flow around the cylinder. It was planned to cover the following aspects:

a The pressure distribution studies on the surface of the cylinder held in the airstream is expected to give the effect of the gap flow on the forces acting on the cylinder.

b The study of the base pressure acting on the plate, having different degrees of scour represented by different curvatures carved out in the plate underneath the cylinder, due to the nearness of the cylinder it will be done for different gap ratios, hoping to get variations in the magnitude of the suction pressure due to the gap flow.

c Under similar conditions, as in (b), the base pressure studies are to be made for a flat unscoured plate for same gap ratios. This is expected to give the effect of onset of scour, when compared with (b), on the flow characteristics.

Gap ratio is defined as the ratio of the clearance between the bed and the cylinder held with its axis parallel to the bed and is denoted by the symbol G to the diameter of the cylinder D. The present work concentrates on the effect of gap

ratio and increasing depth of scour, with the cylinder held at same fixed positions corresponding to the unscoured plate, on the pressure acting on the circular cylinder and the base pressure variation on the rigid scoured and unscoured walls.

1.2 Literature Review

The study of flow around a circular cylinder near a plane surface has received fresh interest in 90's as more submarine pipelines are being laid. Earlier the main work has been done by Bearman(1978)[1], Chiew(1991)[4],[5], Chao(1972)[2], Fredsoe(1990)[8] etc. The flow around a circular cylinder in a free stream is symmetric, so the pressure distribution is also symmetric about the centreline parallel to the flow. On the other hand, the boundary layer flow past a circular cylinder, which is held with its axis parallel to the boundary and perpendicular to the flow, causes asymmetry in the surface pressure distribution. The proximity of the cylinder causes the concentration of positive and higher negative pressure on the boundary plate, the magnitude of this pressure depends on the gap ratio and the diameter of the cylinder.

The major contributions to the mechanics of the local scour around submarine pipelines was summarized by Chiew (1991) [4]. The literature can be broadly classified into two categories namely,

1. Development of the empirical relations for the maximum scour depth in terms of parameters such as velocity, pipe diameter, bed grain size and flow depth.

   Contribution to this category are Kjeldsen et al(1973)[1], Ibrahim and Nalluru(1985)[10], Chao and Hannessy(1972)[2], Fredsoe and Hansen(1987)[7], Hansen et al(1988)[8] and Mao(1986-88)[13].

2. The effect of gap on the scour depth.

   Contributors to this category are Bijker and Leeuwestein(1984)[8], Kjeldsen et al (1973)[1], and others.

1.2.1 Surface Pressure Distribution on the Cylinder and along the Bed Plate

The surface pressure distributions on the cylinder and along the bed plate have been studied by Bearman and Zdravkovich (1978)[1]. They, while concentrating on thin boundary layers, i.e. boundary layers thinner than the diameter of the cylinder, investigated experimentally the flow around a cylinder placed at various heights above a plane boundary. Time averaged pressure distributions were measured around the cylinder and along the plate for various gap ratios, pressure was presented non-dimensionally in the form of pressure coefficients C_p, which is defined as:

$$C_p = \frac{p - p_\infty}{0.5\rho U^2} \tag{1.1}$$

where p is the pressure at the point of interest, p_∞ is upstream undisturbed pressure, U is maximum (free stream) velocity and ρ is the density of the fluid.

When the cylinder touched the plate the minimum pressure was at the point of contact. In the range of strong interference when the cylinder was near the wall for G/D = 0 to 0.4, the pressure peak on the bed plate became more pronounced and its position moved downstream. At G/D = 0.4 the pressure peak reached its maximum magnitude and occurred underneath the ream of the cylinder, at 0.5D. The peak remained at this point for all G/D > 0.4 . The pressure distribution on the cylinder was nearly symmetric about he front stagnation point. A continuous recovery of the pressure along the plate was found after the minimum C_p and the magnitude of this minimum pressure decreased as the gap ratio was increased.

The base pressure was observed to change very little above G/D = 1.0. As gap-ratio was increased the pressure distribution around the circular cylinder assumed a symmetrical form with the axis of symmetry approaching the free stream direction. At small gaps the separation point on the side nearest to the plate moved down stream of the nearest point of the gap. Y.M. Chiew(1990)[3] observed very high

magnitude of positive pressure on the upstream face of the cylinder in comparison to the wind tunnel observations of the Bearman and Zdravkovich (1978)[1]. This indicates that the nearness of the free surface to the cylinder position causes higher magnitude in the upstream pressures and the downstream phase pressure remain fairly similar to the wind tunnel studies.

Fredsoe's(1990) [8] experiments indicate the following observations. When the cylinder was subjected to the wave flow motion, the stagnation point which is characterised, by maximum value of the coefficient of pressure moves to the lee side of the cylinder before the free stream flow reverses. The distribution pattern changes sharply at some phase values during the course of the wave motion. The nearness of the cylinder increases the negative pressure on the plate side surface of the cylinder.

1.2.2 Vortex Shedding

The vortex shedding in case of flow around a circular cylinder near a plane surface exists but it is not similar as in case of a cylinder in a free stream. Bearman and Zdravkovich's (1978)[1] and Prasad's (1993)[15] flow visualization studies indicate the existence of vortices on both upstream and downstream sides of the cylinder when the gap ratio is zero. These vortices detached from the cylinder surface and got attached to the plate for small gap-ratio flows. Existence of counter rotating vortices on the rear side of the cylinder for small gap flow was also observed.

Taneda(1965)[19] observed a single row of vortices for G/D = 0.1 and a strong regular stream of vortices for G/D = 0.6. Wavelengths of the single row vortices increased with downstream distance and after a few wavelengths the wake became unstable and broke down. Experiments conducted by Bearman and Zdravkovich (1978)[1] showed that the strouhal number St varies with G/D as indicated in Table 1.1.

Strouhal number St is defined as

$$St = \frac{\omega D}{U} \tag{1.2}$$

Where ω is the frequency of the vortex shedding.

Table 1.1: Effect of Gap ratio (G/D) on Strouhal Number (St).

S.No.	G/D	St
1	0.0	0.085
2	0.2	0.190
3	0.3	0.207
4	0.4	0.202
5	0.6	0.203
6	0.8	0.213
7	2.0	0.215
8	2.5	0.195
9	3.5	0.203
10	∞	0.208

Roshko et al (1975)[16] also observed that the magnitude of St is of the order of 0.198 in free stream and 0.206 at G/D = 0.5.

1.2.3 Scour Underneath Submarine Pipelines

Interaction between a submarine pipeline and an erodible bed has attracted much attention because of its importance in offshore engineering. In connection with the development of oil and gas fields in offshore regions, additional submarine pipelines are being laid on the ocean bed to transport crude oil to offshore refineries.

Experiments have shown that how local scour develops around submarine pipelines in noncohesive sediments. Most research investigations conducted ion scour around submarine pipelines are confined to establishing empirical equations. In general, these equations relate the depth of the scour to the parameters such as velocity, pipe diameter, grain size, and flow depth.

Bijker and Leeuwestein (1984)[8] identified three basic forms of erosion around a submarine pipeline:

1. Luff erosion which occurs at the upstream side of the pipe and is caused by an eddy formation upstream of the pipe.

2. Lee erosion, which occurs at the upstream of the pipe and is caused by an eddy formation upstream of the pipe.

3. Tunnel erosion, which occurs under the pipe and is a direct consequence of the increased velocity underneath the pipe compared with the undisturbed velocity.

Mao (1988)[13] reported the formation of three types of vortices around a submarine pipeline. As illustrated in Fig.1.1(a), one of the vortices, A, formed at the nose of the pipe, the other two vortices B and C, formed down stream of the pipe.He also cited pressure distribution near a pipe in unidirectional flow measured by Bearman and Zdravkovich (1978)[1] and deduced that the pressure difference between the upstream and the downstream side of the pipe may cause seepage underneath the

pipe. The onset of scour (fig 1.1) is thus, according to Mao, due to the combined action of the vortices and the underflow, which leads to the formation of a small opening under the pipe as more and more sand particles are carried away.

Yee-Meng Chiew (1990)[3] explored the temporal development of the scour around the submarine pipelines resting on an initially flat bed composed of uniform, cohesionless sediments and exposed to uniform steady flows. The study showed that piping is the dominant cause of the scour formation. Piping and the stagnation eddy combined to undermine the pipeline, and mark the onset of scour. The critical hydraulic gradient associated with the initiation of the scour was found equal to the floatation gradient of the bed sediments. The pressure drop between the stagnation pressure upstream and wake pressure downstream of the pipe induces this hydraulic gradient.

The process of scour of the bed in the vicinity of a pipe is due to the disturbance of the flow caused by the presence of the pipeline. In the case of scour around a pipe exposed to a steady current, the scour profile is characterised by a steep upstream slope, as shown in fig 1.2. The asymmetric shape is due to the difference in the flow pattern on the upstream and downstream parts of the pipe, where the potential flow dominates the upstream part.

Leeward of the pipe, flow separation occurs, and a vortex sheet is formed over a long stretch downstream of the pipe. This downstream flow erodes more heavily that the upstream flow due to following:

1. The higher level of turbulence, and

2. The instantaneous velocity in the downstream vortices exceeding the undisturbed flow velocity by a factor of two or more(Summer et al., 1988)[18].

As a result of this erosion, the downstream slope becomes more gentle.

Summer and Fredsoe (1990)[8] undertook an experimental investigation on the scour below pipelines exposed to waves. They concluded that :

1. The effect of lee wake of the pipe is the key element in the process of scour formation,

2. The effect of position of the pipe with respect to the bed is an important parameter in determining the equilibrium scour depth, and

3. The surface roughness of the pipe imposes practically no influence on the scour process.

Chao and Hannessy (1972)[2] were amongst the first to investigate the problem of local scour occurring underneath the offshore pipelines and its effect on the structural stability of the pipe. They developed and presented a simple analytical method for estimating the maximum scour depth under an offshore pipeline, caused by subsurface currents. Due to lack of experimental information, their method only provided an order of magnitude estimation of the possible scour hole depth.

Chiew (1991)[4] critically reviewed the research works conducted since Chao and Hannessy's (1972)[2] estimation of the maximum scour depth, and proposed a semiempirical method for estimation of maximum scour depth based on understanding of the physics of the flow and sediments transported around the pipeline. The study proposed an iterative method for estimating maximum scour depth at submarine pipelines which occurs when the applied shear stress is equal to the critical shear stress for sediments entrainment. Their predicted value compared well with the experimental data obtained from the study.

Chiew (1992)[6] carried his work further and exploited the self burial potential of the pipelines by placing spoilers on the pipelines to increase scouring, thereby stimulating the self burial process.

1.3 Motivation of the Present Work

Apart from most research investigations confined to establishing empirical equations, few experimental investigations have been carried out with a circular cylinder laid on a flat bed which is rigid (Bearman, 1978[1]), mobile (Prasad, 1993[15]) or carved out rigid (Tiwari, 1994[20]) and subject to unidirectional currents.The objective of these experiments, in a broad sense, were to find out the mutual effect of the cylinder and the bed on each other; and in turn relating the pressure distributions around the cylinder and along the bed to the onset of scour, studied by (Mao, 1988[13]), Summer et al., 1988 [18], Fredsoe et al., 1988 [7];etc.)

Not much work has been done, to date, to explore the possibility of subjecting the cylinder, placed near a plane bed, to a real scour like situation, and then measuring the flow around the the circular cylinder and along the boundary to study the change in flow parameters with the on set of scour, and the increase in scour depth. In other words, the flow change along the wall during the various phases of interference with the cylinder, in the form of creation of scour and change in gap ratio, needs to be examined.

Formation of vortex is an important aspect in the formation of scour and this plays a major role in the failure of the pipelines due to vortex induced oscillations. The aspect of the suppression of the vortex induced oscillations by means of the protrusion has not been studied in case of the flow around a cylinder near a plane surface. The protrusion on the cylinder will change the pressure distribution on the bed considerably for smaller gap-ratios, and affect the erosion of the bed.

Helical strakes have been effectively employed on the tall cylindrical chimney to suppress the vortex induced oscillations (Kumar M., 1996 [12]). Will helical strake fitted circular cylinder also modify the flow field near a plane bed so as to reduce the local scour ? this appears to be an interesting problem worth studying in greater detail.

1.4 Objective of the Present Work

The problem put forward by Bearman and Zdravkovich(1978)[1], How does the flow change along the wall during the various phases of interference with the cylinder?, largely remains unanswered. The present study ,"Pressure Measurements around a Circular Cylinder With and Without Strake near Carved-out Boundary", is an attempt to look at this problem, in combination with the problem of the development of scour around the submarine pipelines resting on an initially flat bed and exposed to uniform, steady flows.

The main aim of the present experimental study is to measure the pressure distribution along the bed, and around the cylinder, with the carved out surface underneath the cylinder to simulate the scour, and then comparing this result with the plane boundary (uncarved) results obtained in the study under similar conditions, and those presented by Bearman and Zdravkovich (1978)[1] for a multiple gap ratios and further study the effect of helical strake on the pressure distribution on the cylinder and on the bed.

The scour created on the sea-bed, initially a plane surface, underneath a submarine pipeline, or a circular cylinder, is approximated by a circular curvature having its centre at the centre of the cylinder, when the cylinder rests on a plane boundary. This curvature is carved out all along the span of the boundary, which forms the bottom surface of a low speed wind tunnel.

The pressure distributions around the cylinder and along the plate are measured for varying degrees of scour, represented by different curvature radii carved-out on the plane boundary, and varying gap ratios, G/D = 0.0 correspond to the cylinder touching the plane boundary, with and without the strake. These results when compared with those obtained for the flow around a cylinder near a plane, uncarved boundary, in the present study as well as Bearman's (1978)[] experiments, may give a good measure of the effect of onset of scour. The cylinder is planned to be held at

same fixed positions for all boundaries with different scour curvatures, and aligned normal to the flow, to study these effects.

The pressures were measured on the cylinder and on the bed to study the effect of the strake on the bed and on the cylinder, and compared with the results obtained for plain cylinder and different location of strake with respect to flow direction, and also see the effect of increase of gap-ratio on the pressure distribution in the scoured region.

Chapter 2

Experimental Set-up And Technique

The experiments for the present investigation were conducted in an open circuit low speed wind-tunnel. Description of the experimental set-ups, details of the model, equipment used and the experimental techniques are presented in the following sections.

2.1 Experimental Equipment

The major equipments used to perform the experiments were:

1. Low speed Wind Tunnel
2. Pitot static tube
3. Electronic digital micro-manometer
4. Thermometer
5. Barometer

2.1.1 The Wind Tunnel

An open circuit low-speed wind tunnel (fig. 2.1) with closed test section was used for the measurement of pressure around the cylinder and along the base. The tunnel is available in the 'Low speed Aerodynamics Lab' of I.I.T.kanpur.

A screen is placed at the entrance of the wind tunnel, after which there is a contraction and then the test-section of 16 inches x 12 inches starts. The total length of the test-section is 40 inches. At the end of the test-section there is a gradual expansion and at the end an exhaust fan is fitted which sucks the air through the test-section. The exhaust fan is operated by a motor which is connected to a 230 V AC through a voltage variac by which the voltage can be varied from 0 to 230 volts and also through a voltage stabilizer ensuring constant speed. The velocity of air through the test-section is controlled by varying the voltage variac.

2.2 Experimental Set-up

The experiments for the present investigation were performed in the 'Low Speed Aerodynamics Lab' of the Department of Aerospace Engineering at I.I.T. Kanpur. An open circuit wind tunnel with a closed rectangular test-section 12 inches high, 16 inches wide and 40 inches long was used. Various experimental arrangements made for the investigation are described in the following sections.

2.2.1 Cylinder Mounting

A hollow brass cylinder of external diameter 2.8 cm spanned the test-section of the wind tunnel and was aligned with its parallel to the bottom plate and normal to the free stream. It was placed 20 diameter downstream of the leading edge of the plate, at the centre of the test-section and near the bottom plate.

A detailed view of the cylinder mounting is shown in fig.2.2,2.3 and fig.2.4. The cylinder was pressure tapped at four stations on the surface, separated from each other by an angle of 90 degrees. A fine external threading was provided, over a length of 2 inches, on the surface of the cylinder at one of the ends. A side plate of width 2 inches and length of about 20 inches was provided with a circular hole of diameter corresponding to the outer diameter of the cylinder. A brass collar was fitted to it having internal threads matching with the external ones on the cylinder surface. A hole was made for the fixing of the pitot static tube in it. The side plate was fitted centrally on one of the sides of the test-section. The end of the cylinder was fitted in a plate such that there are no flow induced vibrations of the cylinder, and also it does not rotate. The other side being transparent for viewing purposes.

The cylinder was fastened to the collar and tightened by means of a brass lock-nut, which prevents it from rotating when the experiment is going on. By loosening the lock-nut it could be rotated to any angular position, as indicated by a protractor fitted on the cylinder, and pressure measurements could be made.

Three holes, at longitudinal distances of 1.4 cm from each other were provided both at the top and bottom portions of the side plate. Now using different combinations of the holes for screwing the side plate to the test-section the cylinder could be moved up and down, to vary the gap between the cylinder and the bottom surface (plate). The height above the plate was varied from zero, the cylinder lying on the surface , to the cylinder diameter; i.e. the gap ratio G/D varying from 0.0 to 1.0 in steps of 0.5.

The remaining portion of the side wall of the test-section was covered by two plywood pieces of size 17in. x 12in. x 0.25in..

2.2.2 Carved-out Boundary (Bottom Surface)

The objective of the present investigation was to measure the pressure distribution along the boundary and around the cylinder, with the boundary carved-out underneath the cylinder to simulate a scour. The results obtained were then compared with those obtained for a plane uncarved boundary, in the study, under similar conditions; and those presented by Bearman and Zdravkovich for multitudinous gap-ratios.

The scour created on the sea-bed, initially a plane surface, underneath a submarine pipeline, or a circular cylinder, is approximated by a circular curvature having its centre of the cylinder, when the cylinder rests on the plane boundary. based on Bearman's observations for the effect of gap-ratios (G/D) on the flow, three different curvatures of radii 0.7D, 0.9D,and 1.2D were selected and these were carved out all along the span (width) of the boundary. Three wooden plates of length 16 inches (equal to test section width), width 5 inches and thickness 1.0 inch were taken and different curvatures carved out on them all over the 16 inch length at the centre (see Fig. and Fig.). These plates represented different degrees of scour created on the boundary, as a result of flow around the cylinder near to it.

One of these plates, was fitted in turn on the bottom frame of the wind-tunnel, at the centre, with the length of the plate corresponding to the tunnel width; so that the curvature carved-out on the plate is just beneath the cylinder and thus both have a common centre. The plates were pressure tapped at the mid-span in the region beneath the cylinder. A central tapping was fitted under the axis of the cylinder and the rest were positioned at 0.25, 0.5, 1.0 and 2.0 cylinder diameters upstream and downstream of it. The pressure tubes taken out of these tappings were connected to a digital electronic micro-manometer which gave the pressure distribution along the plate.

Wooden plates having dimensions of 17.5 in x 16.0in x 1.0in were prepared and

finished as shown in Fig. ,and they formed the leading edges of the boundary. They were fixed respectively at the leading and trailing ends of the wind tunnel on the bottom frame. Now, these two plates and a carved-out one, at the centre, constituted the bottom surface (boundary) of the tunnel. The three plates, viz. the leading edge, the central one and the trailing edge were matched properly and the minute gaps between them filled and surface smoothened using moulding clay.

A flat plate of dimensions 16in. x 5in. x 1in. was also located, in turn, at the centre in place of the carved out plates to measure the flow around a circular near a plane boundary under similar conditions.

2.3 Experimental Technique

The present investigation aims at measuring the pressure distribution around the cylinder and along the boundary, for a uniform steady subsonic flow around a circular cylinder near rigid plane scoured (carved-out) and plane boundaries.

The experiments were performed in an open circuit subsonic wind tunnel with a closed rectangular test-section. The procedure adopted in conducting the experiments is described below:

2.3.1 Measurement of Pressure Distribution around the Cylinder and along the Boundary

First of all, the atmospheric pressure and temperature were noted down with the help of a standard barometer and thermometer mounted in the 'Low-speed Aerodynamic Lab'. Then the cylinder and three different plates, forming the boundary (bottom surface) of the wind tunnel, were mounted, as described in section 2.2, in the wind tunnel test-section and the test-section was closed.

The pressure tappings coming out of the cylinder and the boundary were numbered from 1 to 13 and accordingly connected to a digital electronic micro-manometer. Another pressure tubing from the pitot static tube, connected to the side plate on which the cylinder is mounted, through a slot, was connected to a different micro-manometer which served as an anemometer. It measures the dynamic pressure and shows the magnitude of the free stream velocity, in meter/second on a digital screen. The experiments were performed for low velocities of 3.0, 4.0 and 5.0 m/s.The manometer was put in mode of measuring the pressure in pascal.

The tunnel was then turn on. By controlling the voltage of its blower the tunnel speed was increased to the required velocity, as indicated by the anemometer. Now the counter, connected to the micro-manometer ,was set at 1, corresponding to station no.1 connected accordingly through a pressure tubing to the manometer. The reading shown by the manometer, digitally, in terms of pascals to the pressure at station 1. The counter was then shifted up from 1 to 13 and again down to 1, and pressures at the corresponding stations noted down.

As stations 1 to 4 represented four points on the surface of the cylinder separated to each other by 90 degrees at mid-span, the cylinder was rotated by 15 degrees and readings taken at all the four stations. Similarly, rotating the cylinder by 30, 45, 60 and 75 degrees, pressure were measured all over the surface of the cylinder, at a step of 15 degrees.

Now the gap-ratio was changed from zero to 0.5 and then to 1.0, by lifting up the cylinder mounting, and pressure measured at all the stations. similar experiments were performed after changing the free stream velocity, by adjusting the voltage variac, from 3.0 to 4.0 and then to 5.0 m/s.

The central plate of the bottom surface having a curvature carved out in it, was then replaced by different plate, having different radii of curvatures, successively, and pressure distribution found out along the plate and around the cylinder at three

free-stream velocities and three gap-ratios. Similar experiments were also performed using a flat (uncarved) plate in the place of carved-out ones.

2.3.2 Pressure distribution with straked cylinder

For the measurements around the straked cylinder the experiments were conducted for three gap-ratios and for two speeds of 3m/s and 5m/s. For the measurements a long the bed the study was conducted for only one speed of 5m/s and for two gap-ratios of 0.0 and 0.5. The results were plotted and compared from the corresponding values for the smooth cylinder.

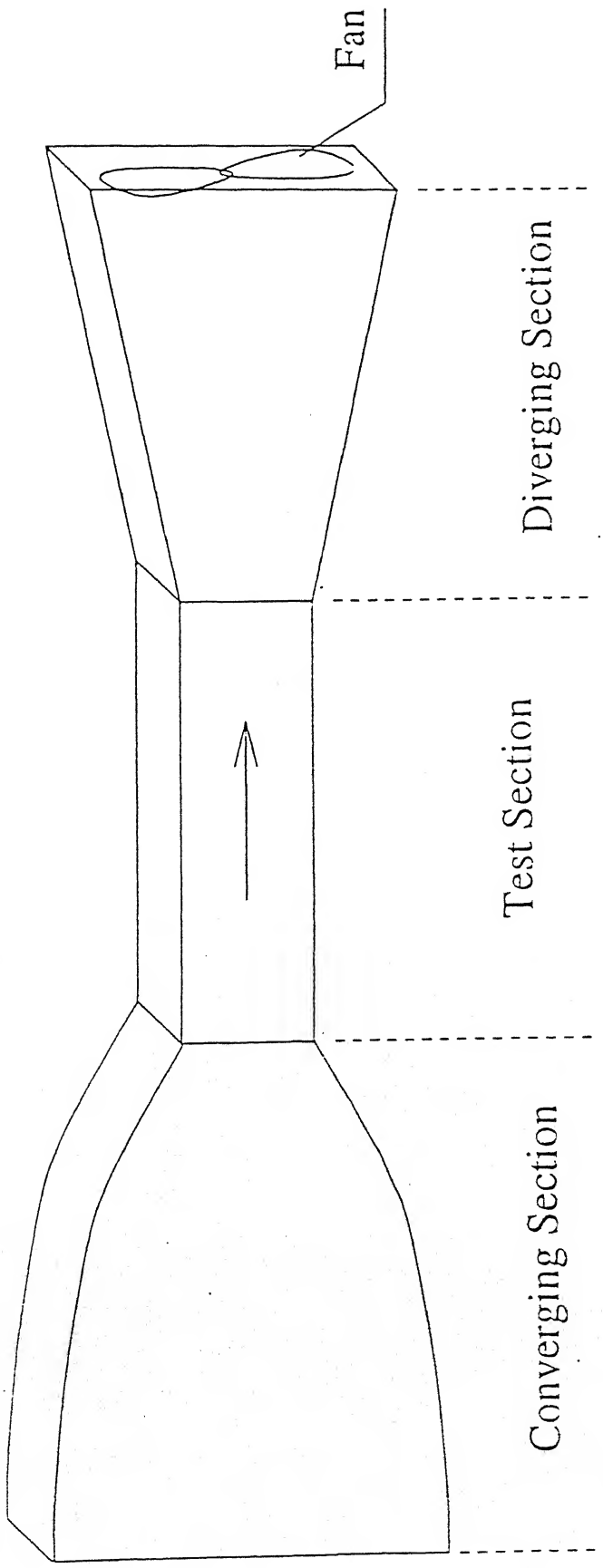

Fig.2.1 Low speed wind tunnel

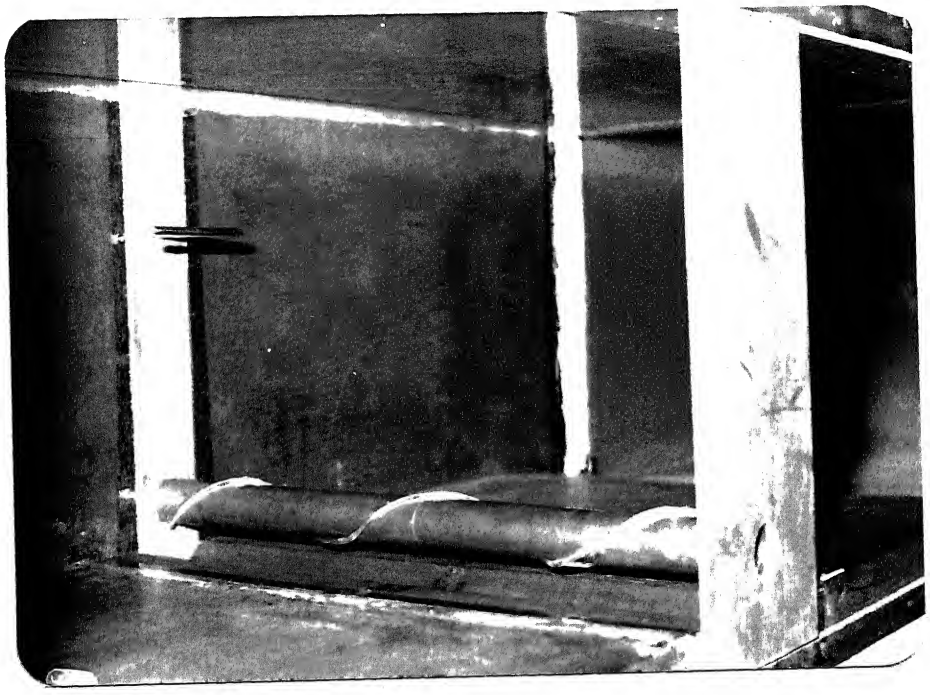

Fig.2.2 Wind tunnel test-section with mountings

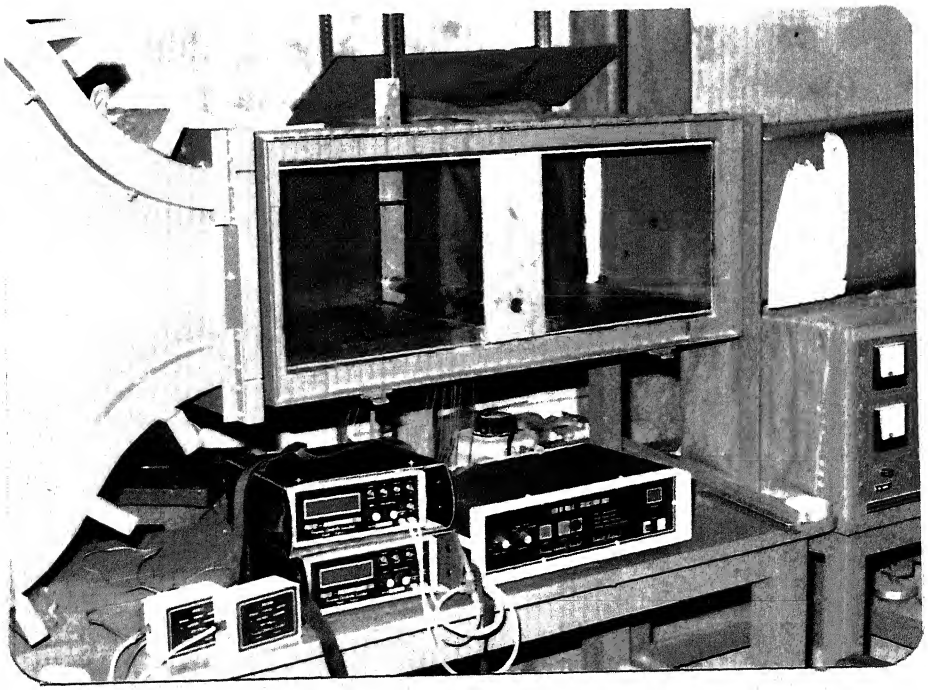

Fig.2.3 Model connected with digital micro-manometer and selection box

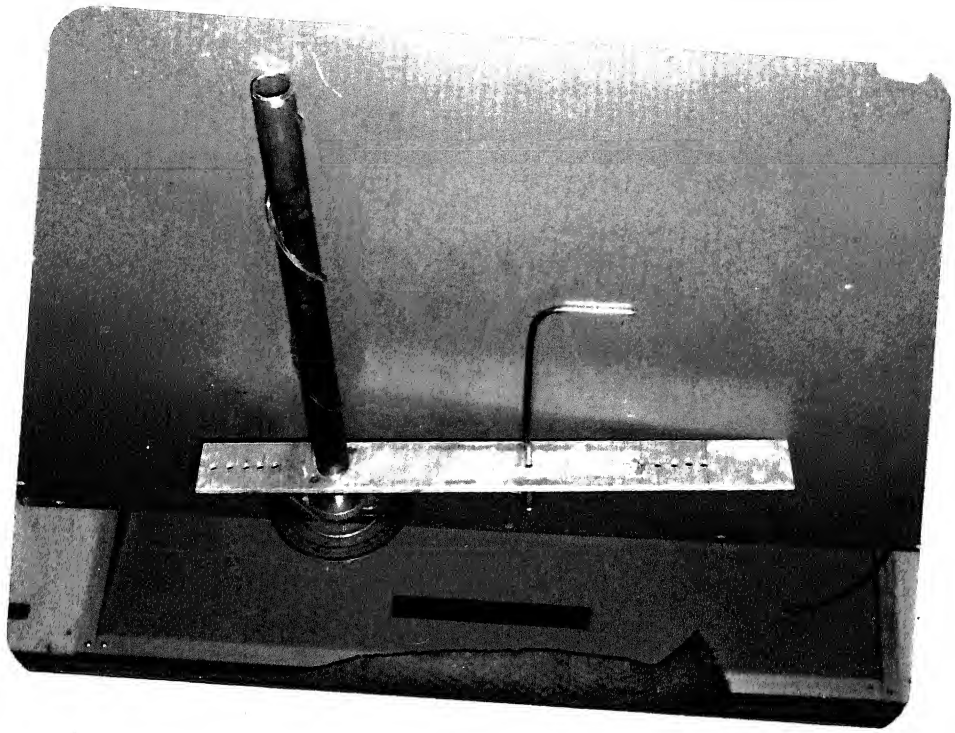

Fig.2.4 Model with helical strake,protector and pitot-static tube

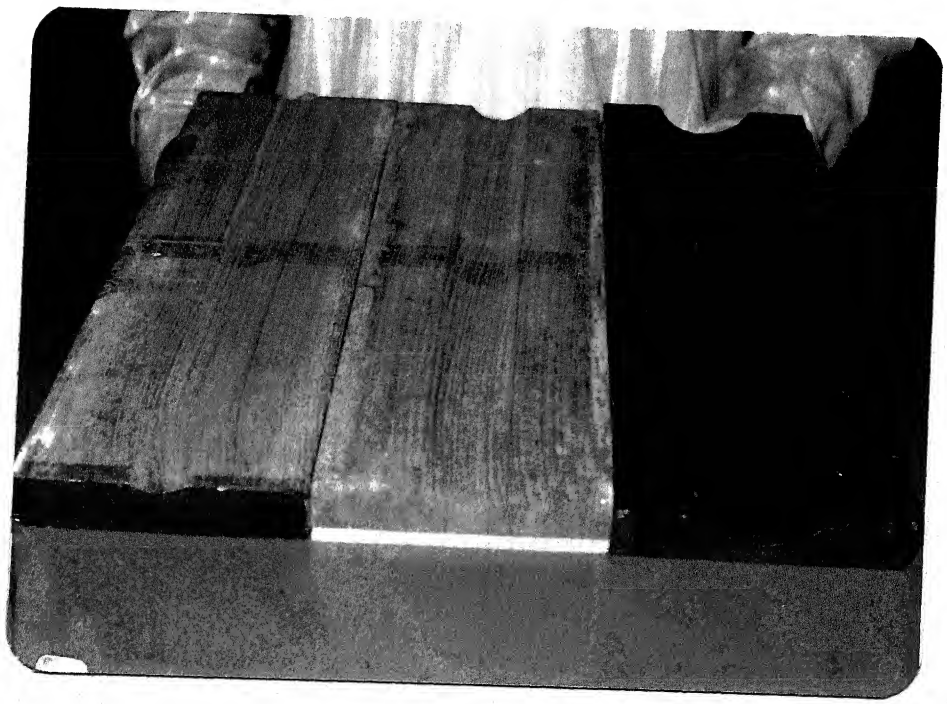

Fig.2.5 Carved-out plates of various curvature

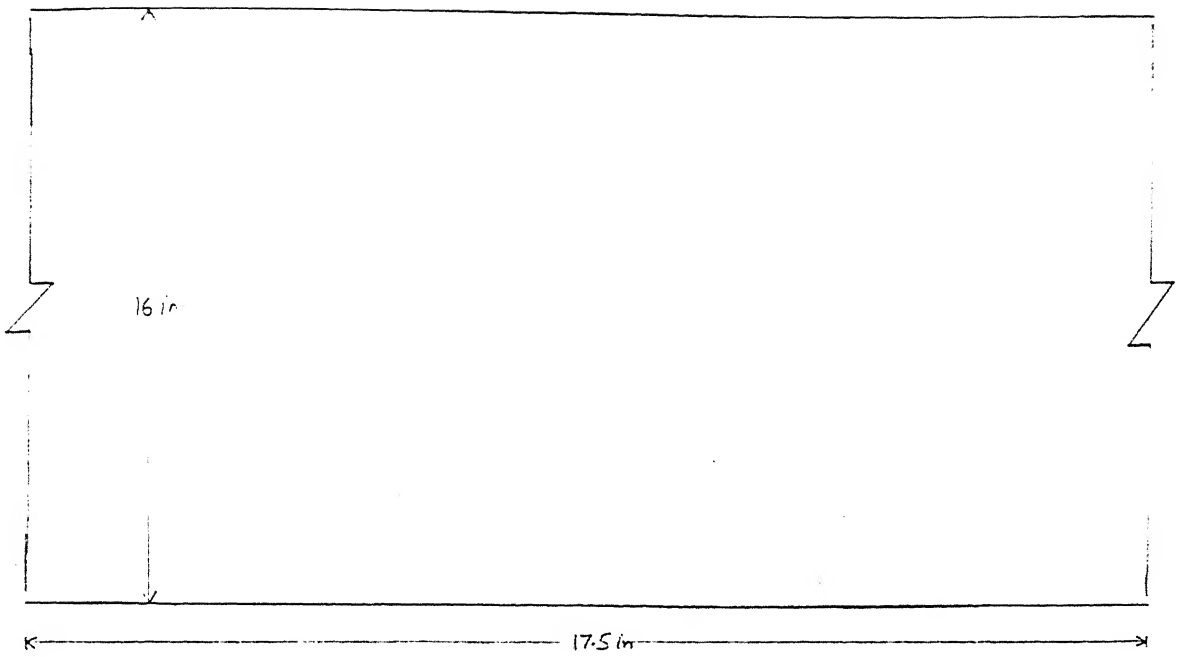

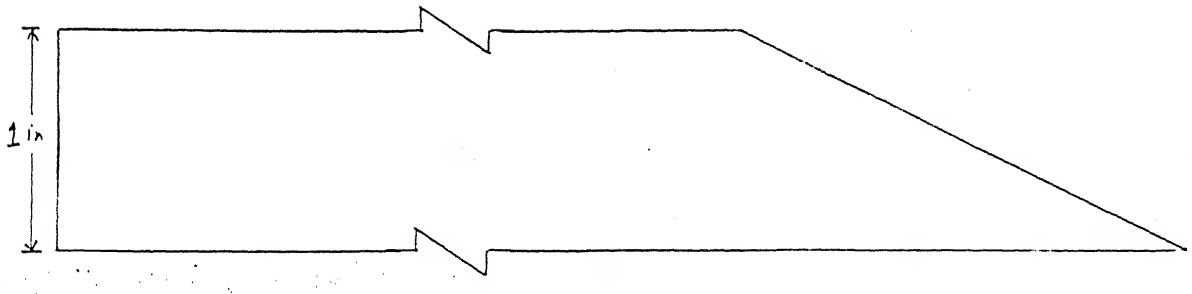

TRAILING - EDGE

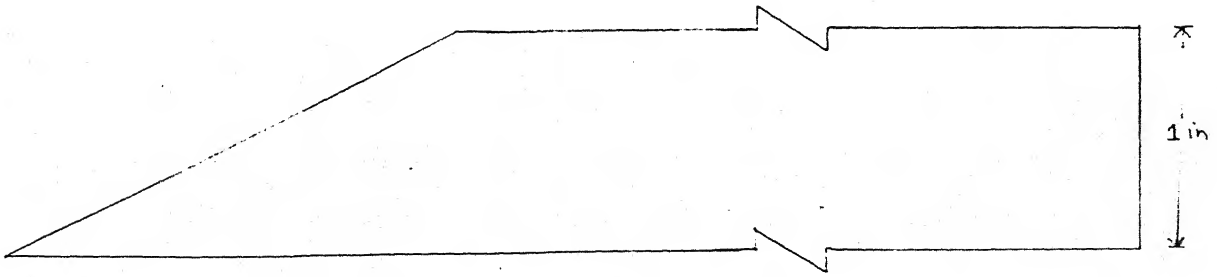

LEADING - EDGE

Fig 2.6 Details of plates forming the leading edge and trailing edge

Chapter 3

Results and Discussion

The objective of the present study was to carry out the pressure measurements around the circular cylinder placed near various carved-out boundaries, successively, also along the boundary, with and without the helical strake. These observations when compared with those made by Bearman for flow near a plane boundary and the flat plate studies made in the present investigations, also when compared along themselves,gives an estimation of variations of the pressure distributions with the initiation and propagation of the scour, represented by three different curvatures carved-out on flat plate viz. plane boundaries and the effect of strake on the pressure distribution on the cylinder, along the bed and on vortex shedding.

The present study deals with thin boundary layer i.e. boundary layers thinner that th e diameter of the cylinder. Assuming the Prandtl's distribution for velocity, the thi ckness of boundary layers midway through the plate , where the cylinder is located, a re less than 7.47mm which corresponds to velocity of 3m/s.

The experiments were conducted at three Reynolds numbers based on the cylinder diameter: Re $= 9.0 \times 10^4$ to 1.5×10^4. This is within the range where the drag coefficient and strouhal number of a circular cylinder are relatively independent of the Reynolds number.

The flow around a cylinder near to a wall has been considered to be analogous to the flow around two cylinders in side-by-side arrangement for values of G/D above about 0.5, the two flows were found to be similar by Bearman.

It is expected that the flow around a cylinder near a wall will depend on the Rey nolds number based on the cylinder diameter, the gap-ratio and the characteristi c of the wall boundary layer.

The present study deals with thin boundary layer i.e. boundary layers thinner th at the diameter of the cylinder. Assuming the Prandtl's distribution for velocit y, the thickness of boundary layers midway through the plate , where the cylinde r is located, are less than 7.47mm which corresponds to velocity of 3m/s.

The flow around a cylinder near to a wall has been considered to be analogous t o the flow around two cylinders in side-by-side arrangement for values of G/D ab ove about 0.5, the two flows were found to be similar by Bearman.

3.1 Pressure Distributions with Smooth Cylinder

Time averaged pressure distributions around the cylinder and along the plates are shown in figures 3.3 to 3.49. The readings are plotted on a magnified scale of 1:3, and the actual position of the boundary relative to the cylinder, shown corresponding to the scale. This is done so because we are actually interested in the nature of the pressure distribution curves and not on the actual values, this being a comparative study.

The pressures are presented non-dimensionally in the form of pressure coefficients C_p, defined earlier; the reference velocity and static pressure are taken as those above the cylinder mounting. The cylinder occupied some place but no attempt was made to apply the conventional blockage correction. The pressure coefficient C_p

has been plotted with the corresponding G/D and velocity, along with the pressure distribution for the plain cylinder, for easy comparison.

3.1.1 Pressure Distribution around the Cylinder

The pressure distributions were measured around the cylinder placed near a carved-out boundary by varying the gap-ratio, the velocity of the flow and the curvature radius itself. Gap-ratio is defined as the ratio of clearance between the bed and the cylinder held with the axis parallel to the bed and denoted with the symbol G to the diameter D, if there were no carving on the boundary. Hence the effective G/D for a carved-out boundary would be actual clearance between the cylinder and the lowest point of the curvature.

For G/D of 0.0, Bearman's observation shows two asymmetric pressure distributions around the cylinder. The cylinder lying on the plate, a discontinuity in the pressure was evident, at the point of contact, on both cylinder and the plate. Fig 3.3 reveals the effect of gap flow on the effect of pressure distribution due to introduction of the carving resulting in an effective G/D of 0.2 for velocity 3m/s. There is a rapid fall of pressure under the cylinder. Similar characteristics were observed for flow velocities of 4m/s and 5m/s (figs. 3.4 and 3.5) except the pressure is more in the front part of the cylinder at low speed of 3m/s. The wake pressure was almost constant for all velocities. These characteristic to a greater extent, resembles Bearman's observations for a plane boundary. In the wake region the pressure remains almost constant on the cylinder.

For the same curvature of 0.7D from the cylinder centre, as G/D is increased to 0.5 and hence an effective gap ratio of 0.7 (figures 3.6, 3.7, 3.8). The minimum pressure is generally found at a point upstream of the bottom point of the cylinder, which is different from the Bearman's observation that minimum pressure point is at the lowest point of the cylinder. With the increase in velocity the wake pressure

decreases further.

With further increase in the G/D to 1.0 And effective gap-ratio of 1.2. (figures 3.9, 3.10, 3.11), the flow around the cylinder remains almost similar to the one without plane surface near it, with boundary disturbances confining to a smaller portion. The pressure distribution becomes almost symmetric about the front stagnation point and resembles with Bearman's observation. In this case there is very little decrease in wake pressure with increase in velocity.

A change in boundary curvature to 0.9D, from the centre of the cylinder, for G/D= 0.0 or effective gap-ratio of 0.4, the figure shows a distinct change in the pressure distribution around the cylinder with increased degree of scour (figures 3.12, 3.13, 3.14). On comparing these with figures (3.3, 3.4, 3.5) shows that the fall in pressure below the cylinder has become less pronounced as there is more area for the flow beneath the cylinder. Velocity has little influence on the pressure distribution in the wake region, but in the front region the pressure has increased indicating that there is increase in drag and may be in the amplitude of oscillation.

An increase in the G/D to 0.5 i.e. effective G/D of 0.9, from figures (3.15, 3.16, 3.17) and comparing these with pressure distribution for G/D= 0.5 and curvature radius of 0.7D and effective gap-ratio of 0.7 (figures 3.6, 3.7, 3.8), we find that the distributions are almost similar except that pressure is slightly less than the pressure in case of plane bed.

For the G/D of 1.0 and the curvature radius of 0.9D, effective gap-ratio of 1.4, the flow around the cylinder is not influenced by the presence of the boundary (figures 3.18, 3.19, 3.20), and the pressure distribution assumes the smooth symmetric shape around the front stagnation point. The change of velocity has no influence on the pressure distribution.

With the boundary curvature being further increased to 1.2D, for G/D of 0.0 the distribution becomes more symmetric than with curvatures of 0.7D and 0.9D, and

the pressure peak becoming less pronounced, as observed by Bearman[1] , Summer B.M. and Fredsoe, J.[17]. For G/D of 0.5 and 1.0 the pressure distribution takes the smooth unobstructed form with the boundary presenting the least influence on the flow past the cylinder. The effect of velocity is that the pressure has decreased more than for curvatures of 0.7D and 0.9D.

3.1.2 Pressure Distribution along the Carved-out Boundaries

Here we see larger pressure in the upstream direction and lower pressure in the downstream direction of the cylinder. The primary objective of the study is to measure the pressure distribution along a carved-out boundary placed near a circular cylinder, and then compare the results with that for a plane (uncurved) boundary obtained in the study under similar conditions and those presented by Bearman et al. (1978)[1] for multitudinous gap-ratios (G/D), and also to compare the various results among themselves.

Figures 3.3 to 3.29 shows the pressure distributions along the carved-out boundaries having different radii of curvatures for three different gap-ratios at three flow velocities.

The pressure distribution along the boundary with curvature of 0.7D from the centre of the cylinder and G/D of 0.0 i.e. the effective G/D of 0.2 are presented in figures (3.3, 3.4, 3.5). With in the span of the pressure tappings on the plate, 2D upstream and downstream of the cylinder axis.

In comparison with Bearman's observations where at point of contact a discontinuity in pressure is evident on the plate figures 3.3 to 3.29 reveal; the effect of the gap flow on pressure distribution along the plate. There is a rapid fall in the pressure under the cylinder in the region of lowest point. However in our observation, in most cases the rapid fall in the pressure is after the downstream

end region of the curvature. In some cases we see the fall in pressure earlier than the upstream end of the curvature (fig. 3.3). In most cases we see that first pressure decreases slightly upstream of the cylinder, than increases below the cylinder and again decreases rapidly downstream of the cylinder. This decrease in pressure may be attributed to the vortices present in the upstream and downstream region, the rapid decrease in the downstream region indicates that the vortices present are of larger strength and are responsible for the erosion of the bed in the downstream region. This also supports the formation of secondary scour downstream fo the cylinder, as observation by Summer, B.M. and Fredsoe, J. [17].

On comparing the figures for a particular carved-out radius of 0.7D, we see that minimum value of pressure coefficient occurs at the G/D of 0.5 at a point after the downstream end of curvature i.e. effective G/D of 0.7, and maximum C_p occuring for G/D of 0.0. At G/D = 1.0 the value of minimum C_p increases. Similar trend is observed for the curvature of 0.9D, where minimum C_p is observed at an effective G/D of 0.9. For the curvature of 1.2D there was no such sharp peak for minimum pressure. The minimum peak at the end of curvature shows that the surface does not have a smooth gradient and there is an optimum curvature for which the C_p is minimum. As earlier seen the peak must lie around gap-ratio of 0.7 and 0.9. The minimum C_p is observed for higher speed of 5m/s.

3.2 Pressure Distribution with Straked Cylinder

The helical strake introduces the three dimensionality in the mean flow field of the circular cylinder. The vortex shedding and associated oscillations are related to the fluctuating flow field.

The effect of the helical strake on the pressure distribution can be studied by dividing the location of the strake at the centre of the cylinder in free stream flow,

in three regions as follows:

1. Forward region for $\alpha_{hs} = 0^o$ to $\pm 20^o$
2. Midriff region for $\alpha_{hs} = \pm 20^o$ to $\pm 85^o$
3. Rear region for $\alpha_{hs} = \pm 85^o$ to $\pm 180^o$

for definition of α_{hs}, refer Fig 3.1.

In the forward Region the radial pressure distribution at the centre of the cylinder shows no local peaks at or near the location of the strake. The pressure in this case is higher in midriff and rear region than the pressure values for a clean cylinder. The pressure distribution is almost the same as that for a clean cylinder.

When the strake is in midriff region the pressure peaks are observed near the location of the strake and also at other points in the rear region the pressure is higher. The pressure distribution in the forward region remains unchanged. These peaks introduces strong assymetry in the flow field as the upper and lower surface show two different preesures. The pressure just downstream the strake is much less than normal pressure. This happens due to separation over the sharp surface of the strake and also upstream of the strake, the region of the positive pressure increases because of the blockage of the flow.

In rear region also the effect of strake is less. Here also we don't see any pressure peak near the strake. In the midriff and rear region the pressure is slightly higher than the corresponding pressure at clean cylinder.

3.2.1 Pressure Distribution around the straked cylinder

For the straked cylinder the experiments were conducted for two velocities of 3m/s an d 5m/s. For the measurements around the cylinder the experiments were conducted for t hree gap-ratios and for the measurements along the bed the study was

conducted for on ly one speed of 5m/s and for two gap-ratios of 0.0 and 0.5.The results were plotted a nd compared from the corresponding values for the smooth cylinder. The effect of the strake on the presure distribution on the cylinder is as folllows:

For plane bed and gap-ratio of 0.12 i.e. strake touching the bed, the results were compared with the flow around a smooth cylinder for G/D of 0.2 (fig.3.30). We see that there is an increase in pressure in the front region, with the increase in velocity the wake pressure decreases. When the gap-ratio is increased to 0.5, the pressure distribution in the wake region is slightly more than that for a smooth cylinder (fig. 3.31), for velocity of 5m/s the C_p increases in the wake region and also under the cylinder. For G/D =1.0, the distribution is almost similar to that of a smooth cylinder except a gain in pressure after the strake for strake angles of $55^o, 40^o, 25^o$ and 10^o (fig. 3.32).

When the curvature radius is 0.7D, when the gap-ratio is 0.0 there is a decrease in pressure in the region under the cylinder for all strake angles α_{hs} for which experiments were performed. However the pressure is slightly more in the wake region (fig. 3.33). In the case with velocity 5m/s the pressure under the cylinder is less and as well as in the wake region.For increased gap of 0.5D the wake pressure is slightly less then that for the smooth cylinder, in this case there is a gain in pressure after the strake for α_{hs} of 55^o, 40^o, 25^o and 10^o (fig. 3.34), but for velocity of 5m/s the pressure in the wake region is more and also under the cylinder. When the gap-ratio is increased to 1.0 we see a significant increase in pressure after the strake for all angles and the wake pressure is slightly less than that for the smooth cylinder (fig. 3.35).

Experiments with curvature radius of 0.9D shows that at 0.0 gap-ratio there is an increase in pressure below the cylinder and decrease in pressure near the front stagnation point region (fig. 3.36). In the wake region the wake pressure is slightly

higher then the smooth cylinder as observed in case of curvature radius of 0.7D. When the speed is increased the pressure under the cylinder increases and also after the strake for $\alpha_h s$of $55^o and 25^o$.In this case on changing the strake angle $\alpha_h s$ we see that intially the pressure is higher for $70^o$and 55^o but it is lesser for other strake angles than that corresponding to the pressure for smooth cylinder. The increase of gap-ratio to 0.5 we see that the wake pressure is slightly lesser then that for smooth cylinder (fig. 3.37). The increase in velocity does not has any effect at G/D = 0.5.On changing the strake angle, there is an increase in the pressure after the strake and is lower for region of front lower region. For gap-ratio of 1.0 the wake pressure increases with strake and the pressure after the strake increases for all +ve values of strake angles (fig. 3.38).

For the curvature radius of 1.2D at G/D of 0.0 the pressure distribution is almost similar to that of smooth cylinder except for strake angles of55^o and 25^o the pressure after the strake has increased (fig. 3.39). Here as the flow area under the cylinder has increased the change in pressure distribution has not been found as observed for curvatures of 0.7D and 0.9D. For increased G/D of 0.5 the pressure decreases slightly in the wake region and the distribution is almost similar except after the strake for strake angles of $55^o, 25^o$ and 10^o for which there is an increase in pressure than that in case of a smooth cylinder (fig. 3.40).

3.2.2 Pressure Distribution along the Carved-out Boundaries

Pressure along the carved-out boundary was measured to know the effect of strake on the pressure along the bed. The pressure were measured at velocity of 5m/s and for two gap-ratios of 0.0 and 0.5.

For plane bed when the strake touches the bed i.e. the gap-ratio is 0.12, the results were compared with effective gap-ratio of 0.2 with smooth cylinder (fig.

3.42), we see that the pressure in the upstream region the pressure is more and in the downstream region the pressure is lower then that for smooth cylinder so the pressure drop is faster with the strake in the region below the cylinder i.e. development of scour is faster. As the strake angle is varied from 70^o to $-5^o$with steps of 15^o, the pressure changes slightly only in the region below the cylinder and remains unaffected in the end regions. When the gap-ratio is 0.5 the pressure in the upstream region is higehr and lower in the down stream region, but the pressure gradient is smaller then that for earlier case, so it seems that the area of scour gets widened in this case (fig. 3.43). On changing the strake angle $\alpha_h s$ the pressure decreases only a little in the region below the cylinder, for smaller angles the flow remains unaffected and in the end region it is almost constant.

When the curvature radius is 0.7D and G/D is 0.0 we see that now the C_p is slightly lower than that for a smooth cylinder except at the downstream end of the curvature, there is a minimum pressure peak (fig. 3.44). Under the bottom region of the cylinder the slope of pressure change is smoother then that for a smooth cylinder. When the strake angle is changed we see that now the C_p variation is significant in the in the upstream end region and slight change under the cylinder. This is because the more flow is to be directed towards upward direction by the strake as the gap in the bottom is less, this changes the flow significantly in the upstream region. Here when the gap-ratio is increased to 0.5 the pressure coefficient is generally higher then that of smooth cylinder thus there is an decrease in the velocity and hence lesser erosion. On changing the strake angle there is negligible change in pressure distribution (fig. 3.45).

For curvature radius of 0.9D and gap-ratio of 0.0, we see that C_p is slightly lower then that for smooth cylinder. When the strake angle is decreased there is slight decrease in pressure except at point just after the upstream end of curvature, where the variation is more (fig. 3.46). When the G/D is increased to 0.5, the pressure

is slightly more than in case of smooth cylinder. The change of strake angle has very little effect on pressure distribution, that is a little decrease in pressure with decrease in strake angle upto 10^o (fig. 3.47).

The experiments with curvature radius of 1.2D shows that pressure distribution is generally higher then that of smooth cylinder but in the downstream end we see almost no change in C_p value (fig. 3.48). The location of the strake with respect to the flow direction has little effect on the flow only in the region of the curvature, here we see no change in pressure in the upstream end as observed in case of smaller radius of curvature. For gap-ratio of 0.5, the C_p is slightly higher then the case of smooth cylinder and see almost no effect of the change of the strake angle, this is due the fact that there is little change in diversion of flow with the change of strake angle (fig. 3.49).

In the experiments we have assumed that the scour developed under the cylinder i s perfactly cylindrical in shape and it is directly under the cylinder with its axis coinciding with that of the cylinder.In our experiments we have not used an y correction for the blockage, which is about 8-section. We have not also observed the effect of increasing boundary layer on t he distribution.

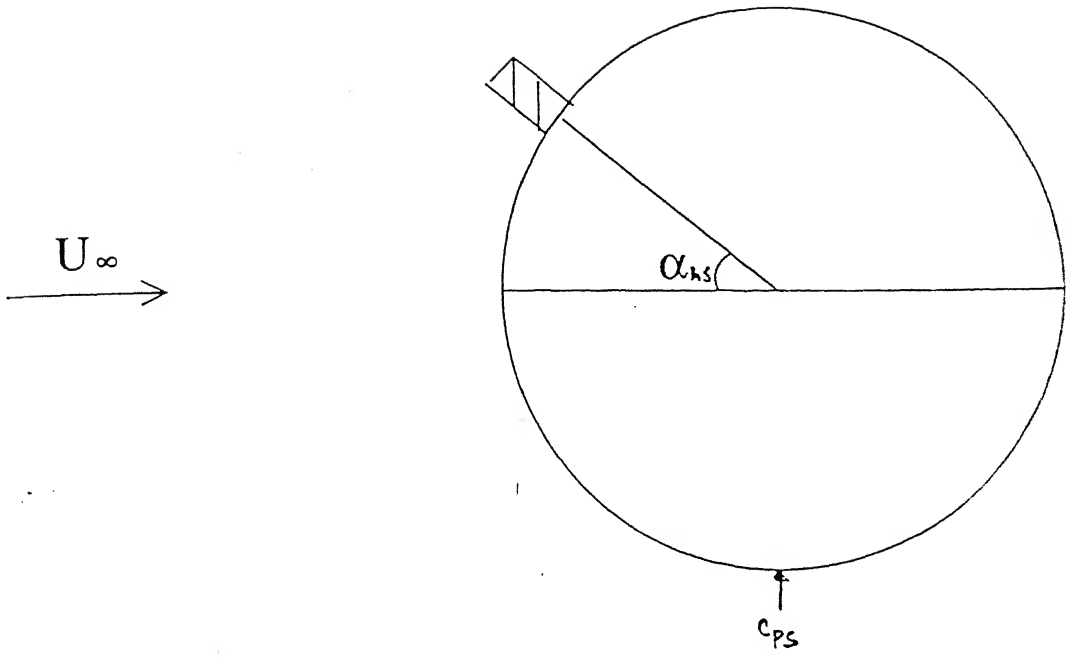

Fig.3.1 Figure showing strake location at Mid-span w.r.t. Flow direction

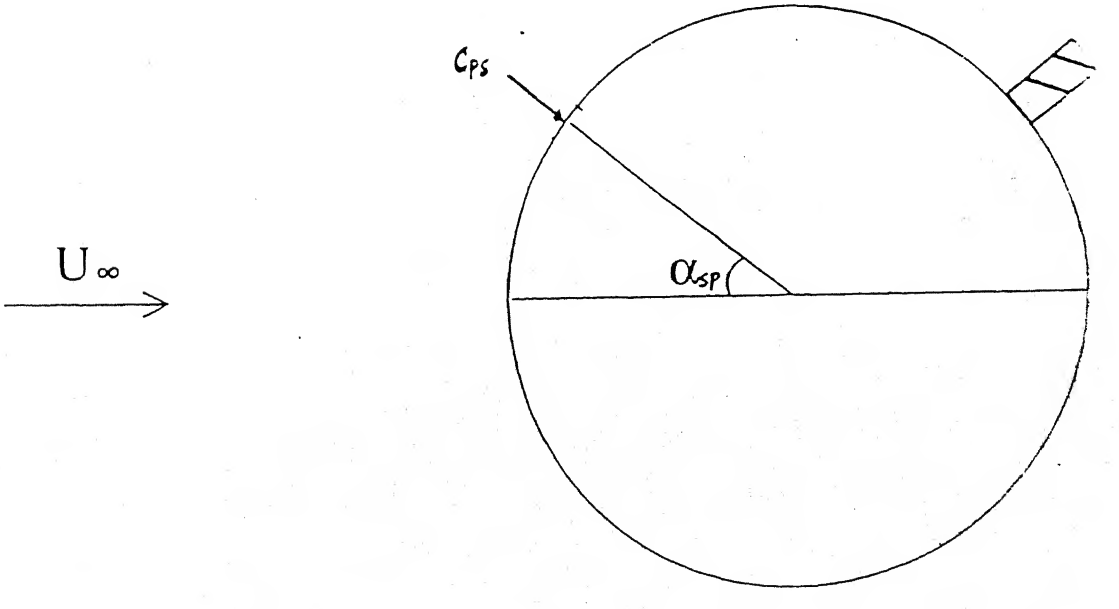

Fig.3.2 Figure showing location of radial station

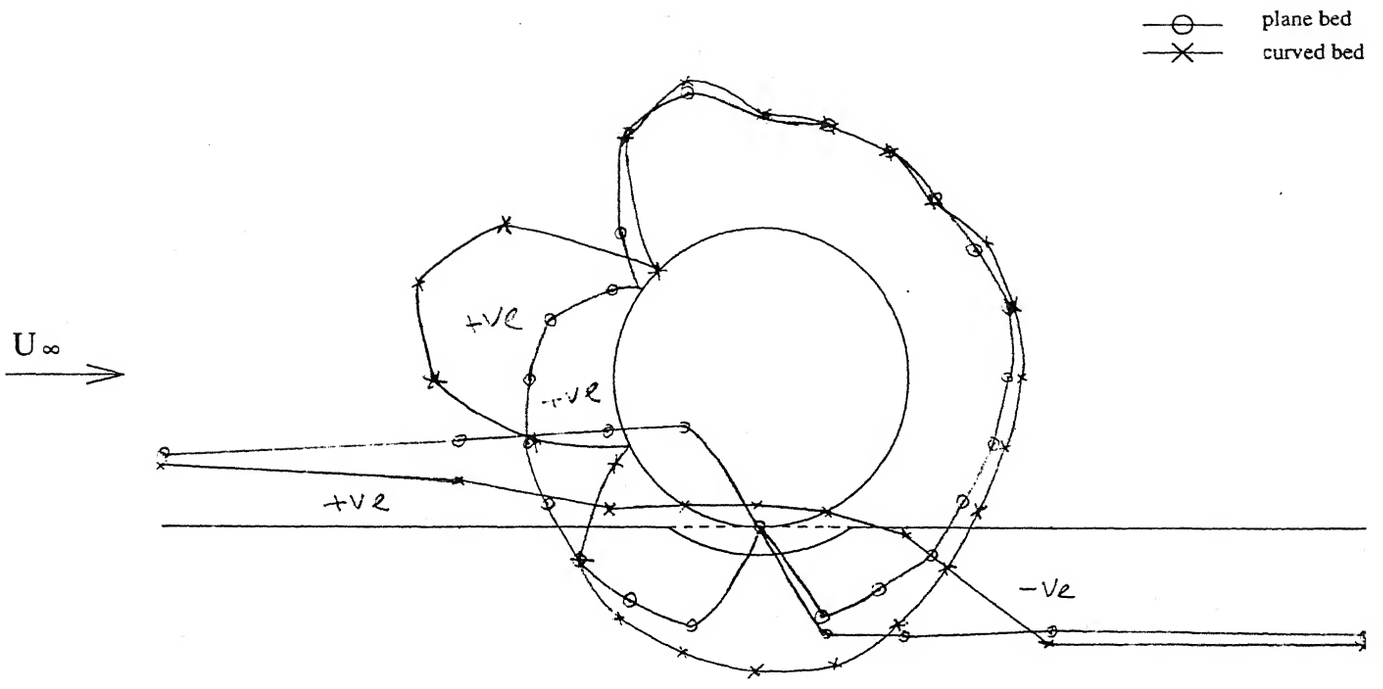

Fig.3.3 Pressure distribution around the cylinder and along the carved-out bed for curvature radius 0.7D; G/D=0.0, at velocity 3 m/s

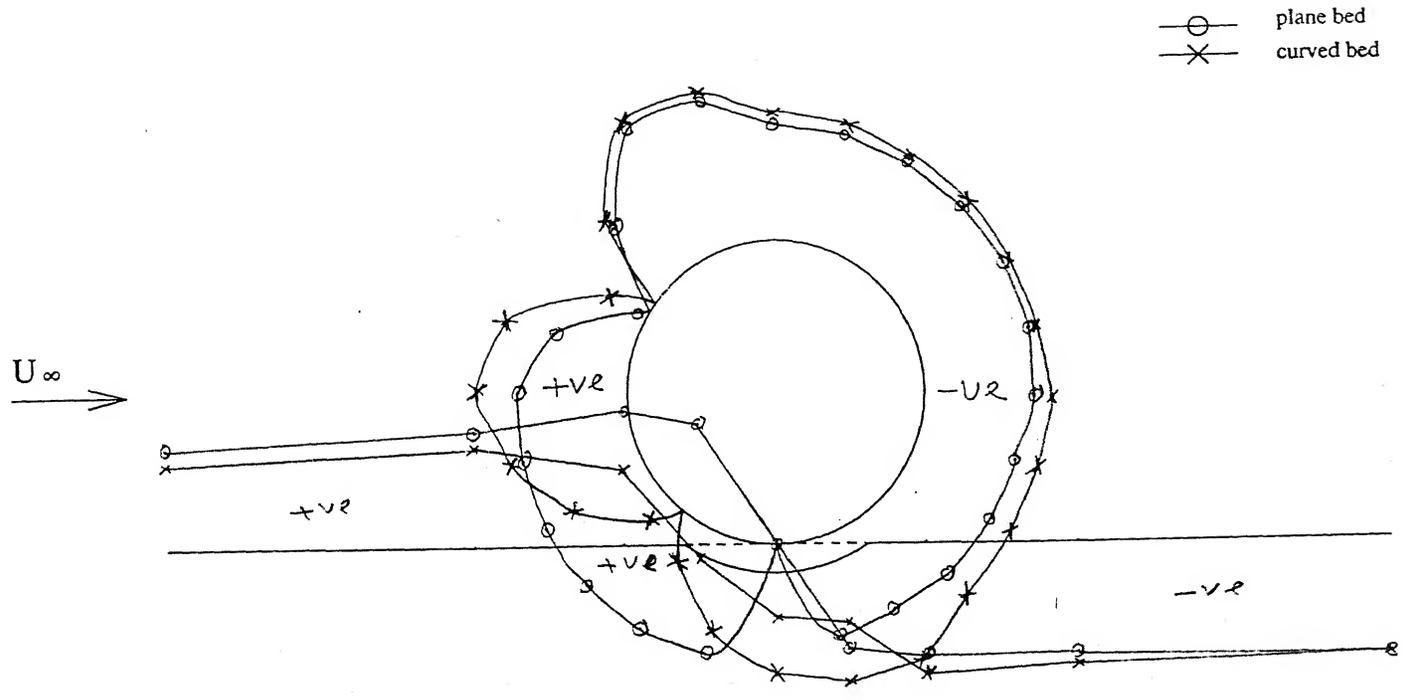

Fig.3.4 Pressure distribution around the cylinder and along the carved-out bed for curvature radius 0.7D, G/D=0.0, at velocity 4m/s

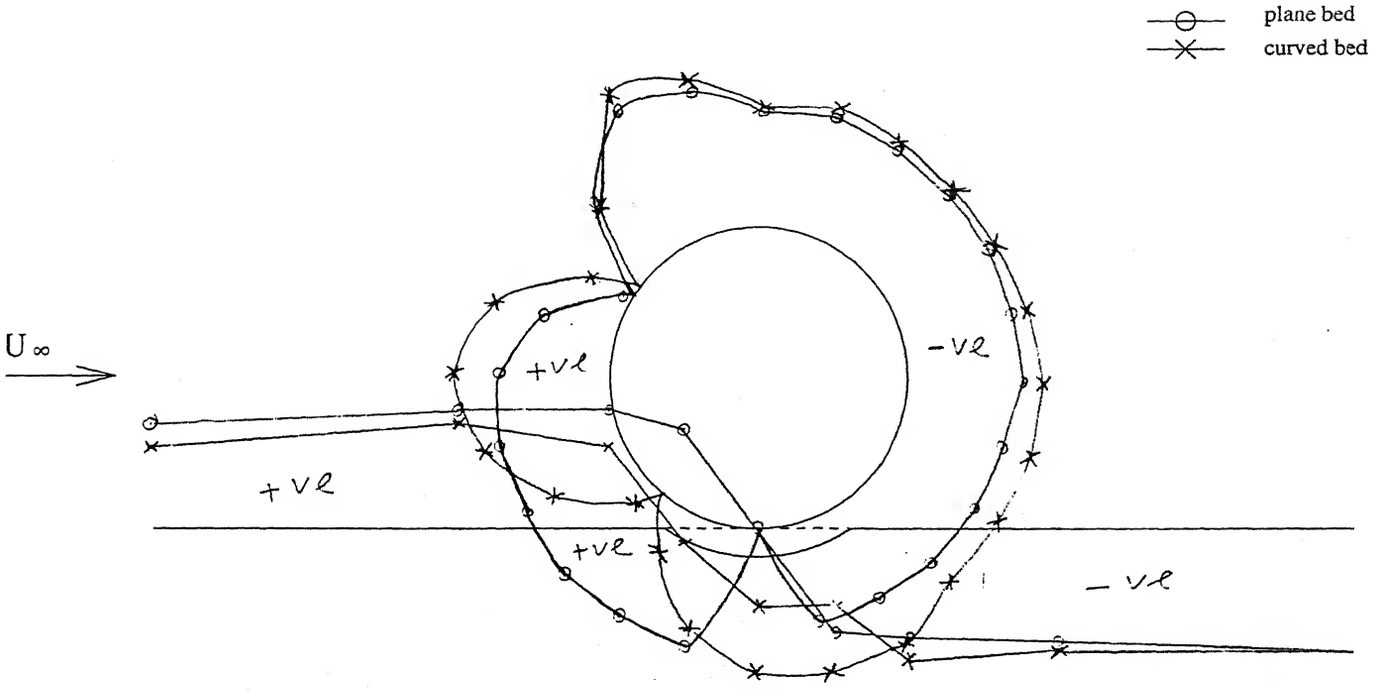

Fig.3.5 Pressure distribution around the cylinder and along the carved-out bed for curvature radius 0.7D, G/D=0.0, at velocity 5m/s

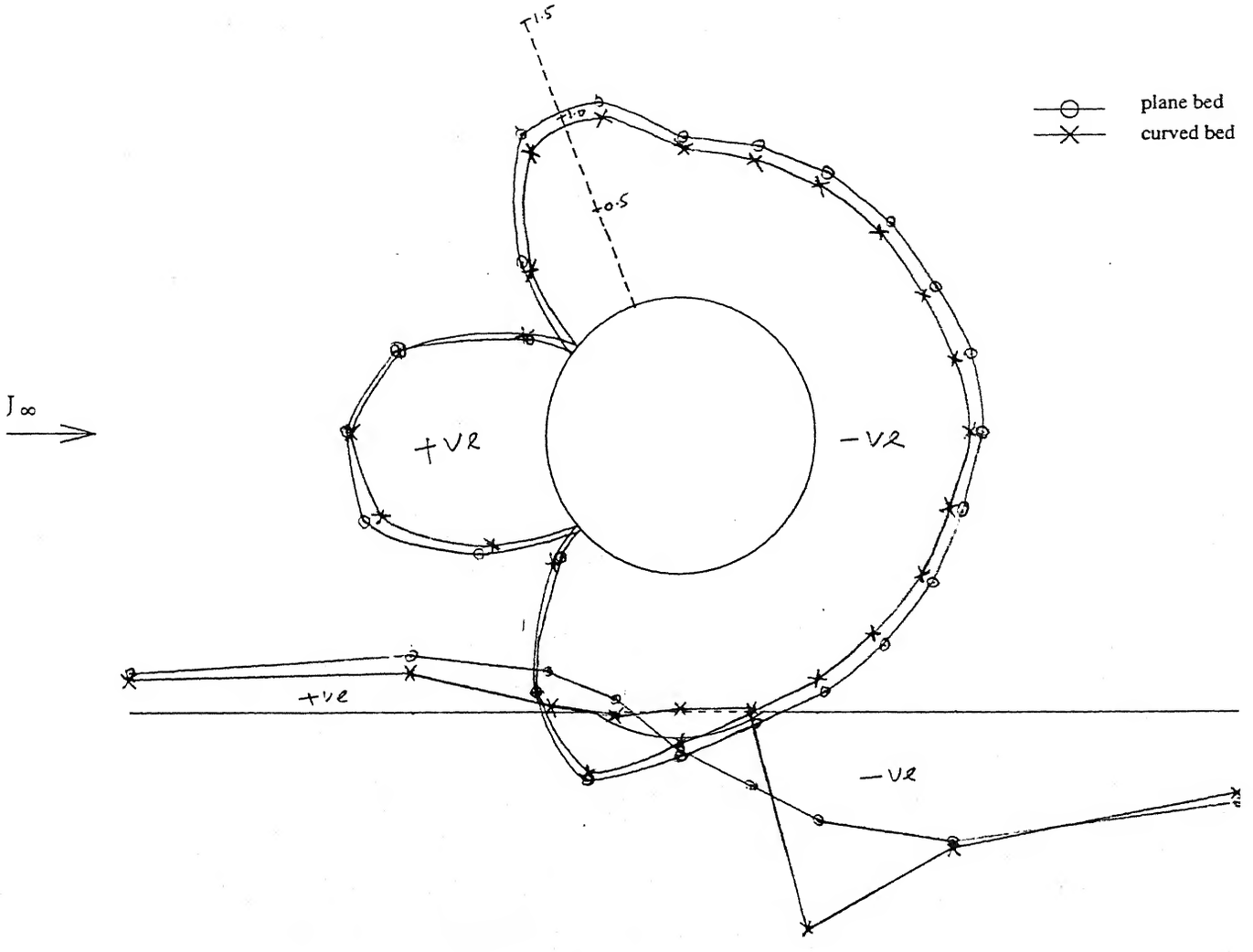

Fig.3.6 Pressure distribution around the cylinder and along the carved-out bed for curvature radius 0.7D, G/D=0.5, at velocity 3m/s

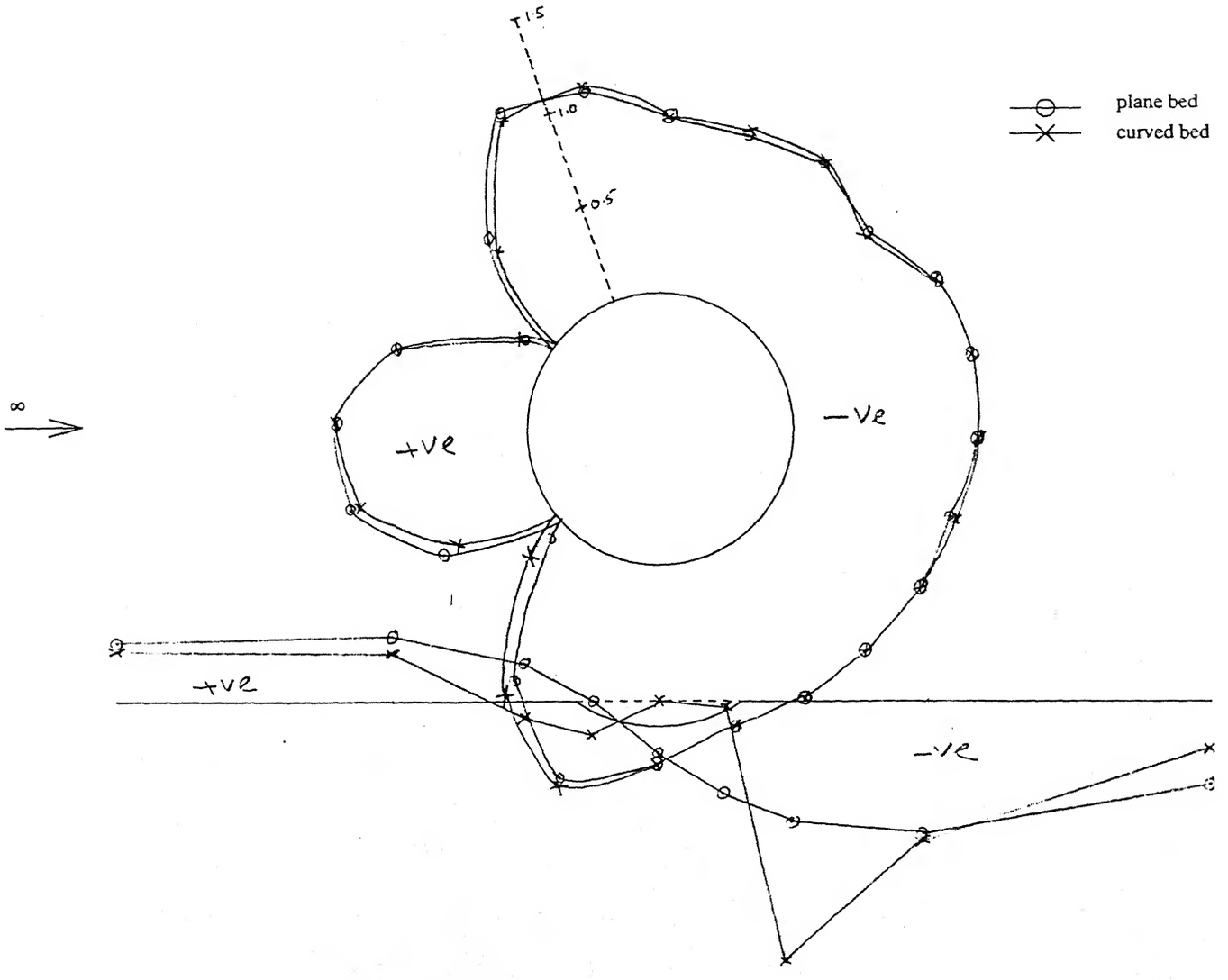

Fig.3.7 Pressure distribution around the cylinder and along the carved-out bed for curvature radius 0.7D, G/D=0.5, at velocity 4m/s

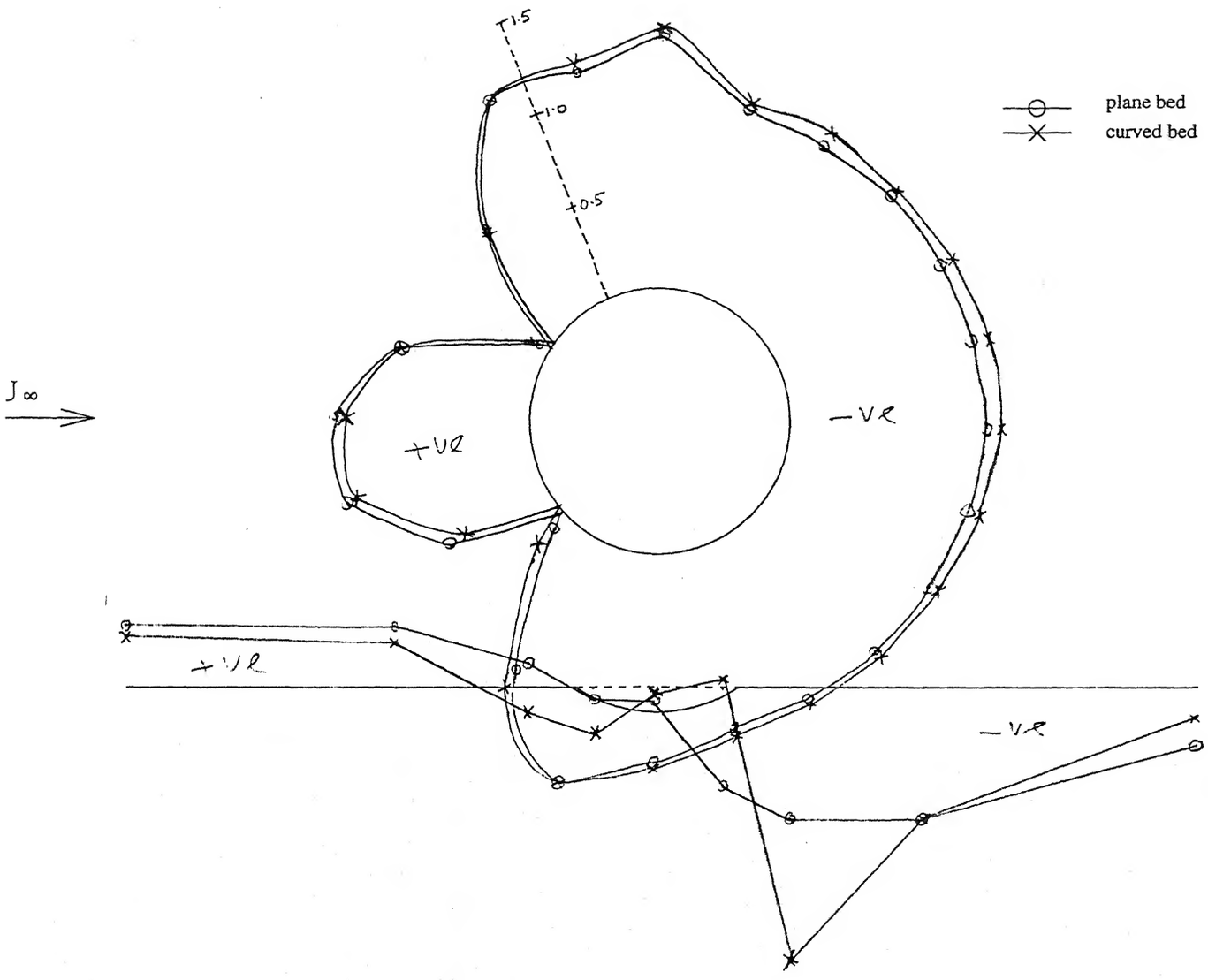

Fig.3.8 Pressure distribution around the cylinder and along the carved-out bed for curvature radius 0.7D, G/D=0.5, at velocity 5m/s

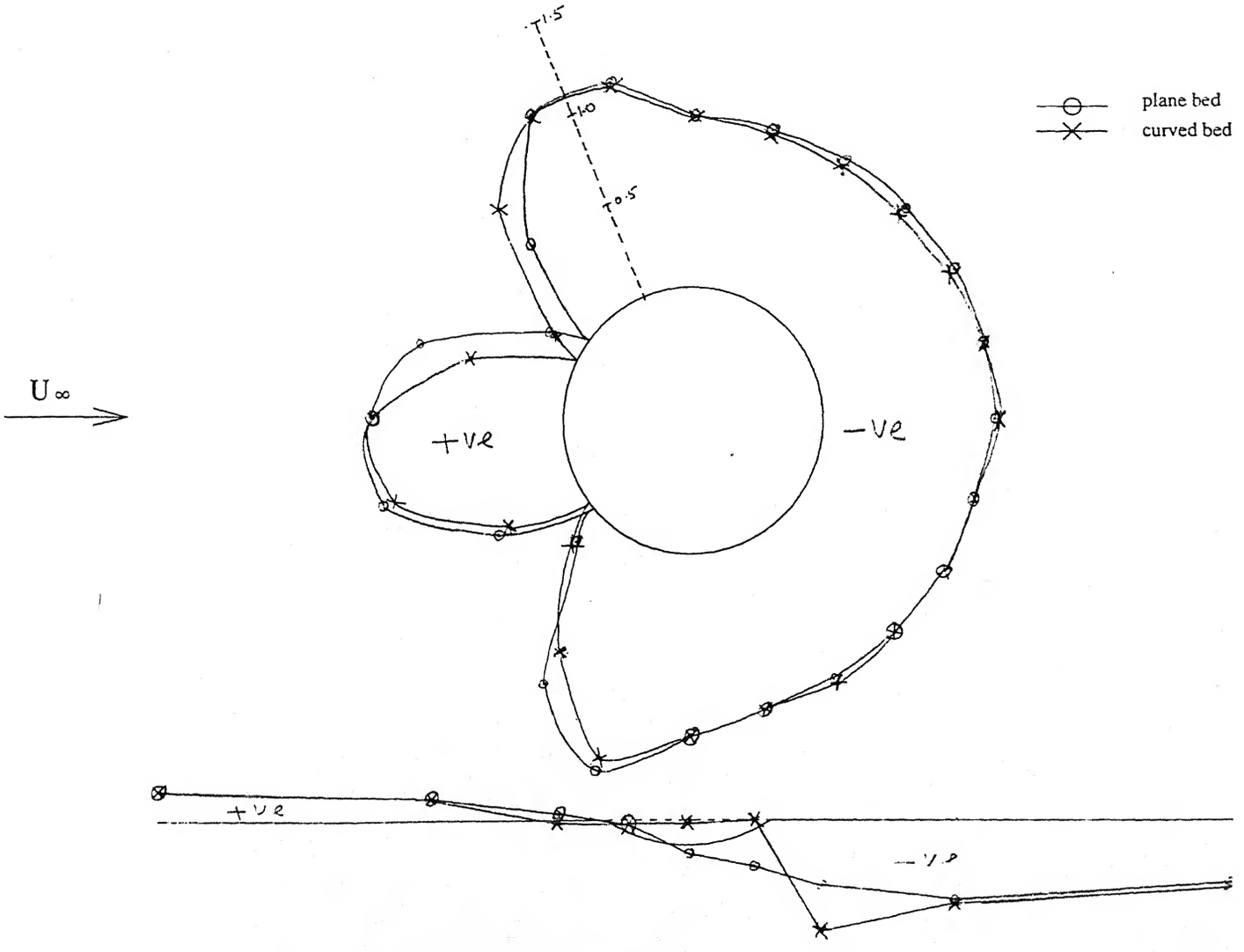

Fig.3.9 Pressure distribution around the cylinder and along the carved-out bed for curvature radius 0.7D, G/D=1.0, at velocity 3m/s

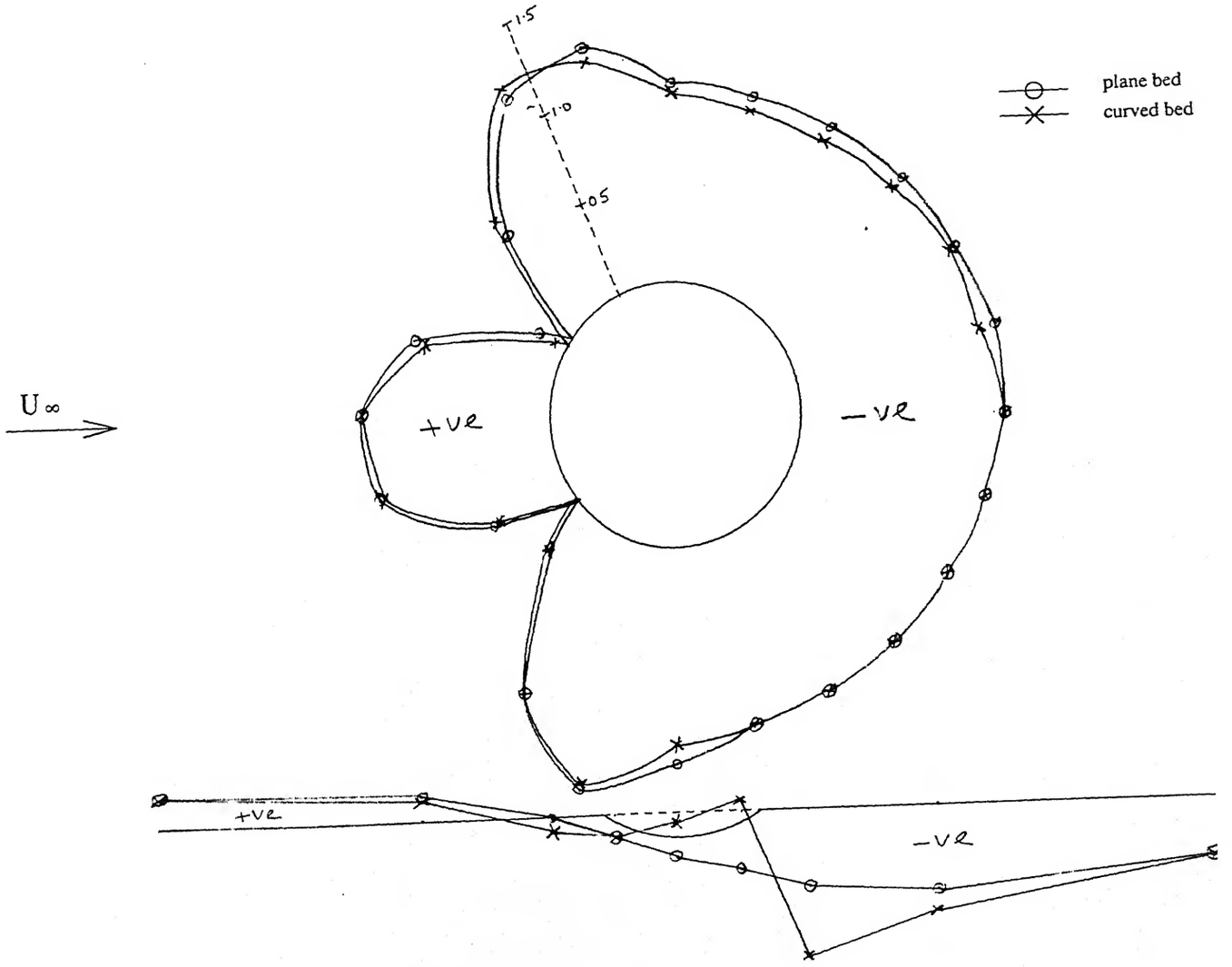

Fig.3.10 Pressure distribution around the cylinder and along the carved-out bed for curvature radius 0.7D, G/D=1.0, at velocity 4m/s

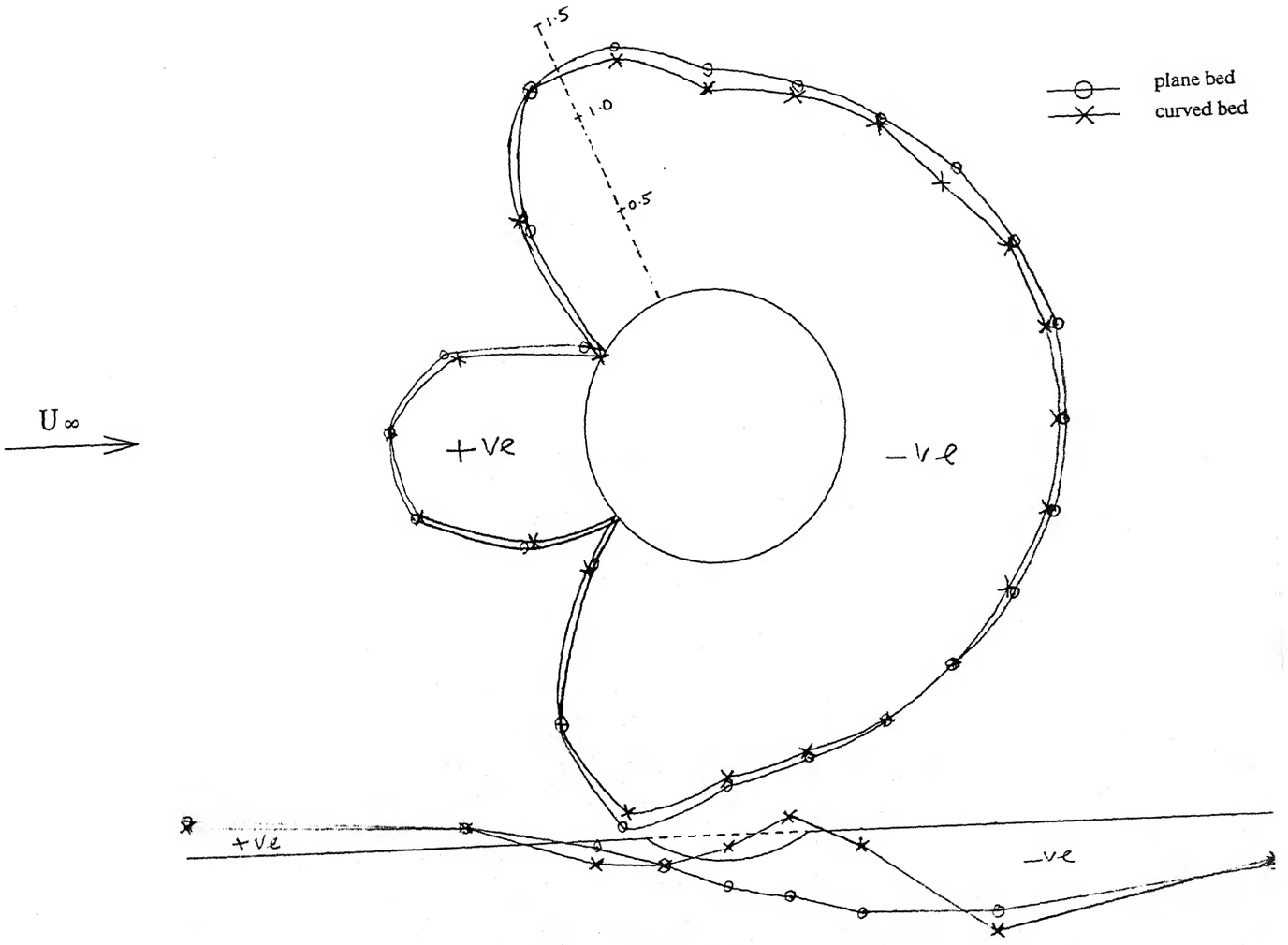

Fig.3.11 Pressure distribution around the cylinder and along the carved-out bed for curvature radius 0.7D, G/D=1.0, at velocity 5m/s

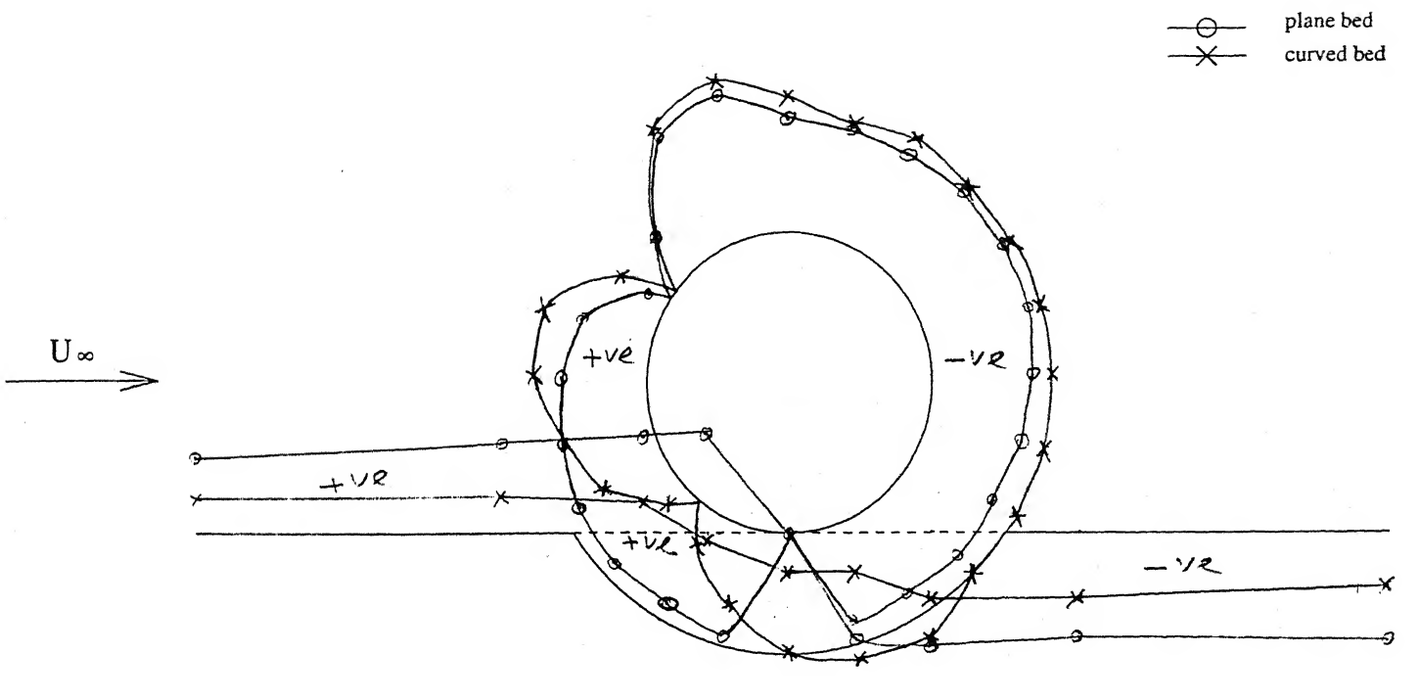

Fig.3.12 Pressure distribution around the cylinder and along the carved-out bed for curvature radius 0.9D, G/D=0.0, at velocity 3m/s

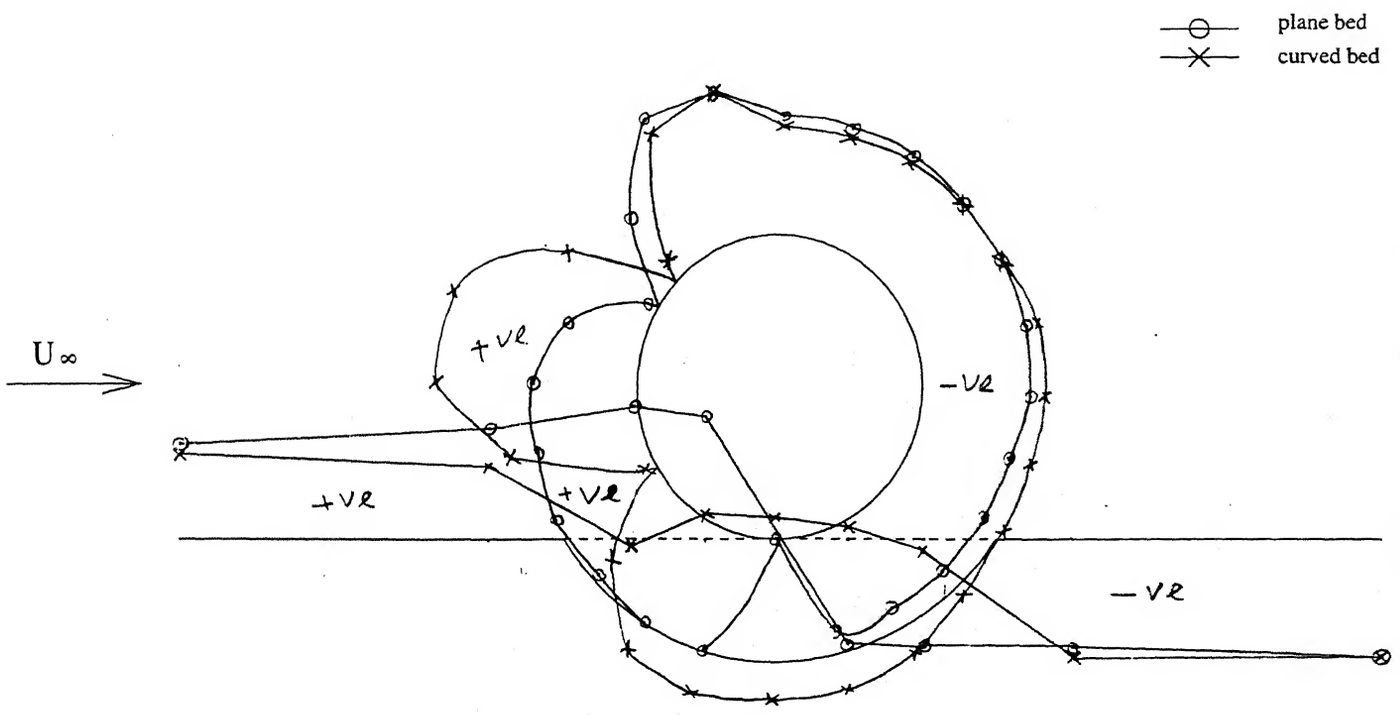

Fig.3.13 Pressure distribution around the cylinder and along the carved-out bed for curvature radius 0.9D, G/D=0.0, at velocity 4m/s

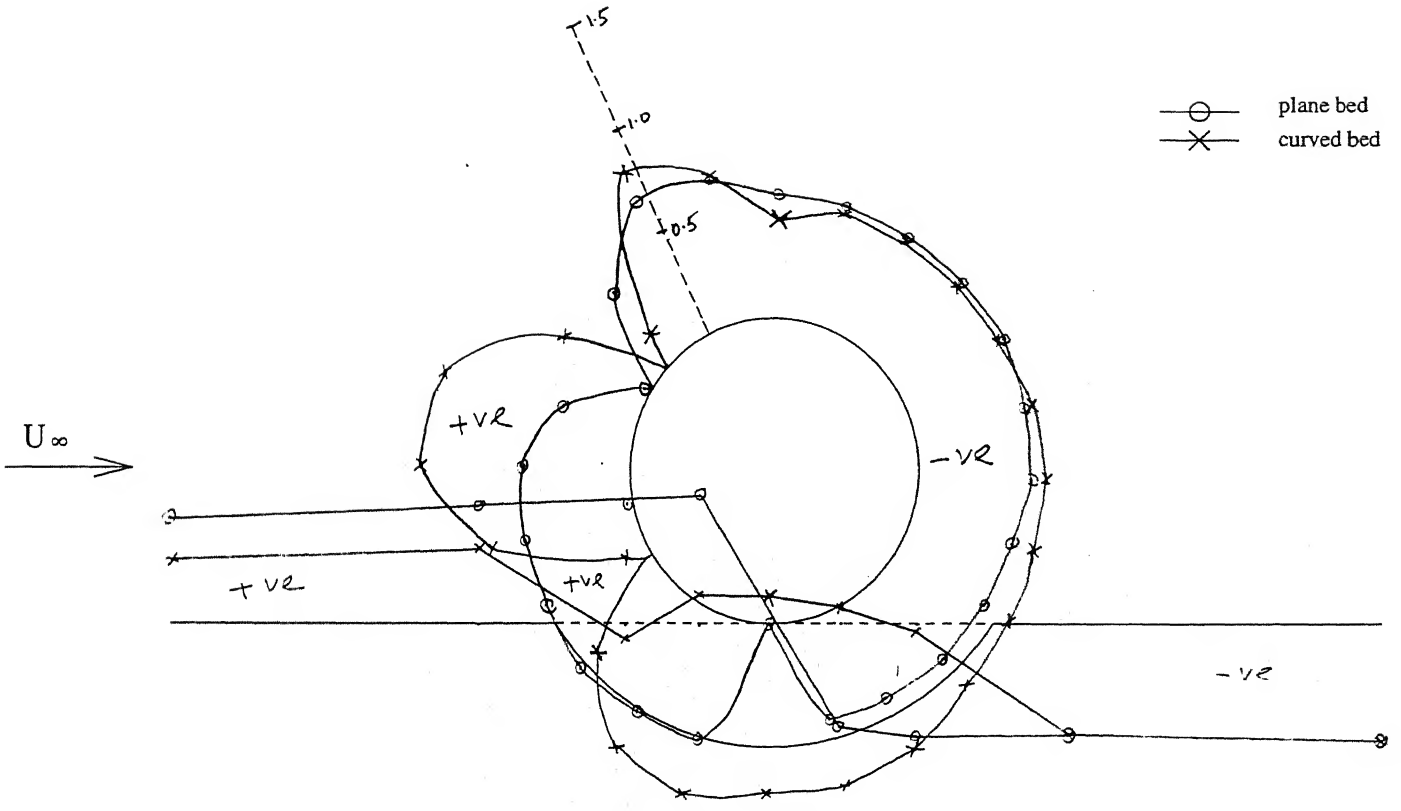

Fig.3.14 Pressure distribution around the cylinder and along the carved-out bed for curvature radius 0.9D, G/D=0.0, at velocity 5m/s

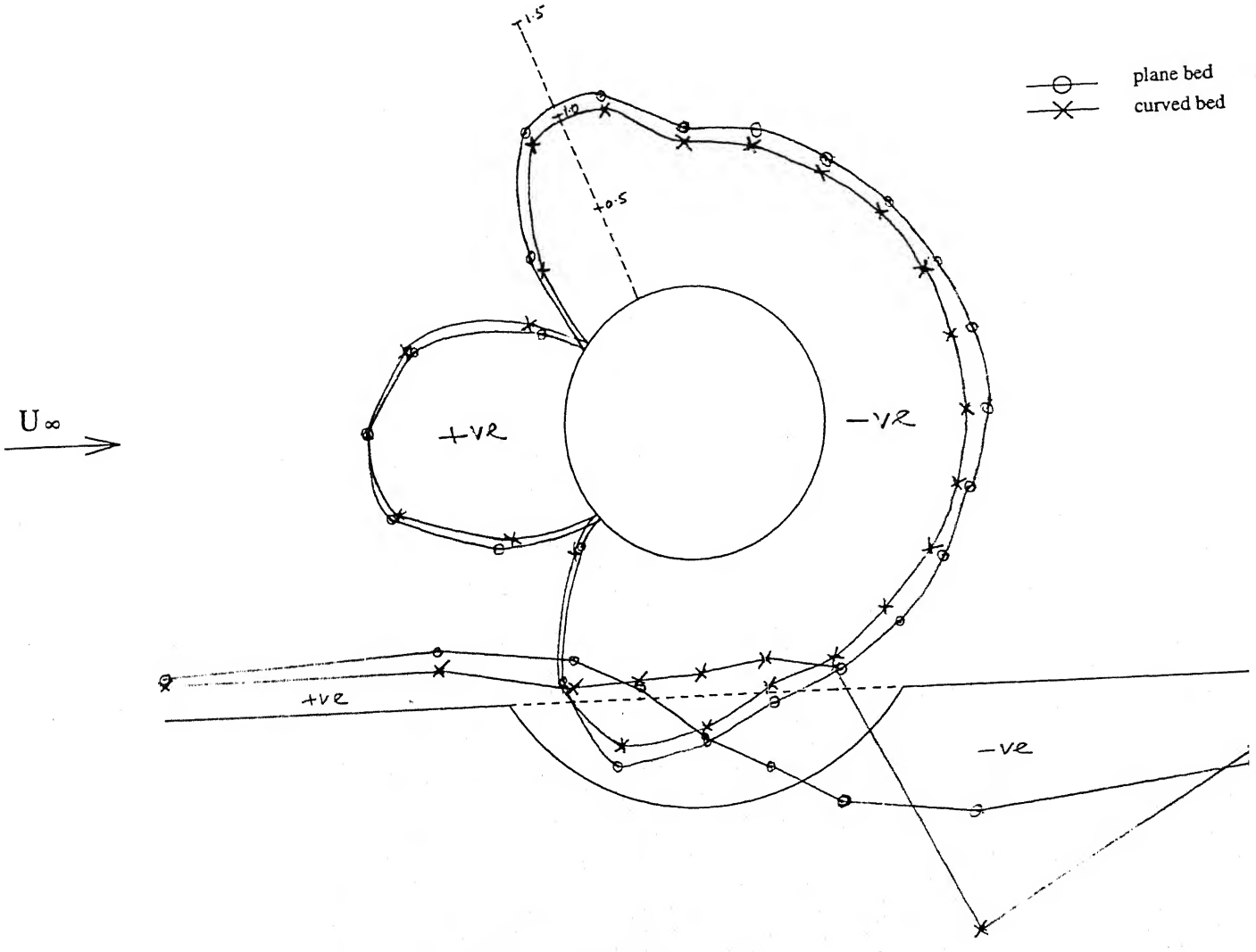

Fig.3.15 Pressure distribution around the cylinder and along the carved-out bed for curvature radius 0.9D, G/D=0.5, at velocity 3m/s

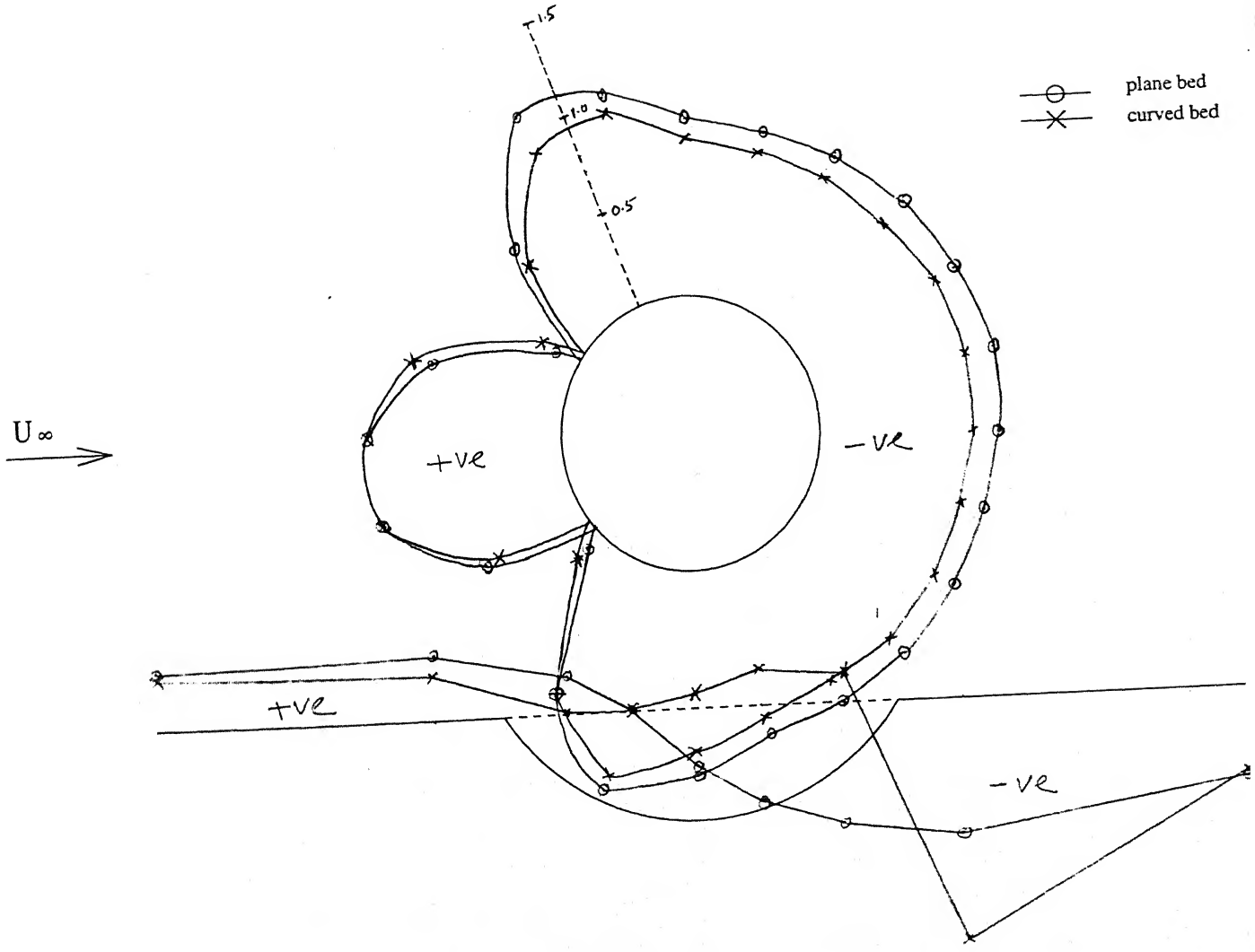

Fig.3.16 Pressure distribution around the cylinder and along the carved-out bed for curvature radius 0.9D, G/D=0.5, at velocity 4m/s

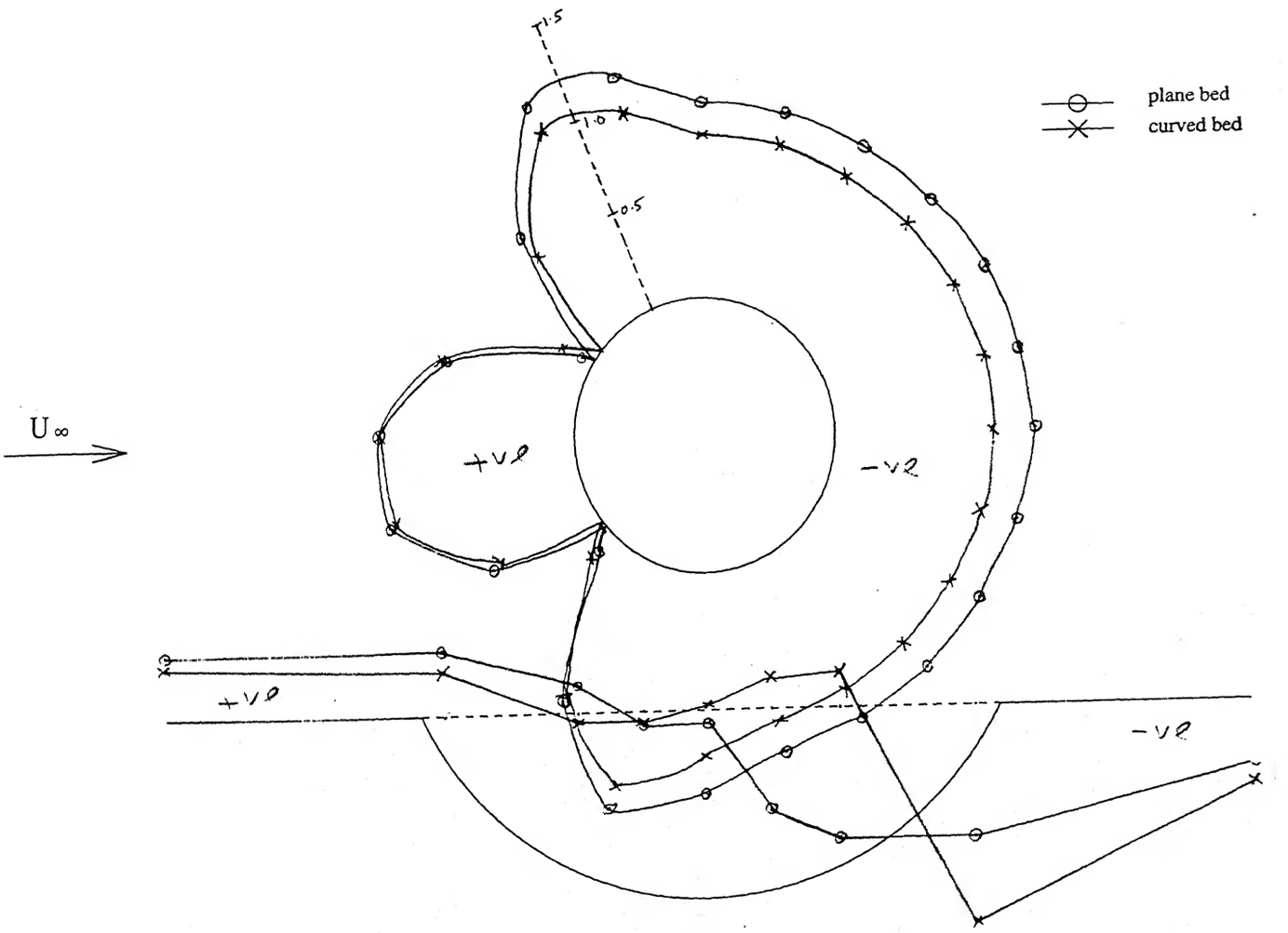

Fig.3.17 Pressure distribution around the cylinder and along the carved-out bed for curvature radius 0.9D, G/D=0.5, at velocity 5m/s

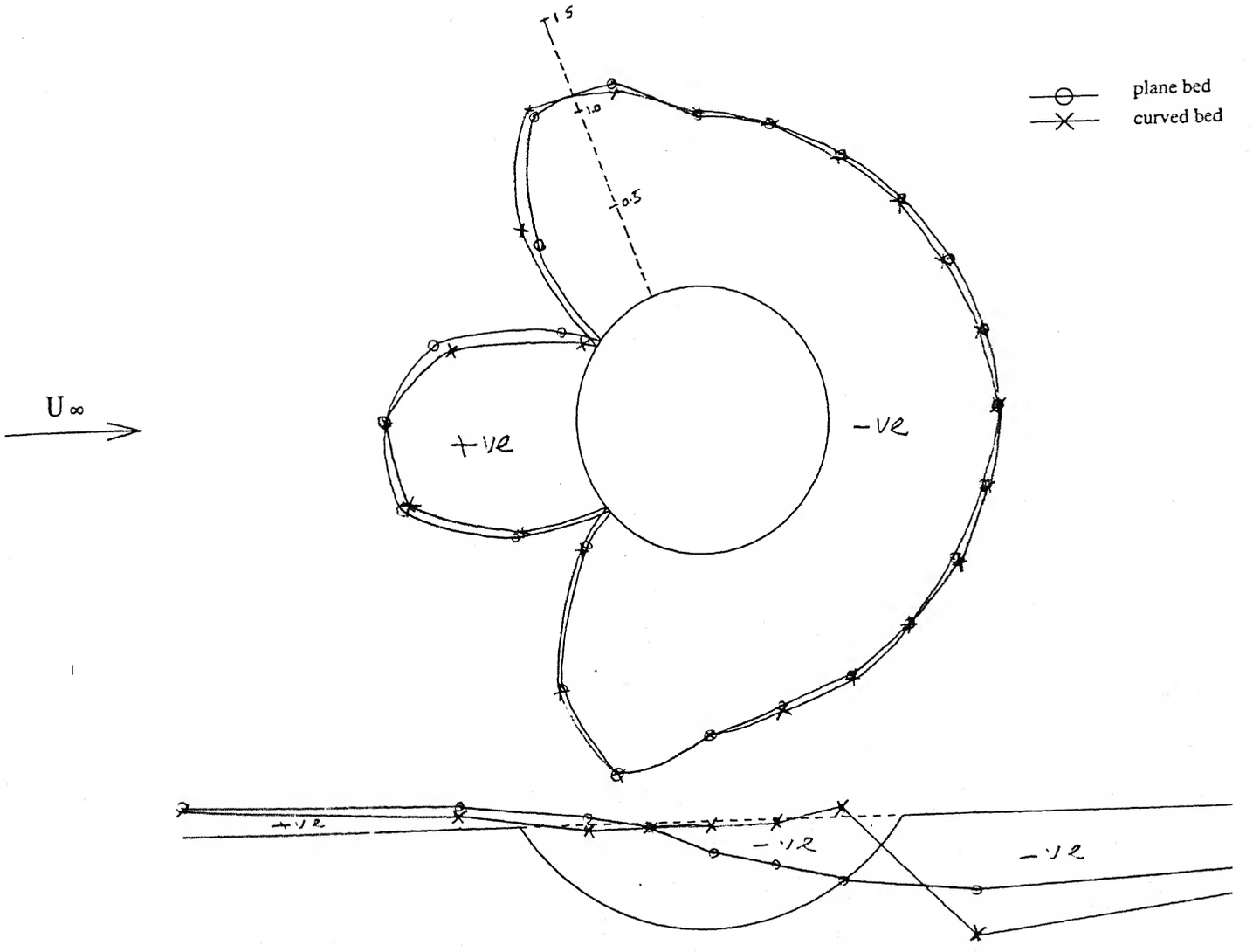

Fig.3.18 Pressure distribution around the cylinder and along the carved-out bed for curvature radius 0.9D, G/D=1.0, at velocity 3m/s

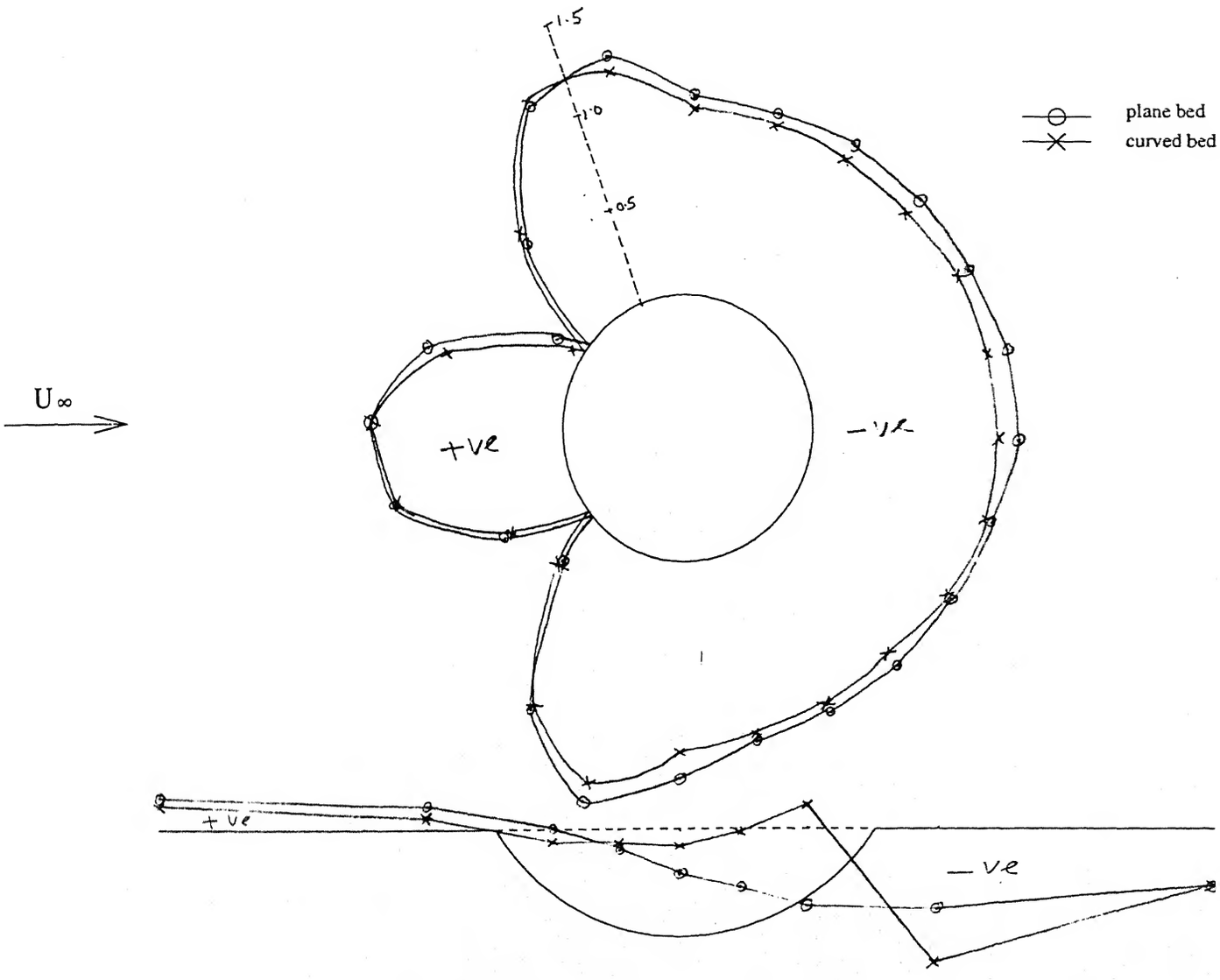

Fig.3.19 Pressure distribution around the cylinder and along the carved-out bed for curvature radius 0.9D, G/D=1.0, at velocity 4m/s

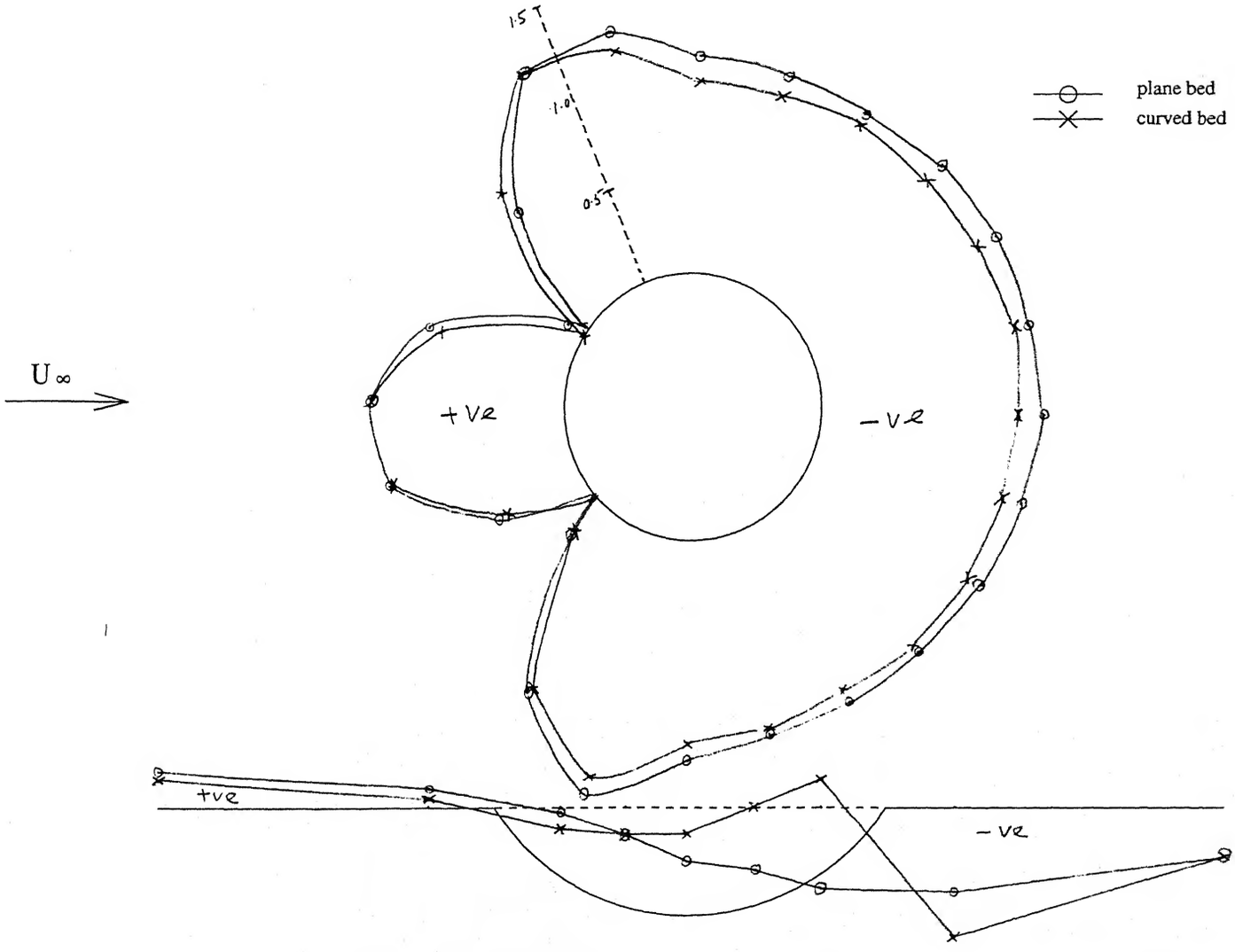

Fig.3.20 Pressure distribution around the cylinder and along the carved-out bed for curvature radius 0.9D, G/D=1.0, at velocity 5m/s

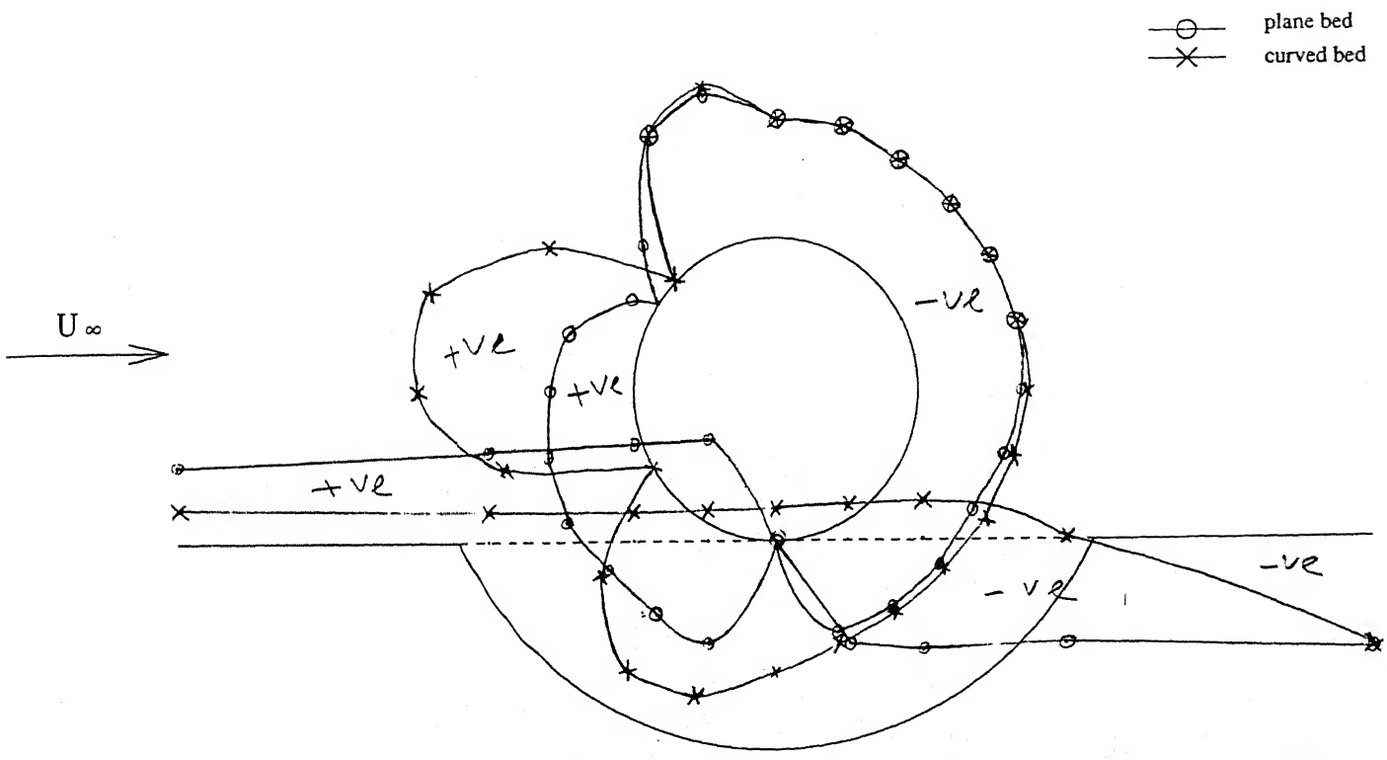

Fig.3.21 Pressure distribution around the cylinder and along the carved-out bed for curvature radius 1.2D, G/D=0.0, at velocity 3m/s

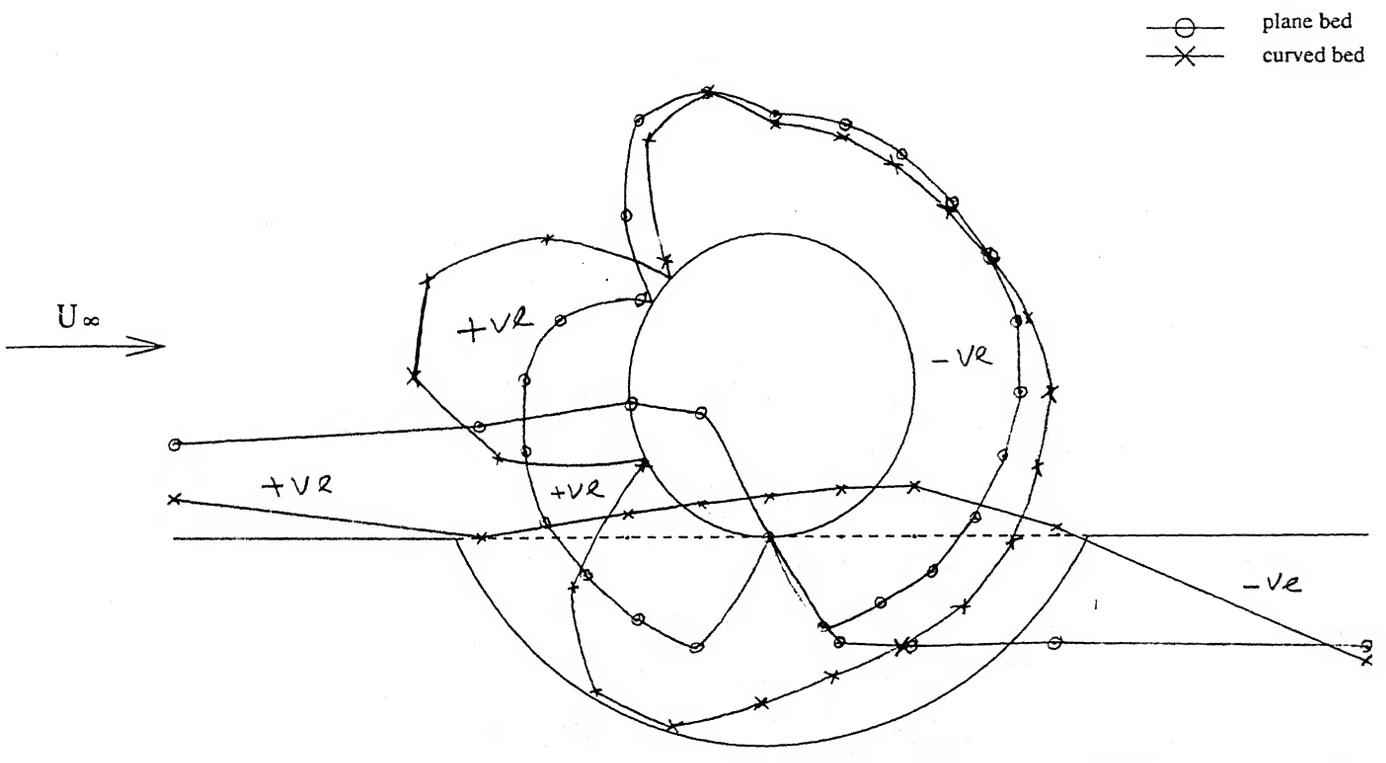

Fig.3.22 Pressure distribution around the cylinder and along the carved-out bed for curvature radius 1.2D, G/D=0.0, at velocity 4m/s

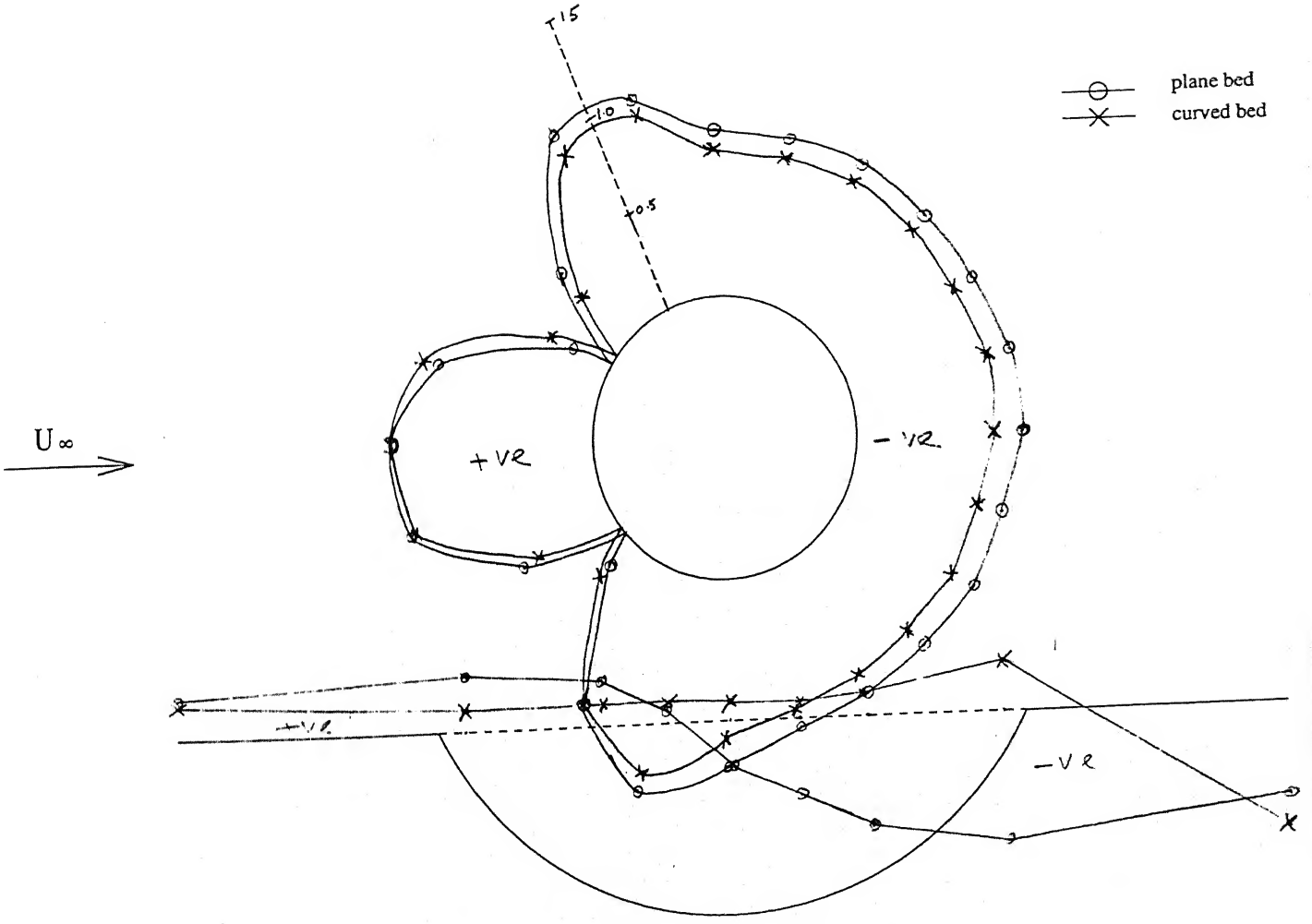

Fig.3.24 Pressure distribution around the cylinder and along the carved-out bed for curvature radius 1.2D, G/D=0.5, at velocity 3m/s

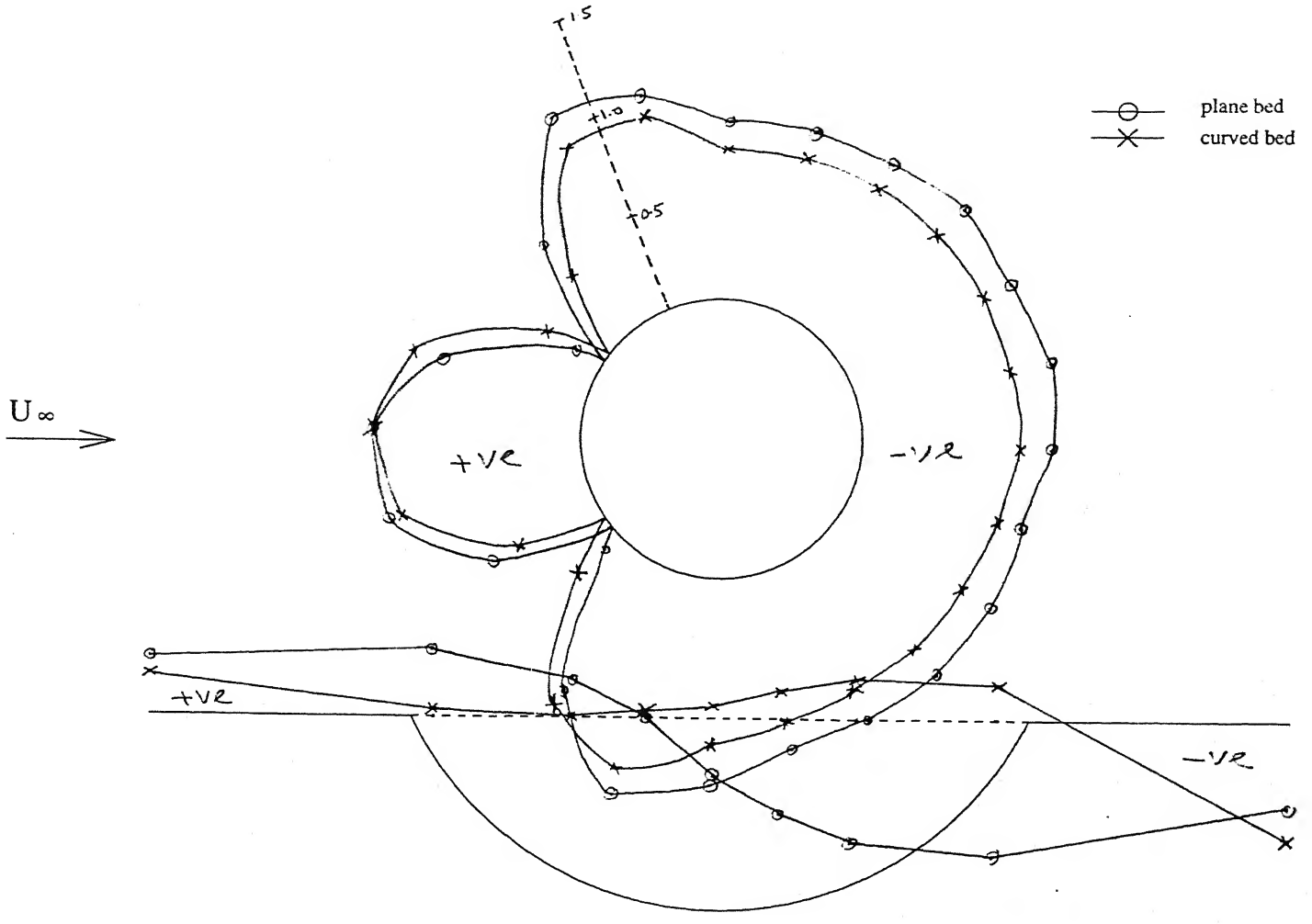

Fig.3.25 Pressure distribution around the cylinder and along the carved-out bed for curvature radius 1.2D, G/D=0.5, at velocity 4m/s

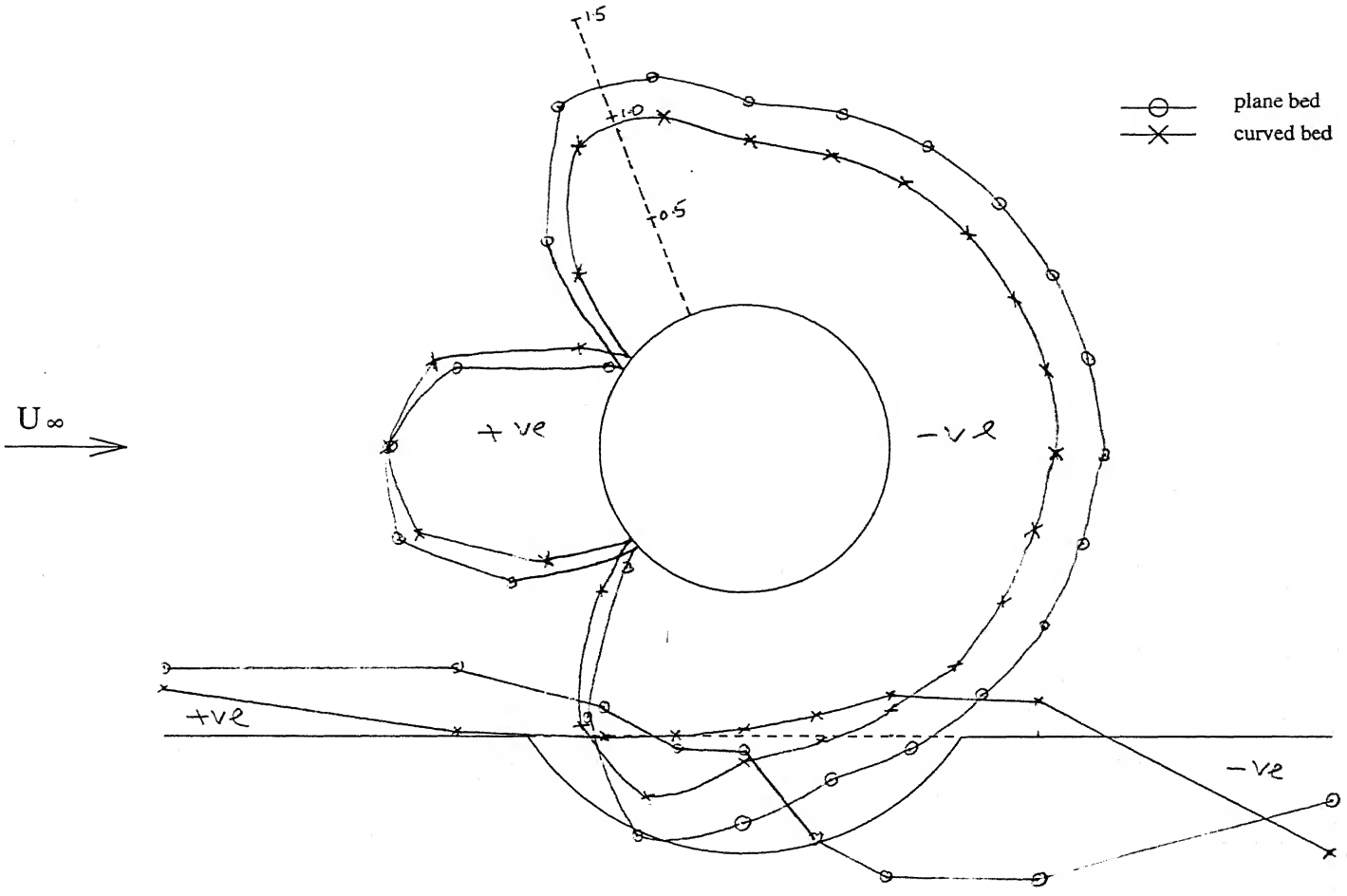

Fig.3.26 Pressure distribution around the cylinder and along the carved-out bed for curvature radius 1.2D, G/D=0.5, at velocity 5m/s

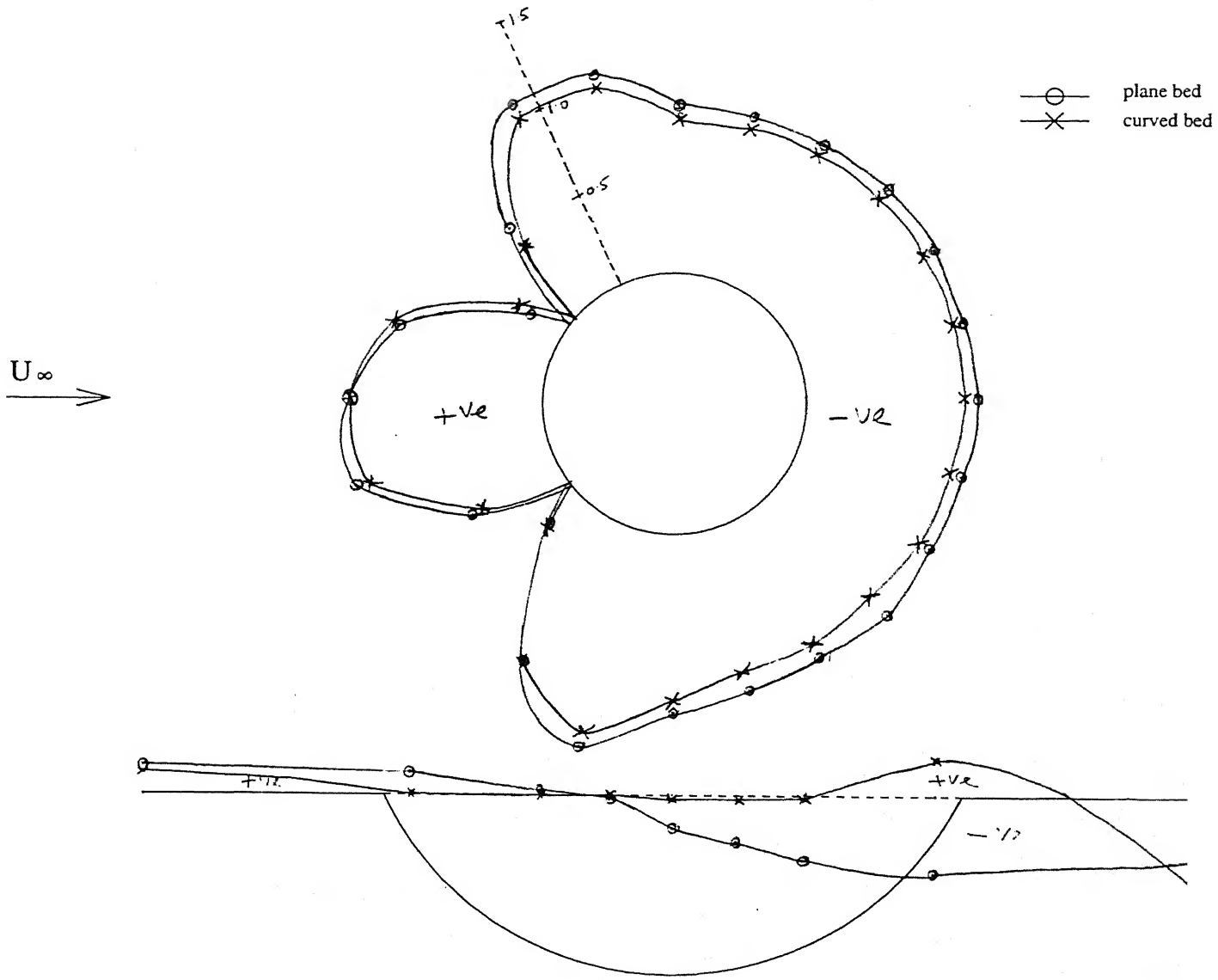

Fig.3.27 Pressure distribution around the cylinder and along the carved-out bed for curvature radius 1.2D, G/D=1.0, at velocity 3m/s

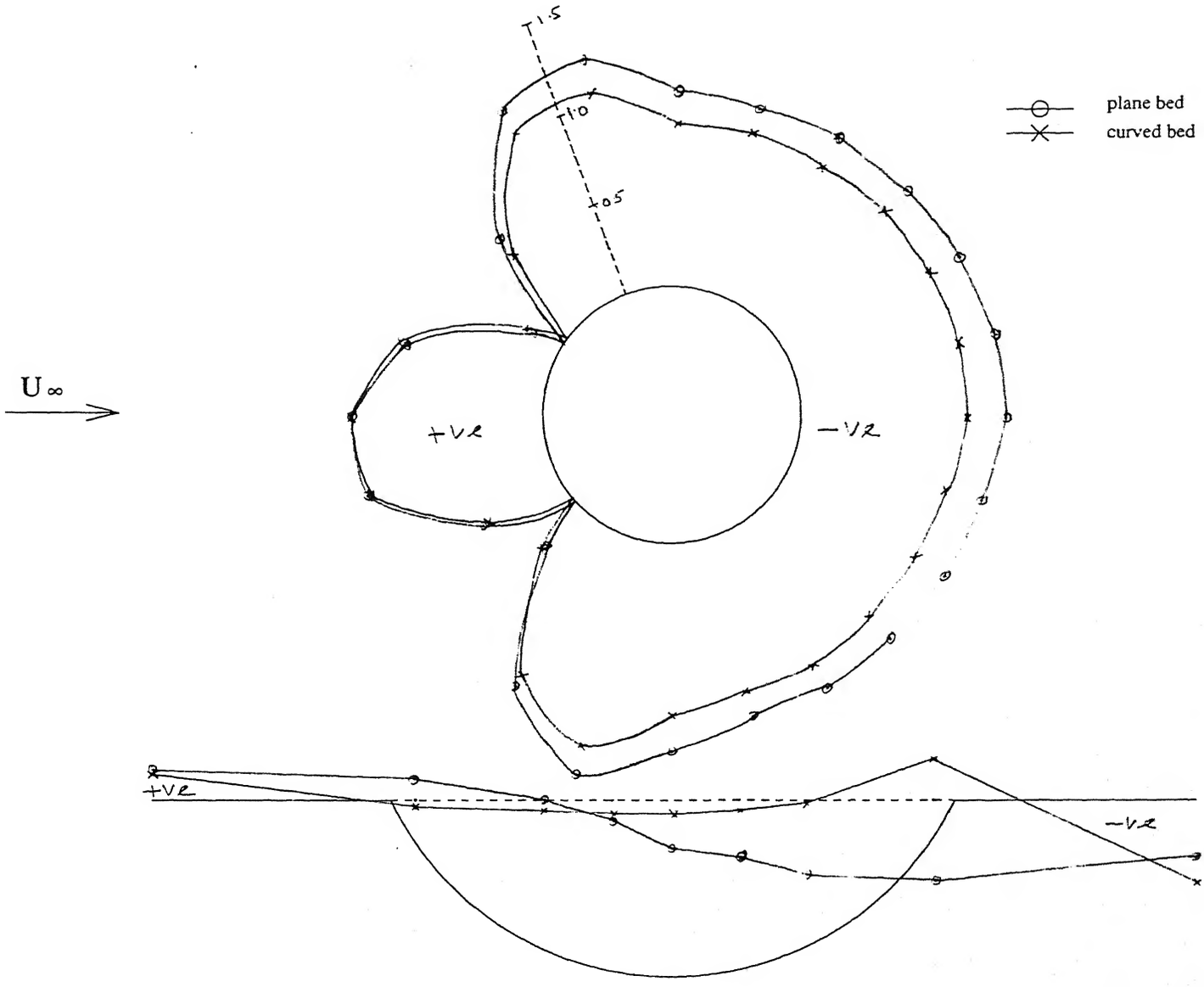

Fig.3.28 Pressure distribution around the cylinder and along the carved-out bed for curvature radius 1.2D, G/D=1.0, at velocity 4m/s

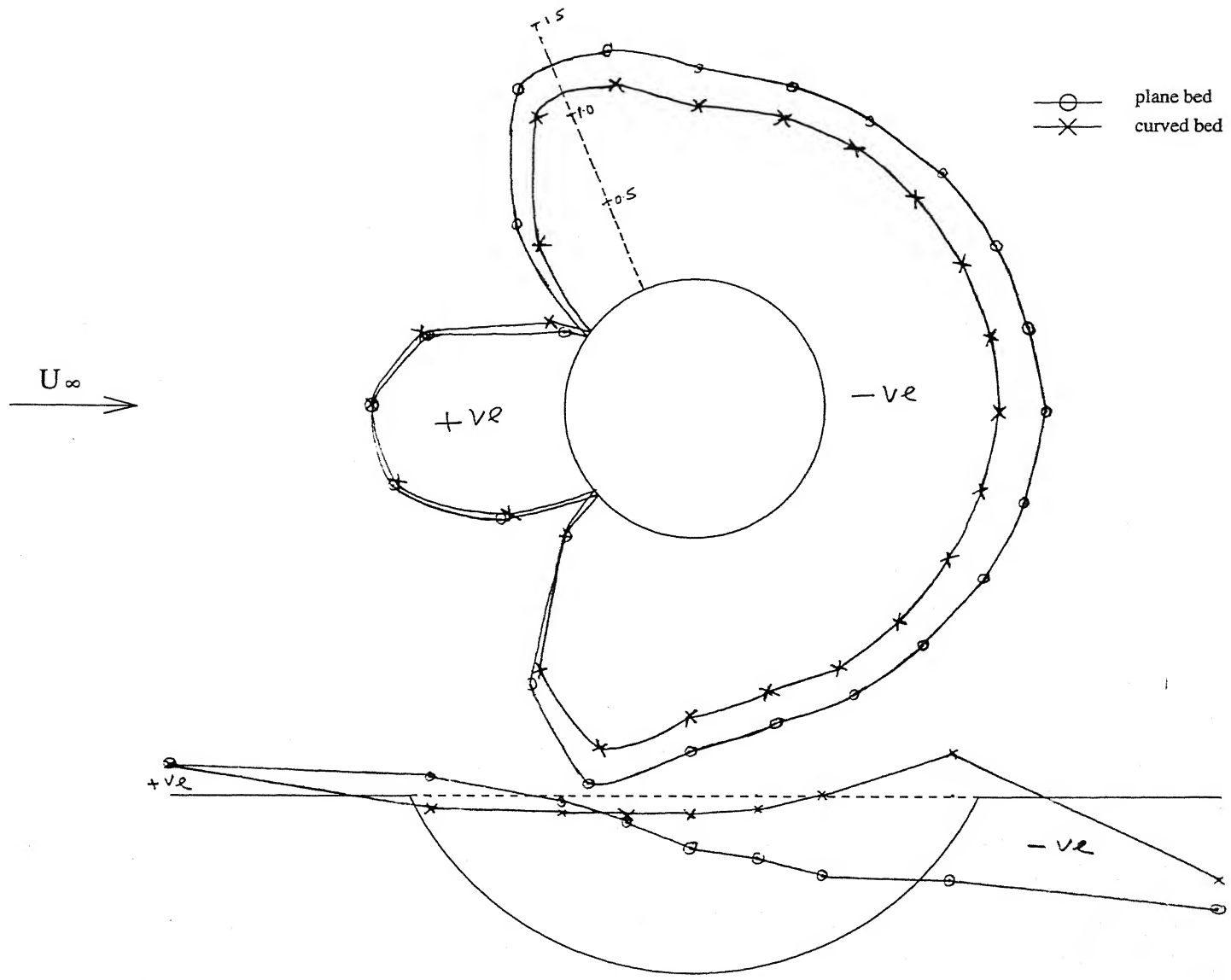

Fig.3.29 Pressure distribution around the cylinder and along the carved-out bed for curvature radius 1.2D, G/D=1.0, at velocity 5m/s

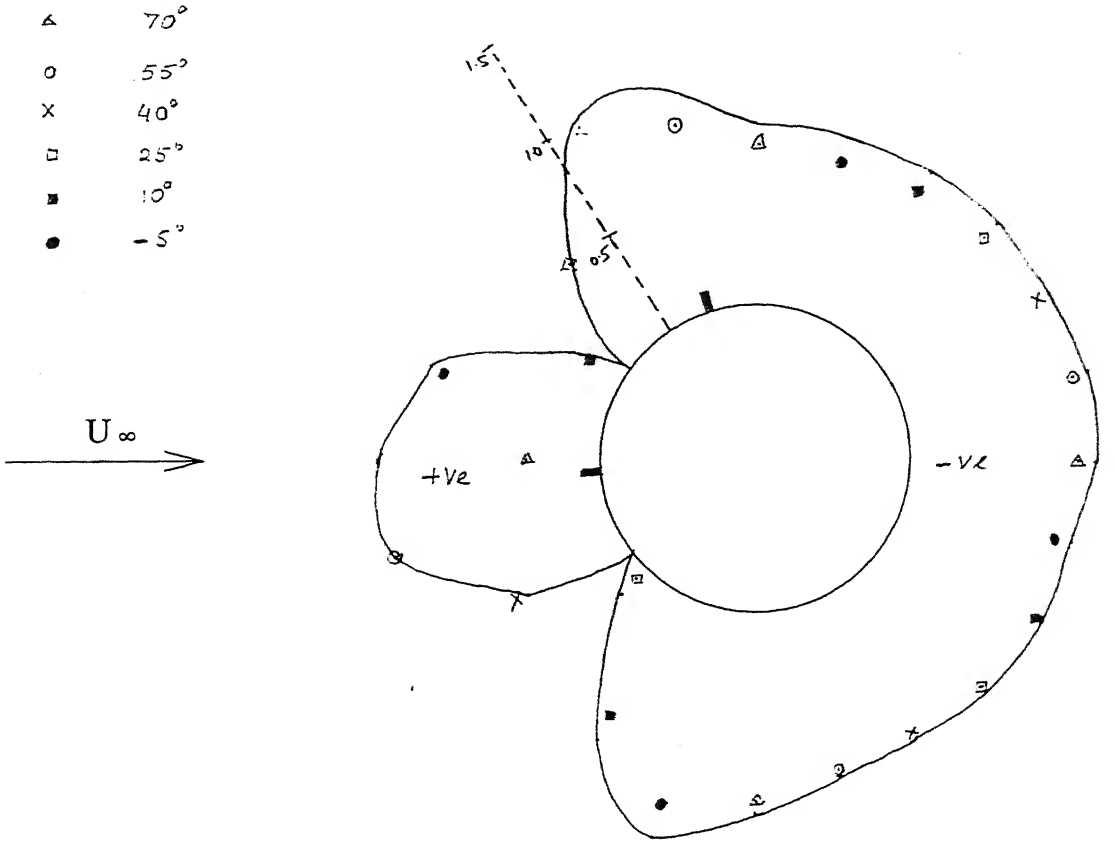

Fig.3.31 Pressure distribution around the cylinder for plane bed, G/D=0.5, at velocity 3m/s

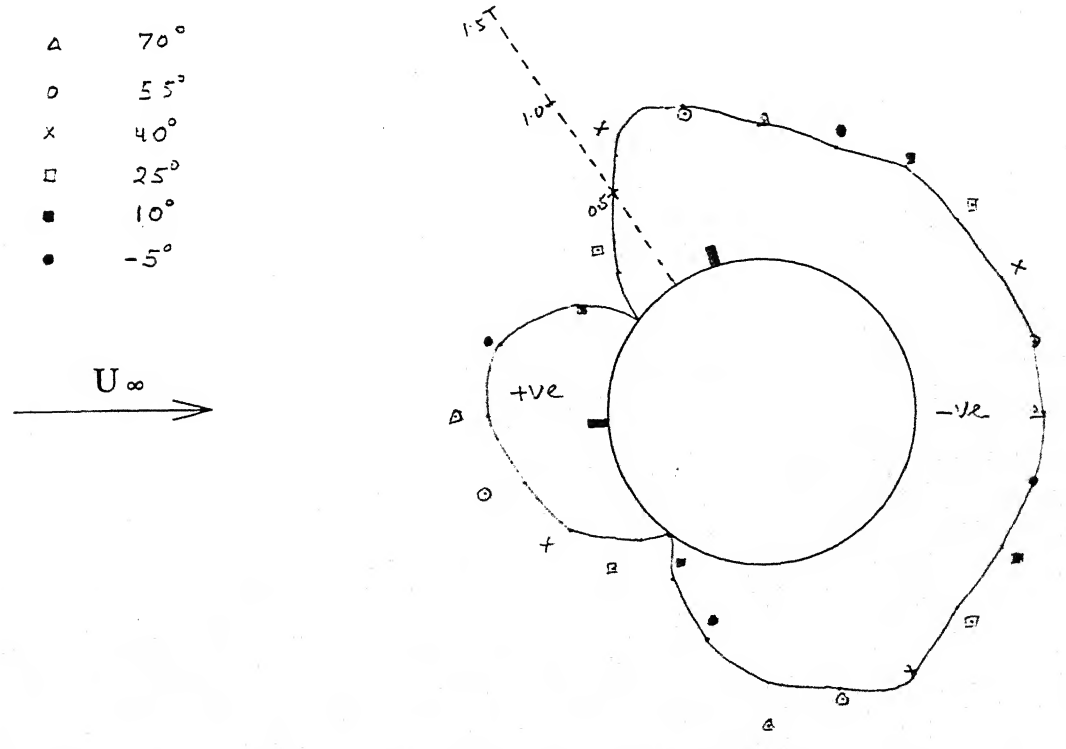

Fig.3.30 Pressure distribution around the cylinder for plane bed,

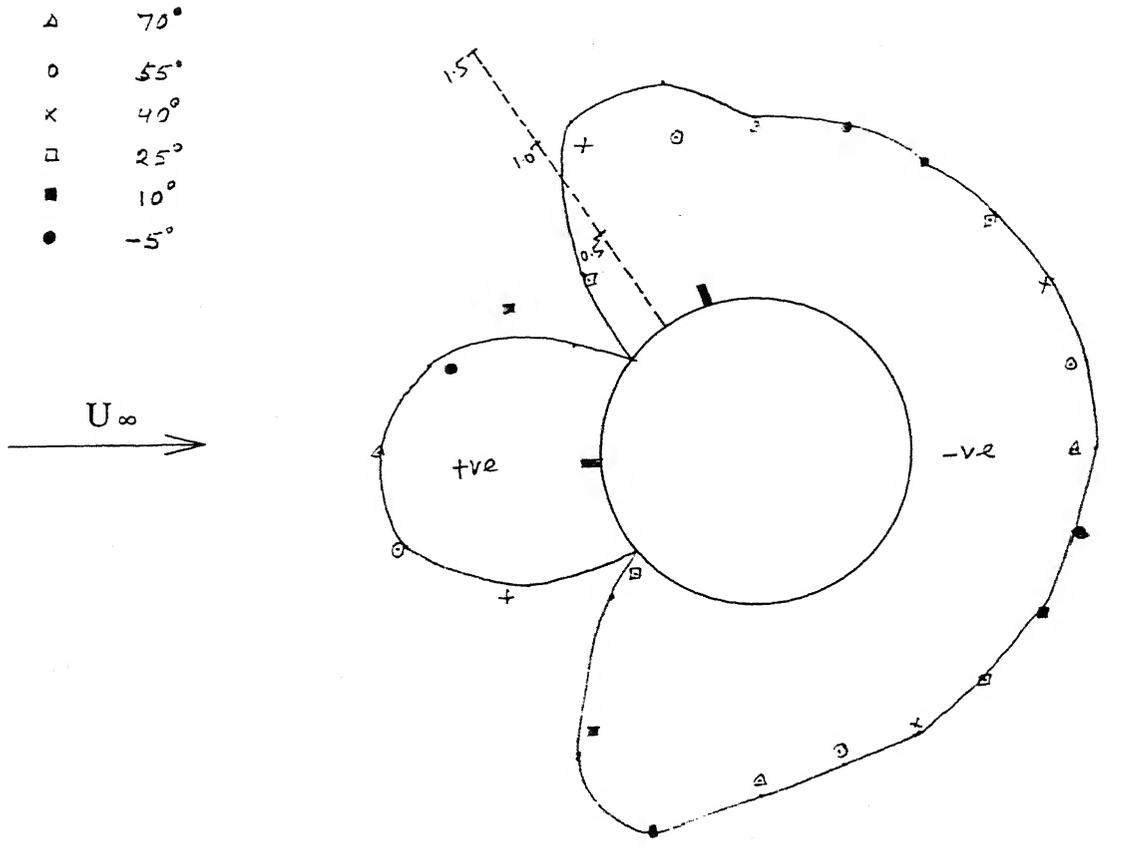

Fig.3.32 Pressure distribution around the cylinder for plane bed, G/D=1.0, at velocity 3m/s

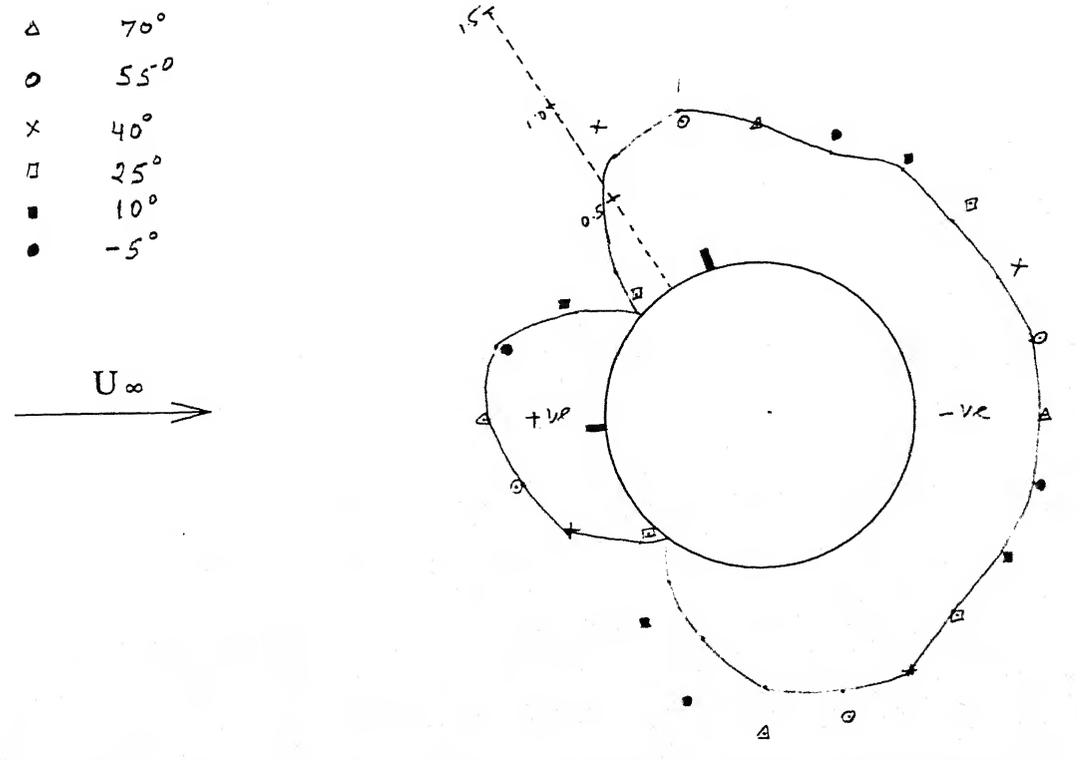

Fig.3.33 Pressure distribution around the cylinder for curvature radius 0.7D, G/D=0.0, at velocity 3m/s

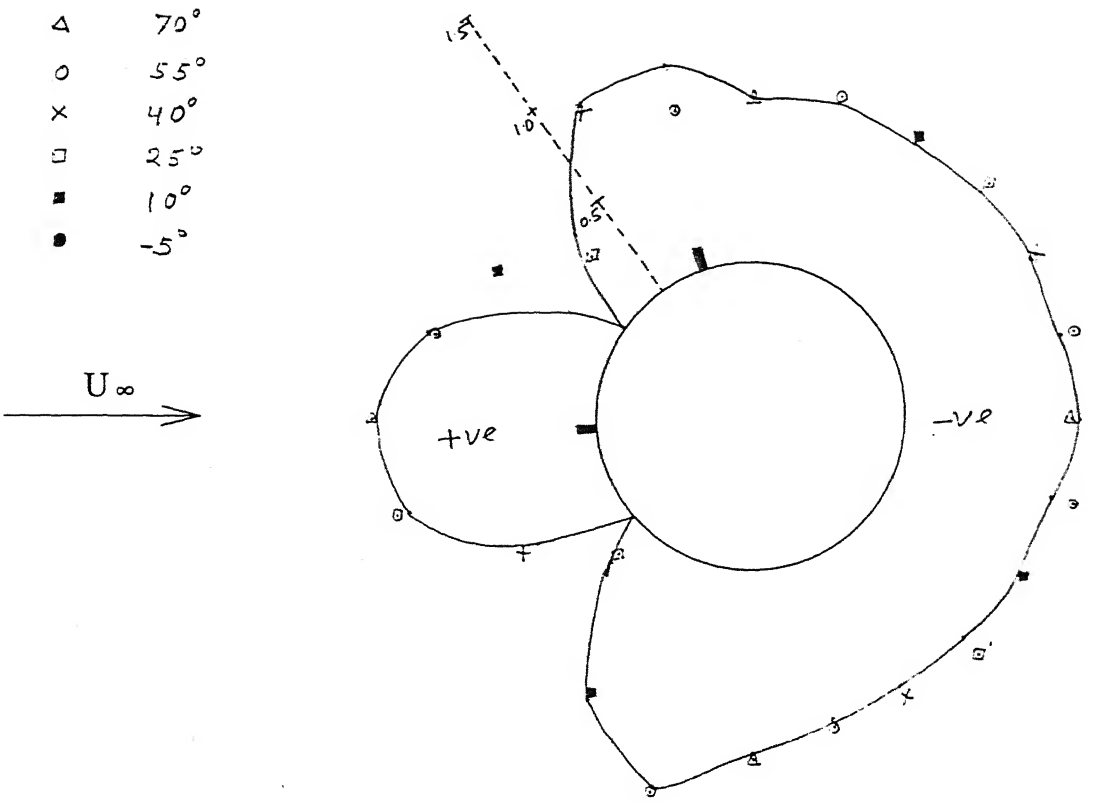

Fig.3.34 Pressure distribution around the cylinder for curvature radius 0.7D, G/D=0.5, at velocity 3m/s

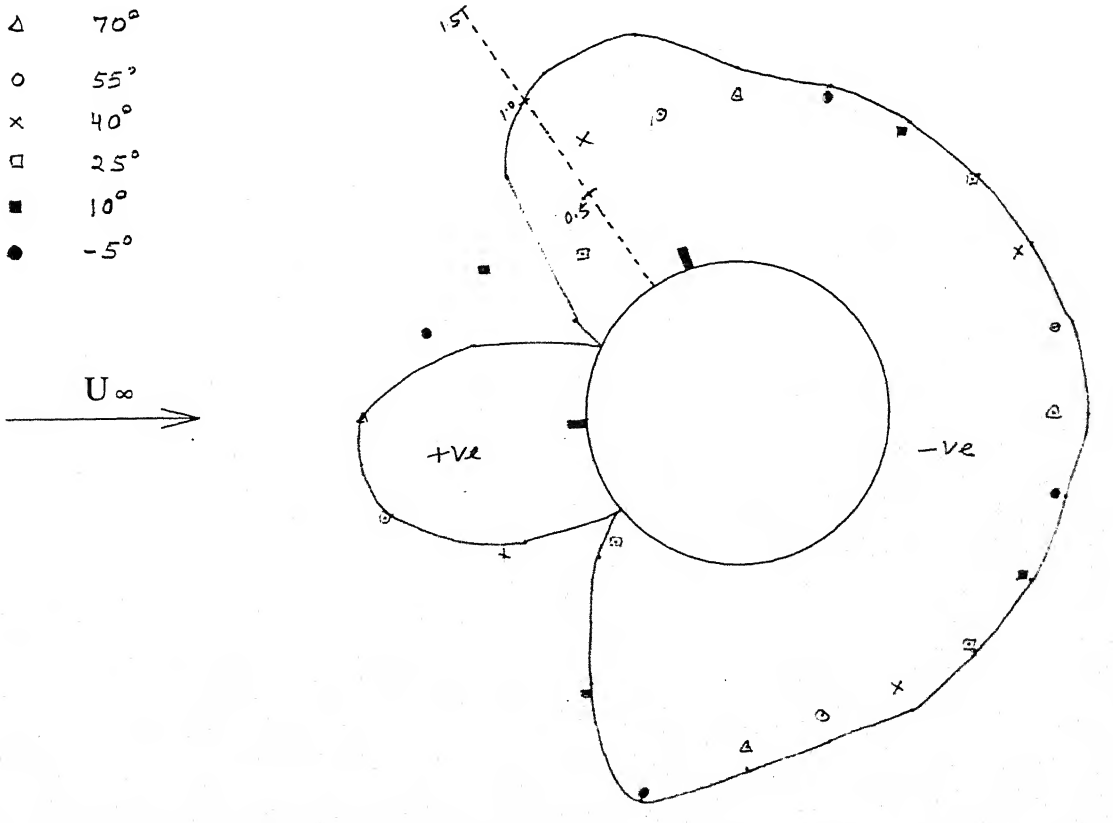

Fig.3.35 Pressure distribution around the cylinder for curvature radius 0.7D,

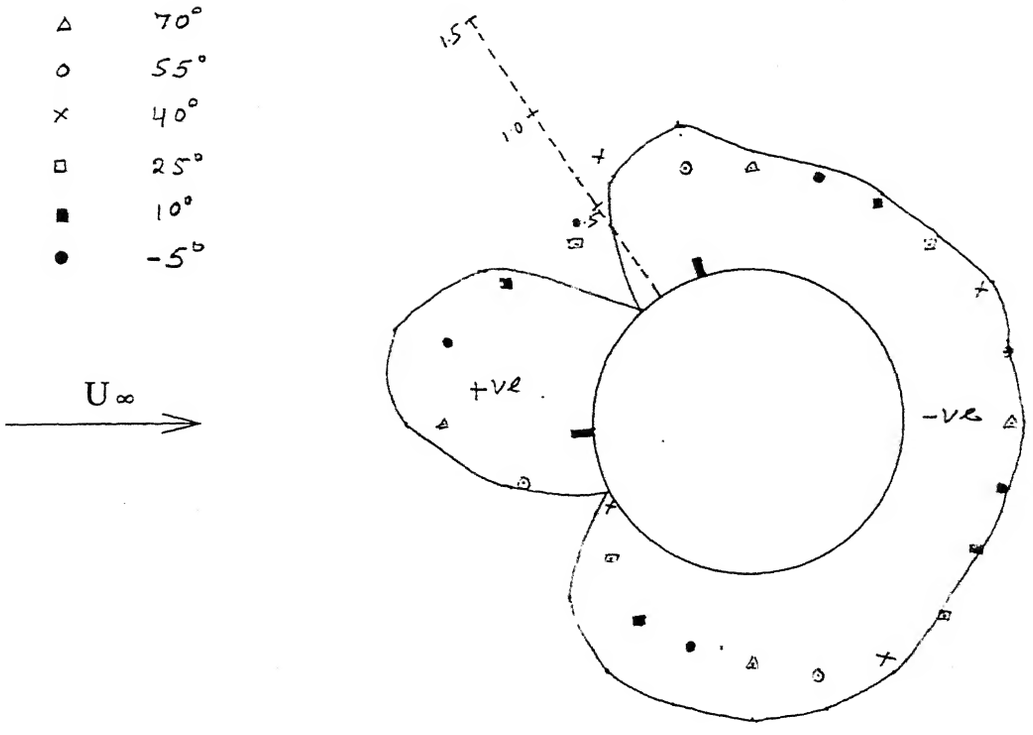

Fig.3.36 Pressure distribution around the cylinder for curvature radius 0.9D, G/D=0.0, at velocity 3m/s

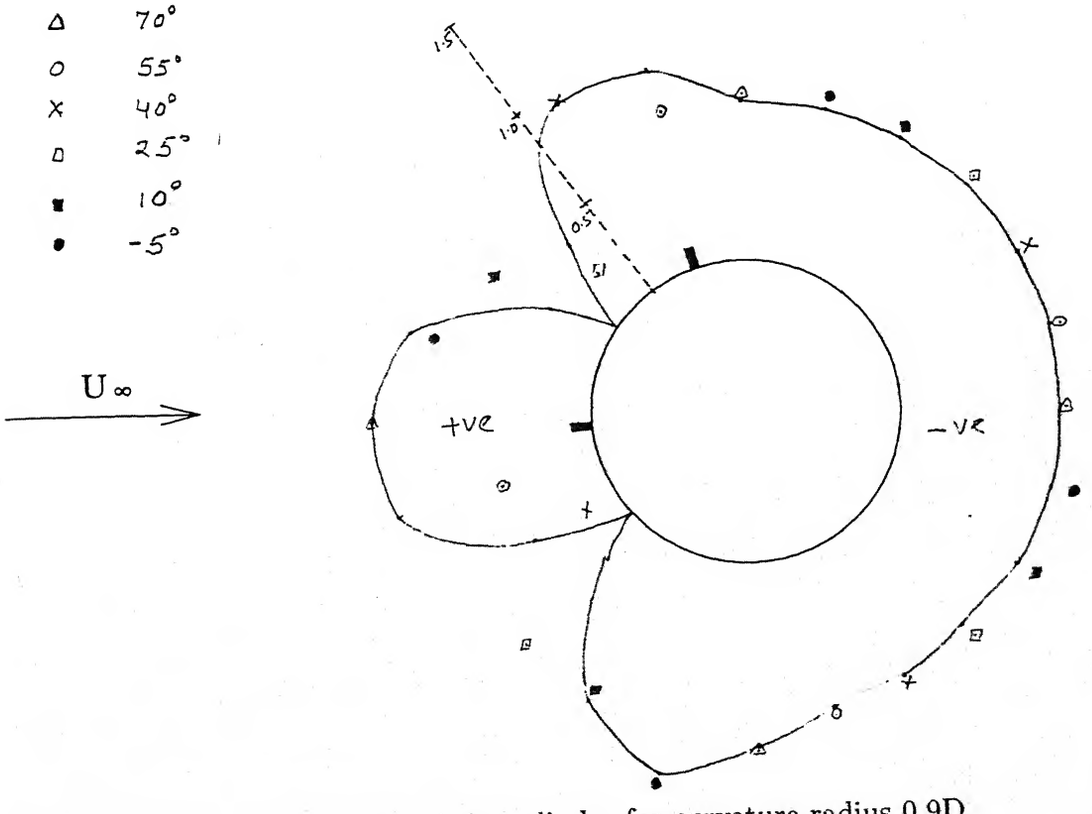

Fig.3.37 Pressure distribution around the cylinder for curvature radius 0.9D, G/D=0.5, at velocity 3m/s

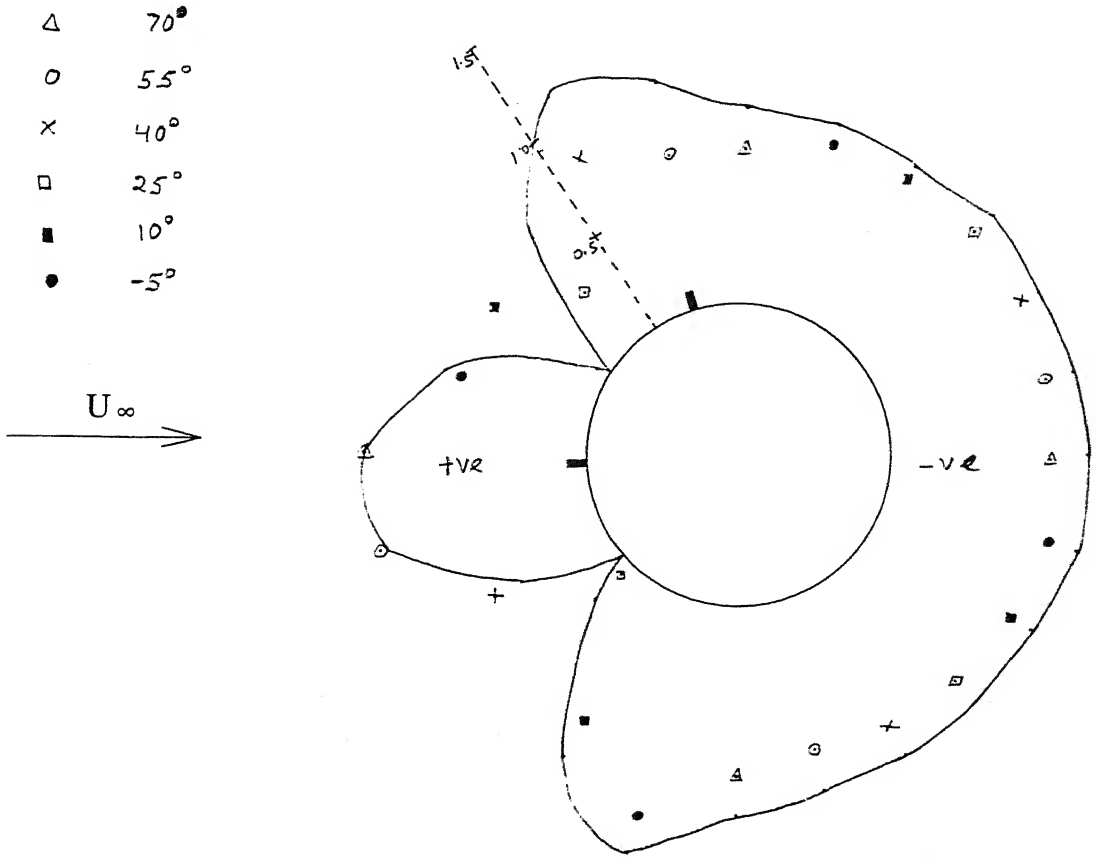

Fig.3.38 Pressure distribution around the cylinder for curvature radius 0.9D, G/D=1.0, at velocity 3m/s

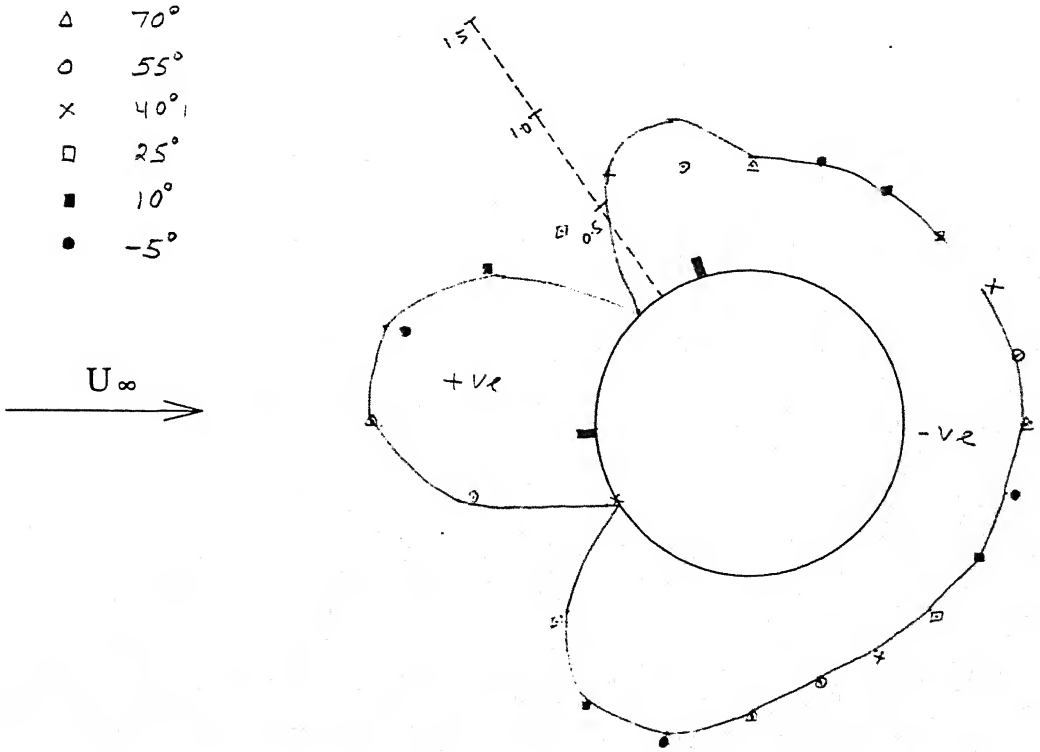

Fig.3.39 Pressure distribution around the cylinder for curvature radius 1.2D, G/D=0.0, at velocity 3m/s

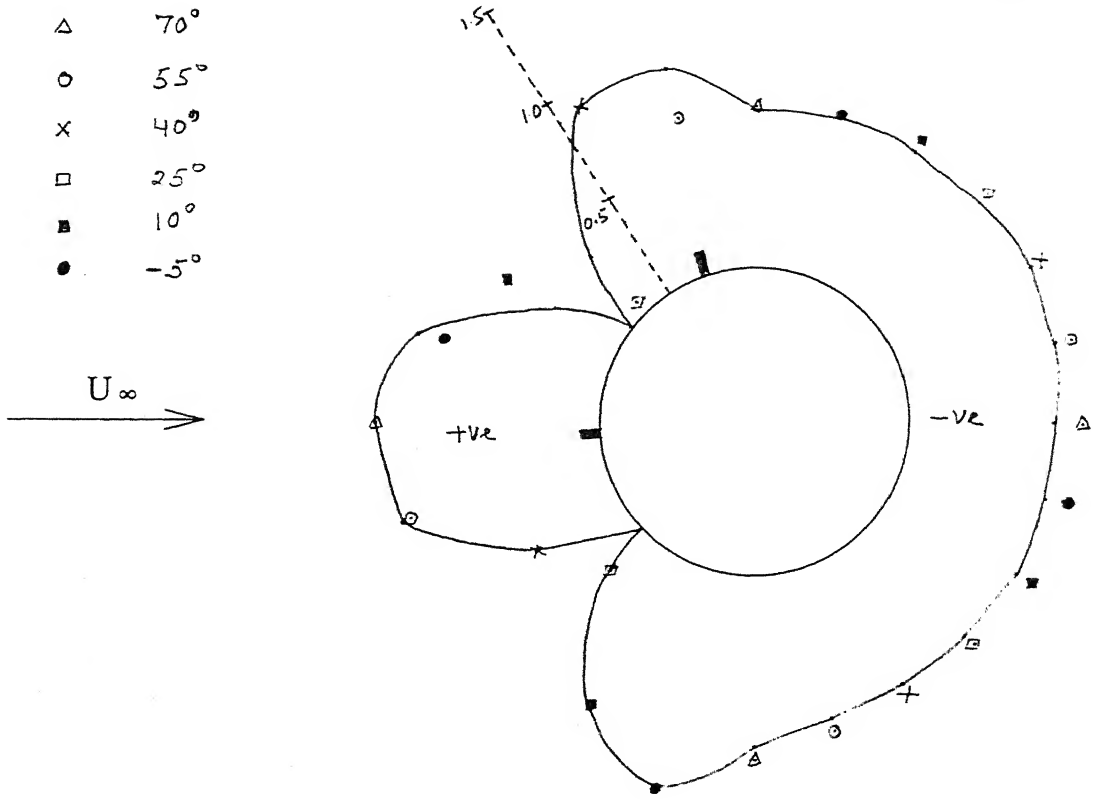

Fig.3.40 Pressure distribution around the cylinder for curvature radius 1.2D, G/D=0.5, at velocity 3m/s

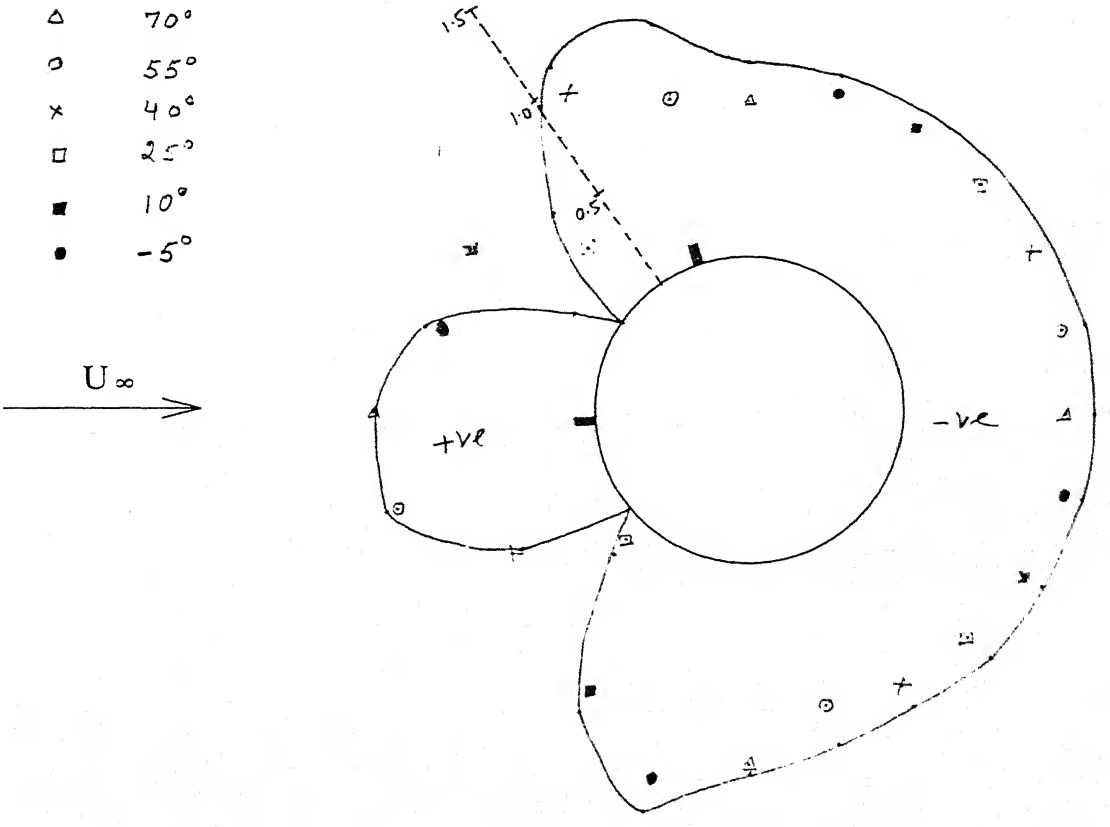

Fig.3.41 Pressure distribution around the cylinder for curvature radius 1.2D,

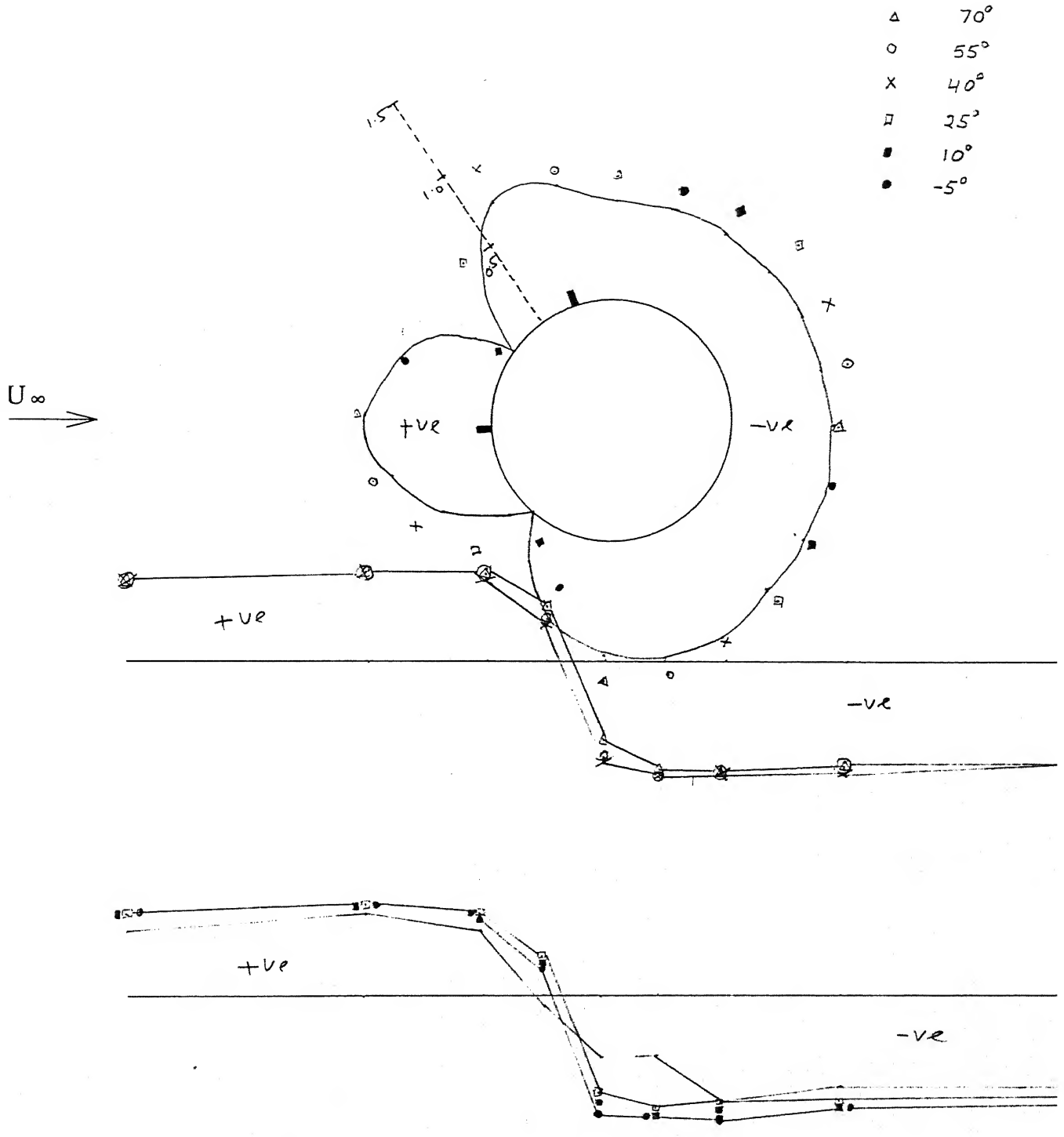

Fig.3.42 Pressure distribution around the cylinder and along the carved-out bed for plane bed, G/D=0.12, at velocity 5m/s

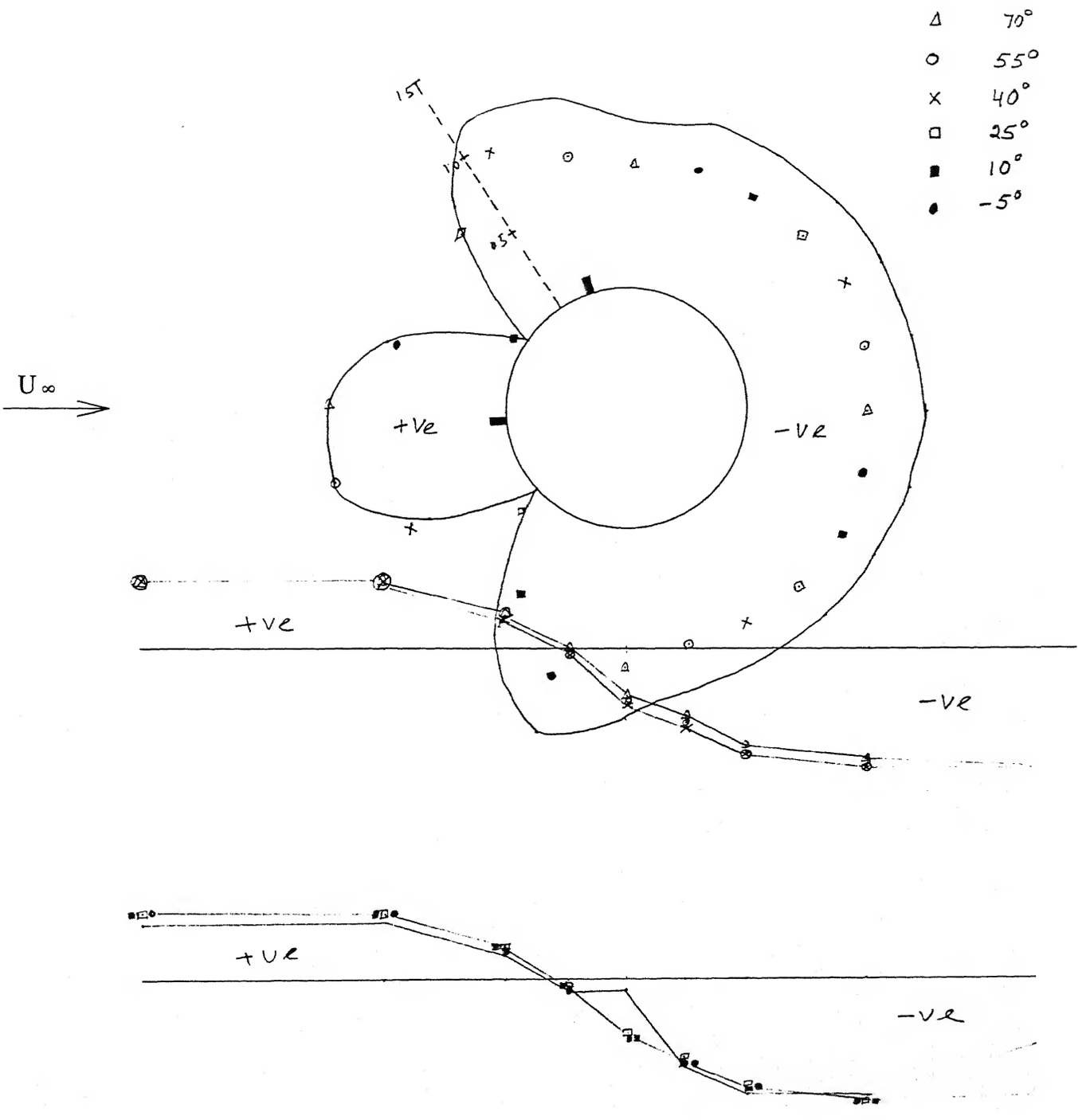

Fig.3.43 Pressure distribution around the cylinder and along the carved-out bed for plane bed, G/D=0.5, at velocity 5m/s

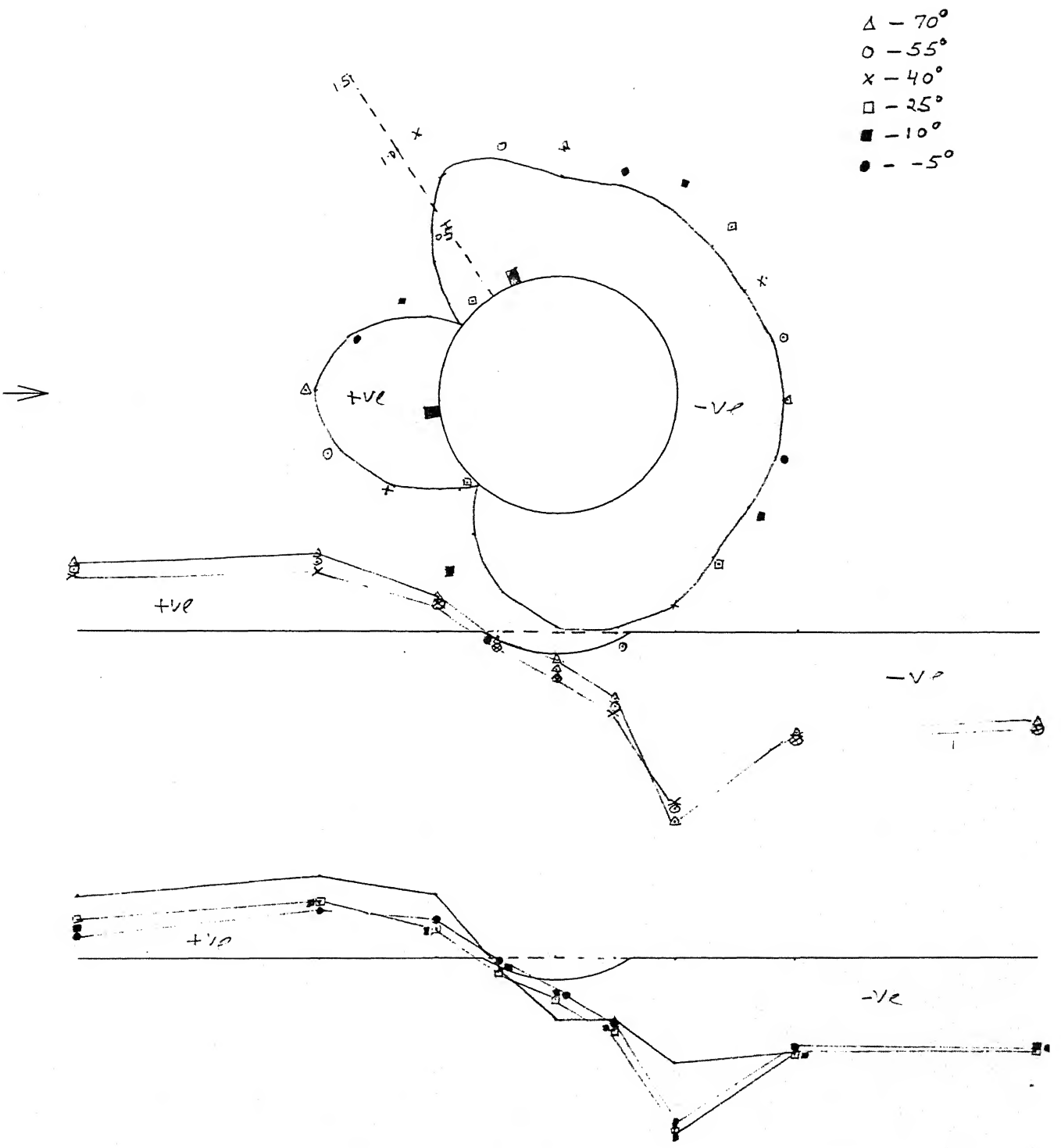

Fig.3.44 Pressure distribution around the cylinder and along the carved-out bed for curvature radius 0.7D, G/D=0.0, at velocity 5m/s

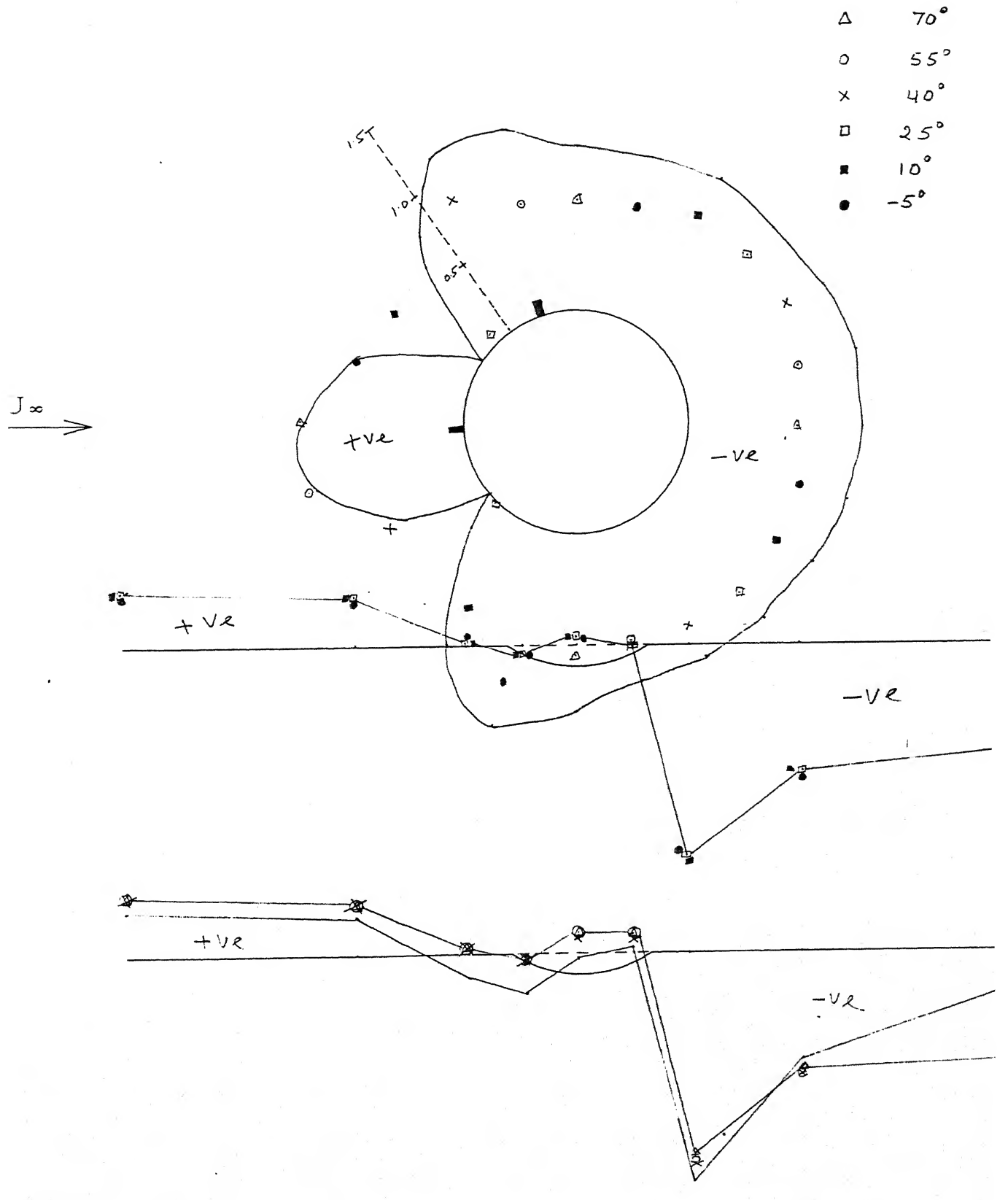

Fig.3.45 Pressure distribution around the cylinder and along the carved-out bed for curvature radius 0.7D, G/D=0.5, at velocity 5m/s

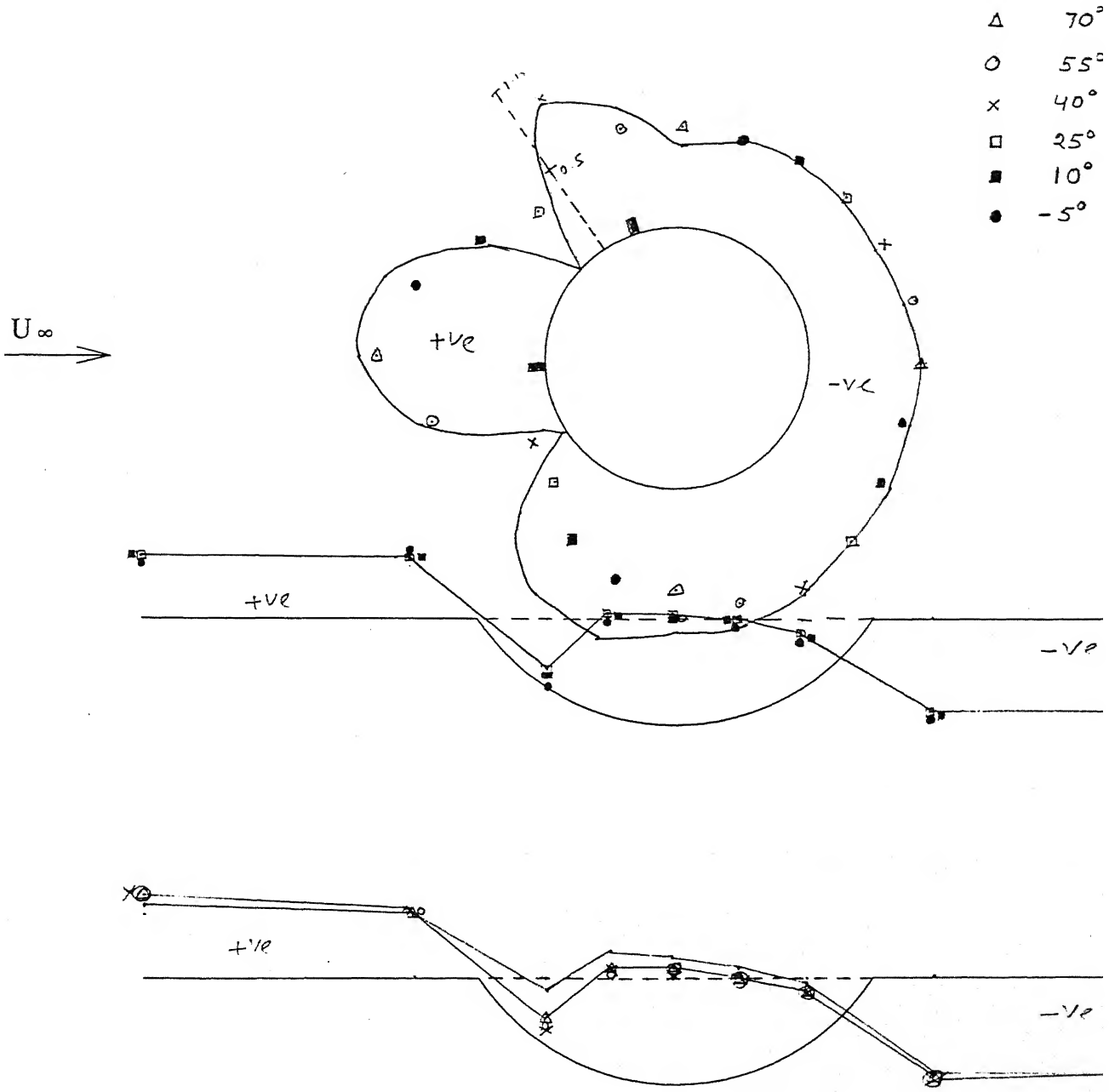

Fig.3.46 Pressure distribution around the cylinder and along the carved-out bed for curvature radius 0.9D, G/D=0.0, at velocity 5m/s

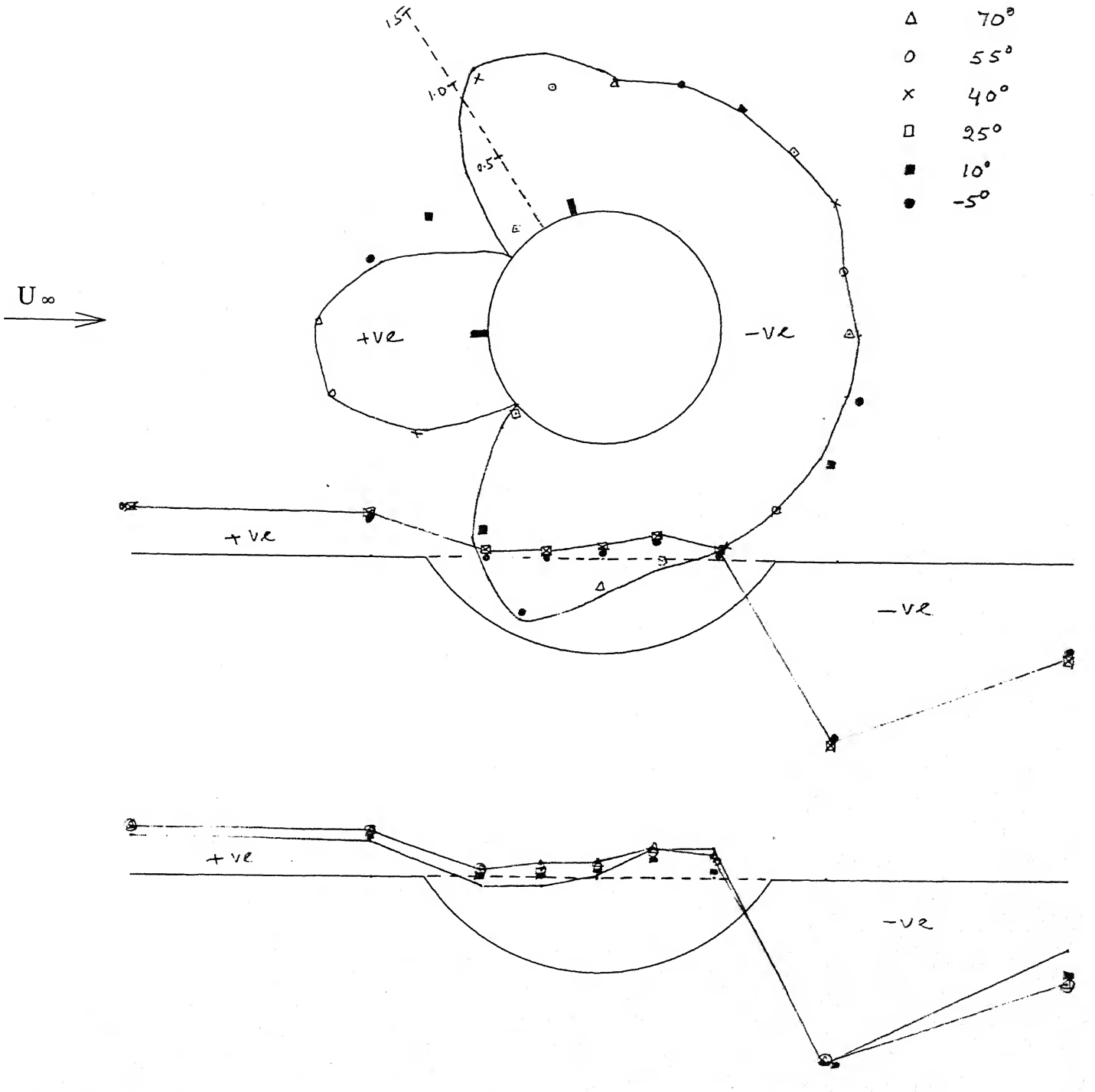

Fig.3.47 Pressure distribution around the cylinder and along the carved-out bed for curvature radius 0.9D, G/D=0.5, at velocity 5m/s

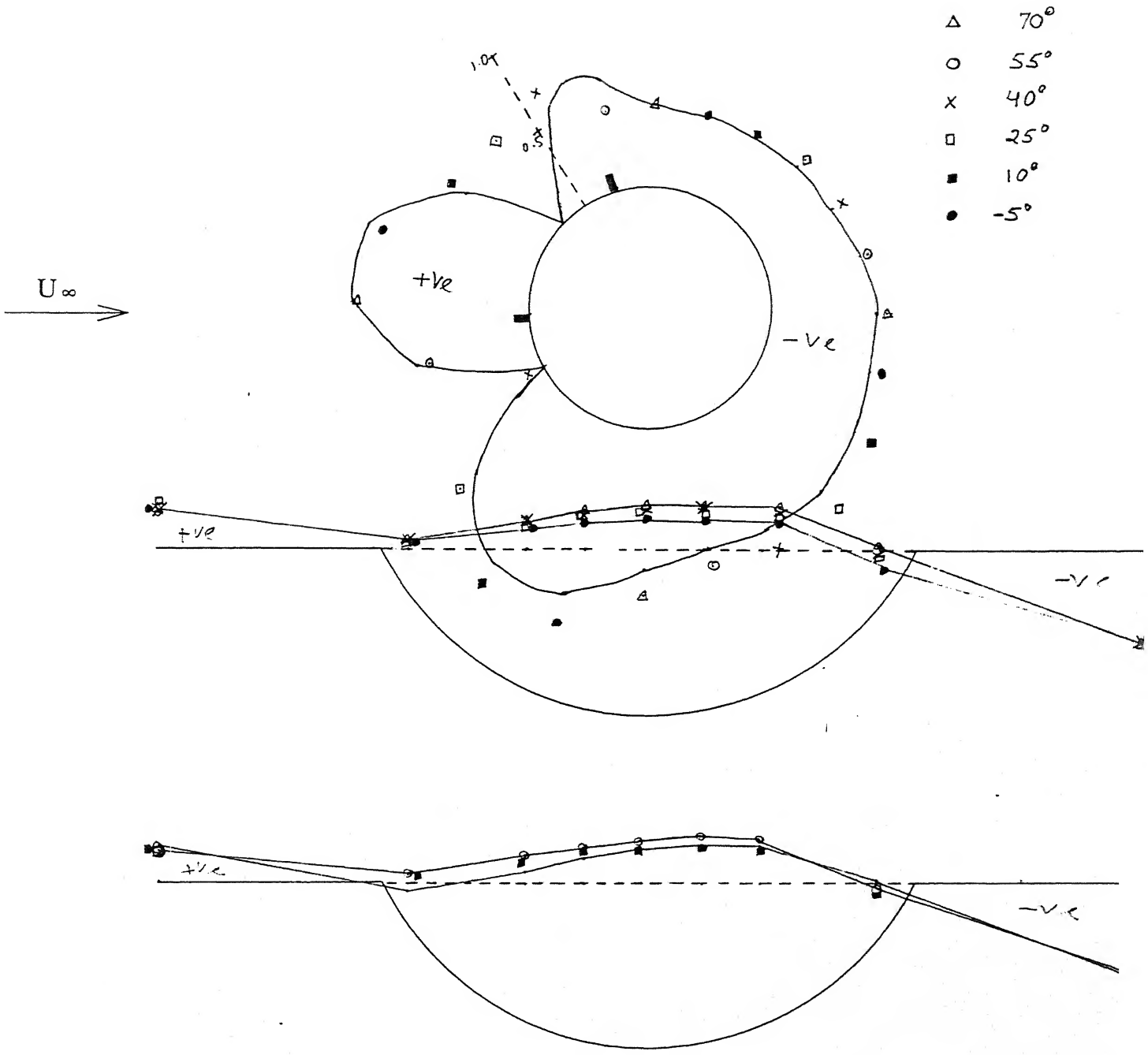

Fig.3.48 Pressure distribution around the cylinder and along the carved-out bed for curvature radius 1.2D, G/D=0.0, at velocity 5m/s

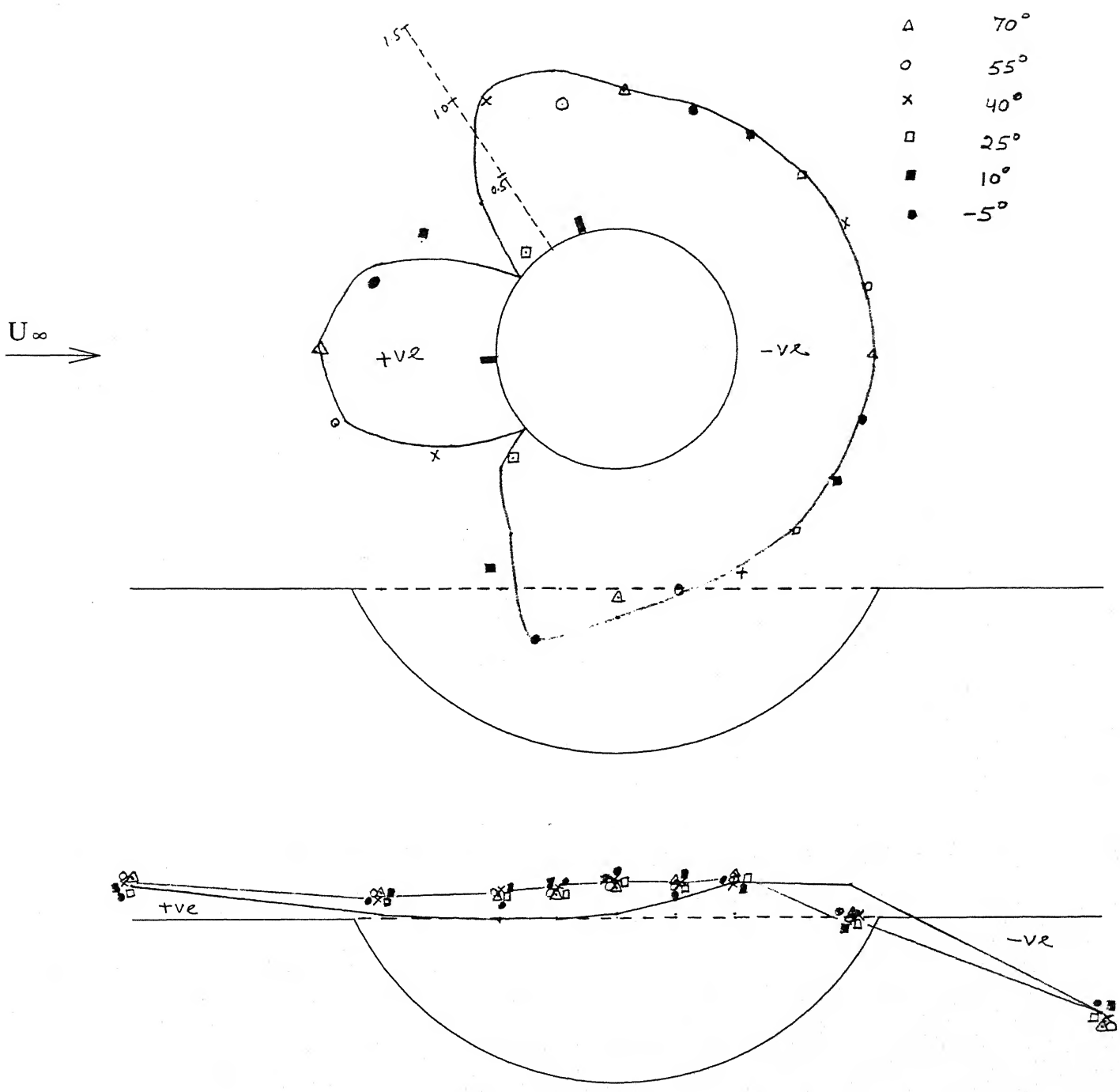

Fig.3.49 Pressure distribution around the cylinder and along the carved-out bed for curvature radius 1.2D, G/D=0.5, at velocity 5m/s

Chapter 4

Conclusions and Suggestions

4.1 Conclusions

The results for a clean circular cylinder are summarised as follows:

a Pressure distribution with the plane boundary.

1 A pressure discontinuity was evident at the point of contact, on both cylinder and on the bed.

2 Front stagnation point was displaced towards the boundary and hence the lack of symmetry of the pressure distribution about the front stagnation point.

3 The increase in velocity(Reynold's Number) makes almost no influence on the C_p distribution around the cylinder, except for a wider and larger negative loop in the pressure distribution.

4 The pressure distribution are in agreement with Bearman and Zdravkovich[1].

b Pressure distribution with carved boundary.

1 With the introduction of an effective G/D of 0.2, in the form of scour a rapid fall in pressure under the cylinder is noted.

2 This fall in the pressure becomes less pronounced with the increase of radius of the carved-out boundary.

3 The pressure distribution around the cylinder takes a more symmetrical form about the front stagnation point, with the axis of symmetry approaching the free stream direction.

4 With the increase in G/D to 0.5 and 1.0, the pressure distribution around the cylinder becomes more and more symmetrical as expected.

5 The C_p in wake region of the cylinder is lesser than that for plane surface for all curvatures at G/D of 0.0.

6 For large scour curvatures and higher gap-ratios the flow remains largely unaffected by the presence of the boundary.

7 The effect of widening the negative loop is more pronounced for lower gap-ratios and smaller radii of curvatures.

8 At G/D = 0.5 and curvature radius of 0.7D the wake pressure decreases with the increase in speed compared to that for a plane surface.

9 For curvature 0.7D and G/D of 1.0 the pressure distribution is almost same, this can be attributed to low curvature radius of bed and large gap-ratio.

10 For all G/D except 0.0 and curvatures except 0.7D, the C_p in the wake region is more then the corresponding values for a plane surface.

11 The wake pressure has increased for higher gap-ratios and higher curvature radii,the force on the cylinder decreases, and there will be vibrations of smaller amplitude.

12 In the wake region pressure coefficient C_p slightly decreases with the increase in velocity(Reynold's Number).

13 Though the C_p distribution pattern is similar but the values may change considerably, and the pressure in the wake region may gain. Thus the Bearman's observations with the plane bed do not truly represent the scour like condition with increasing gap.

c Surface pressure distributions along the boundary.

1 Here we see larger pressure in the upstream direction and lower pressure in the downstream direction of the cylinder.

2 We see a minimum pressure coefficient (C_p) just after the curvature for all values of curvature radius. This may be attributed to the separation caused by the sharp edge of the curvature.

3 This minimum pressure peak becomes less pronounced when the curvature radius is increased.

4 The distribution also shows that the for higher gap-ratios the recovery of negative pressure is more evident.

5 The increase of gap-ratio to 0.5 makes the minimum pressure peak more pronounced. The further increase of gap makes the peak less pronounced.

6 Minimum C_p value occurring for 0.7D and speed of 5m/s.

7 The pressure distribution almost remains similar except that the value at the minimum peak is more pronounced for larger speeds.

8 In most of the cases with gap of 0.5D the C_p, in the region under the cylinder is positive, showing a reduction in velocity and hence lesser erosion on the bed.

9 The results of the present study can not be directly comparable to the Bearman's observations due to differing values of G/D for carved-out boundaries.

The results for a straked circular cylinder are summarised as follows:

a Pressure distribution on the straked cylinder.

1 The pressure distribution around the cylinder changes mainly in the wake region and at point after the strake.

2 In the wake region the C_p is slightly less in the case of plane bed for gap-ratio of 0.5, and it is almost same for values of G/D.

3 There is gain in pressure after the strake for all positive strake angles (α_{hs} of $55^o, 40^o, 25^o$ and 10^o.

4 When the curvature radius is 0.7D the wake pressure is slightly more for G/D = 0.0 but it is lesser for other gap-ratios.

5 For higher gap-ratio and larger curvature radius the effect of the strake is less significant.

b Pressure distribution along the carved-out boundaries with straked cylinder.

1 For lower gap-ratio of 0.0, we see faster pressure drop just beneath the cylinder. This shows that the onset of the scour is faster.

2 On decreasing the strake angle the pressure in the unstream and downstream end remains almost same, but increases a little under the cylinder.

3 For higher gap-ratios, the pressure change becomes smoother than the earlier case and the pressure is little higher then that for a smooth cylinder.

4 On decreasing the strake angle the pressure decreases slightly under the cylinder and remains constant on other points.

5 We do not observe the sharp negative peaks with strakes on the cylinder.

6 This also shows that the pressure distribution is not symmetric with the change of the strake angle thus there is decrease in the pressure induced vibration.

7 In the initial phase of development of scour the process may be fast as the pressure gradient is high but later the gradient becomes less and more spread thus decreasing the scour depth. This may be also helpful in selfembeded pipelines.

4.2 Suggestions

4.2.1 Suggestions for Future Course of Work

In the future following things can be attempted in this field of work:

1. In this work we have done the experiments for only three speeds, it is needed to study for various higher real life values of Reynold's number

2. To study the real effect on the onset of scour we must study for larger number of gap-ratios between the values of 0.0 and 1.0.

3. With strakes on the cylinder the study is preliminary. So the effect of strakes can be studied for various heights and various pitch of the strake.

4. The effect of strake can also be studied for increased number of strakes.

5. The study can be done for strake angles covering the complete round.

6. For making the experiments faster we must have larger number of pressure ports.

7. For proper understanding of mechanics of formation of scour we can have flow visualization.

8. Since local scour is an unsteady phenomena mainly due to the vortex shedding from the cylinder and it's interference with the boundary, hot wire probe investigation coupled with spectral analysis will shed more light on the phenomena.

References

[1] Bearman, P.W. and Zdravkovich, M.M. 1978,"Flow around a Circular Cylinder near a Plane Boundary",*Journal of Fluid Mechanics*, Vol.89,part I,pp 33-47.

[2] Chao, J.L. and Hennessy, P.V. 1972,"Local Scour under Ocean Outfall Pipelines",*Journal of Water Pollution Control Federation*, Vol.44, No.7,pp 1443-1447.

[3] Chiew, Y.M. 1990,"Mechanics of Local Scour around Submarine Pipelines ",*ASCE Journal of Hydraulic Engineering*, Vol.116, No.4,pp 515-529.

[4] Chiew, Y.M. 1991,"Flow around Horizontal Circular Cylinder in Shallow Flow",*ASCE Journal of Hydraulic Engineering*, Vol.117, No.2,pp 120-135.

[5] Chiew, Y.M. 1991,"Prediction of Maximum Scour Depth at Submarine Pipelines ",*ASCE Journal of Hydraulic Engineering*, Vol.117, No.4,pp 452-466.

[6] Chiew, Y.M. 1992,"Effect of Spoiler on scour at Submarine Pipelines",*ASCE Journal of Hydraulic Engineering*, Vol.118, No.9,pp 1311-1317.

[7] Fredsoe, J. et al. 1988,"Three Dimensional Scour below Pipelines",*Journal of Offshore Mechanics and Arctic Engineering*, Vol.110, No.10,pp 373-379.

[8] Fredsoe, J. and Summer, B.M. 1990,"Scour below Pipelines in Waves",*ASCE Journal of Saterway, Port, Coastal and Ocean Engineering*, Vol.116, No.3,pp 307-323.

[9] Gartshore, I.S., Khanna, J. and Laccinole, S. 1978,"The Effectiveness of Vortex Spoilers on a Circular Cylinder in Smooth and Turbulent Flow",*Proc. 5th Int. Conf. on Wind Engineering, Fort Collins,CO.*

[10] Ibrahim, A. and Nalluri, C. 1985,"Three Dimensional Scour around Pipelines under Submarine Environment",*ASME Proc. Foruth Int. Offshore Mechanics and Arctic Engineering Symposium*, Vol.1,pp 569-575.

[11] Kokkalis, A. and Wong, H.Y. 1982,"A Comparative Study of Three Aerodynamic Devices for Suppressing Vortex Induced Oscillation ",*J. Wind Engg. Ind. Aerodyn.*, Vol.10,pp 21-29.

[12] Kumar, M. 1996,"An Experimental Investigation of Pressure Distributions on a Straked Cylinder",*M.Tech. Thesis, Dept. of Aerospace Engg.*, I.I.T. kanpur.

[13] Mao, Y. 1988,"Seabed Under Pipelines",*Proc. 7th Int. Conf. on Offshore and Arctic Engg., Houston, Tex.*,pp 33-38.

[14] Maybrey, J.F.M. and Woodgate, L. 1959,"Further Experiments on the use of Helical Strakes for Avoiding Wind-excited Oscillations of Structures of Circular and Nearly Circular Section ",*Natl. Phys. Lab.(U.K.), Aero Rep. 384.*

[15] Prasad, K.M. 1993,"Flow around a Circular Cylinder near Plane Rigid and Mobile Bed",*M.Tech. Thesis, Dept. of Civil Engineering*, I.I.T. Kanpur.

[16] Roshko, A., Steinolfson, A. and Chattoorgoon, V. 1975," Flow Forces on a Cylinder near a Wall or near another Cylinder",*Proc. 2nd U.S. Conf. Wind Engg. Res., Fort Collins, paper 4-15.*

[17] Scruton, C. and Walshe, D.E. 1957," A means of Avoiding Wind-excited Oscillation of Structures with Circular or nearly Circular Cross Section",*Natl. Phys. Lab. (U.K), Aero Rep. 335.*

[18] Summer, B.M. et al. 1988,"Effect of Lee-wake on Scour below Pipelines in Current",*ASCE Journal of Waterway, Port, Coastal and Ocean Engineering*, Vol.114, No.5,pp 599-614.

[19] Taneda, S. 1965, "Experimental Investigation of Vortex Streets ",*J. Phys. Soc. Japan*, Vol.20,pp 1714-1721.

[20] Tiwari, S. 1994,"Flow around a Circular Cylinder Near Carved-out Boundary ",*M.Tech. Thesis, Dept. of Aerospace Engg.*, I.I.T. Kanpur.

[21] Vickery, B.J. and Watkins, R.D. 1964,"Flow Induced Vibrations of Cylindrical Structures ",*Proc. 1st Aust. Conf. on Hydraulics and Fluid Mechanics, Pergamon*, pp 213-241.

[22] Zdravkovich, M.M. 1981,"Review and Classification of various Aerodynamic and Hydrodynamic means of Suppressing Vortex Shedding ",*J. Wind Eng. Ind. Aerodynamics*, Vol.7,pp 145-189.

Date Slip

This book is to be returned on the date last stamped.

122050

AE-1996- M-GUP PRE